DISSERTATION / DOCTORAL THESIS

Titel der Dissertation /Title of the Doctoral Thesis

„Geometrical and statistical properties of almost Anosov flows“

verfasst von / submitted by

Hector Homero Canales Farias MSc

angestrebter akademischer Grad / in partial fulfilment of the requirements for the degree of

Doktor der Naturwissenschaft (Dr. rer. nat.)

Wien, 2022 / Vienna 2022

Studienkennzahl lt. Studienblatt / degree programme code as it appears on the student record sheet:	UA 796 605 405
Dissertationsgebiet lt. Studienblatt / field of study as it appears on the student record sheet:	Mathematik
Betreut von / Supervisor:	Univ.-Prof. Dr. Henk Bruin, PhD
Betreut von / Supervisor:	Assoz. Prof. Mag. Dr. Roland Zweimüller, Privatdoz

ACKNOWLEDGEMENT

I would first like to thank my thesis advisor Prof. Dr. Henk Bruin of the Faculty of Mathematics at University of Vienna, whose door office was always open whenever I ran into a trouble or had a question about my work. He consistently allowed this thesis to be my own work, but steered me in the right direction whenever he thought I needed it.

Secondly, I would like to thank the members of the Ergodic Theory research group for all the given help and all the time we spent together despite the situation given due the pandemic.

I would also like to express my very profound gratitude to my parents, brother and my aunt for providing me with unfailing support and continuous encouragement throughout my years of study and through the process of researching and writing this thesis. This accomplishment would not have been possible without them. Thank you.

I thankfully acknowledge the financial support by the Austrian Research Fund FWF (stand-alone project P 31950-N35) which financed me for my PhD studies. Finally, I would also like to thank the support provided by the the Vienna School of Mathematics (VSM).

Abstract

In this work we give an example of a flow with finite SRB-measure satisfying polynomial decay of correlations. To do that, we take the construction of the geometrical Lorenz flow and proceed by changing the nature of the saddle fixed point at the origin by a neutral fixed point. This modification is accomplished by changing the linearised vector field in a neighbourhood of origin for a neutral vector field. This change in the nature of the fixed point will allow us to obtain a polynomial flow time, which will lead us ultimately to the proof of the polynomial decay of correlations for the modified flow.

Kurzfassung

In dieser Arbeit geben wir ein Beispiel eines Flusses mit endlichem SRB-Maß, der den polynomialen Zerfall von Korrelationen erfüllt. Dafür nehmen wir die Konstruktion des geometrischen Lorenzflusses und fahren fort, indem wir die Natur des Sattelfixpunkts am Ursprung für einen neutralen Fixpunkt ändern. Diese Modifikation wird erreicht, indem das linearisierte Vektorfeld in einer Ursprungsumgebung für ein neutrales Vektorfeld geändert wird. Diese Änderung in der Natur des Fixpunkts wird es uns ermöglichen, eine polynomiale Flusszeit zu erhalten, was uns schließlich zum Beweis des polynomischen Zerfalls von Korrelationen für den modifizierten Fluss führen wird.

Contents

Introduction

The study of flows in surfaces and higher-dimensional manifolds has caught the interest of many scientists because of its numerous applications such as Hamiltonian flows, which arise from energy-preserving dynamical systems, billiard flows, flows from meteorological models, most notably the Lorenz model. These flows are equipped with a natural invariant measure μ, for instance SRB-measures, Liouville measures, Margulis entropy maximizing measure among other measures.

The main goal is to have a better understanding of the properties of these flows, such as hyperbolicity, ergodicity, mixing and weak mixing and, in chaotic settings, rates of mixing; that is, we would like to investigate the asymptotic behaviour of the correlation coefficients

$$\rho_t(v,w) = \left| \int_M v \cdot w \circ f^t d\mu - \int_M v d\mu \int_M w d\mu \right|,$$

where $f^t : M \to M$ is a flow acting on a manifold M and μ its invariant measure, and for observables v, w chosen from an appropriate Banach space.

Since mixing rates are one of the strongest statistical properties to have, other statistical laws, such as the Central Limit Theorem (CLT), usually follow. Therefore, investigate the rates of mixing is a major tool for proving other ergodic properties. The rates of mixing are certainly connected to the type of flow. For example, convexity of scatters in billiard maps and flows produces hyperbolicity and over the past years, a lot of effort has been dedicated to prove exponential mixing of such systems, see for example [14, 23, 50]. To obtain sharp estimates of mixing rates in the polynomial setting, the operator renewal theory techniques developed by Sarig [41] and Gouëzel [27] are the only ones available.

One of the first major successes of ergodic theory in mathematical billiards was the proof of ergodicity of Sinai billiards in the 1970s [44]. Over the past decades, a lot of effort has been done in proving rates of mixing considering different settings. For example, [25] proved that Anosov flows enjoy exponential mixing.

Other example and probably the most emblematic one is the Lorenz flow. In the mid seventies Afraimovich, Bykov and Shil'nikov [1] and Guckenheimer and Williams [28] introduced independently the geometric Lorenz attractors to model the original Lorenz attractors. It was not until the end of the nineties that Tucker [47] gave a rigorous proof for the existence of the non-uniform hyperbolic Lorenz attractor originally suggested by E. Lorenz. More recently, Araújo and Melbourne in [8] proved that the geometrical Lorenz flow (and hence the classical Lorenz flow), see Figure 1, also enjoys exponential mixing.

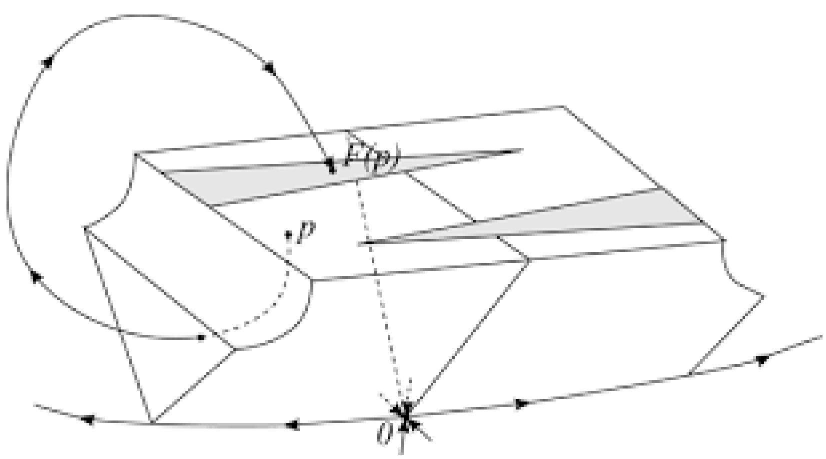

Figure 1: The Guckenheimer-Williams geometric model of the Lorenz flow.

Among the different techniques in the literature we will use the following: any flow can be regard as a suspension flow over a Poincaré map $P : \Sigma \to \Sigma$ with roof function $r : \Sigma \to \mathbb{R}^+$. The flow becomes now a vertical, parallel flow $f^t(x, u) = (x, u + t)$ on $\Sigma^r = \{(x, u) \in \Sigma \times [0, r(x)]\}/\sim$, where $(x, r(x)) \sim (P(x), 0)$. The flow-invariant measure $d\mu = d\mu_P \times du$, where $d\mu_P$ is an P-invariant measure. If $P : \Sigma \to \Sigma$ is not hyperbolic, hyperbolicity can be regained by looking at a return map $P_Y = P^\tau : Y \to Y$, for some induce time $\tau : Y \to \mathbb{N}$, preserving a measure μ_Y. If τ is the first return map, then

μ_Y and $\mu_{P|_Y}$ coincide up to a multiplicative constant. The induce map has its own suspension flow with induced roof function $r_Y = \sum_{j=0}^{\tau(x)-1} r \circ P^j(x)$.

Indeed the geometrical Lorenz flow can be seen as the natural extension of a suspension flow built over a certain type of one-dimensional expanding map f. To obtain the one-dimensional map f we first consider the cross-section Σ which is transversal to the flow and the Poincaré map $P_{\mathrm{Lor}} : \Sigma \to \Sigma$ given by $P_{\mathrm{Lor}}(x) = \mathrm{L}_{r_{\mathrm{Lor}}(x)}(x)$, where $\mathrm{L}_t : \Lambda \to \Lambda$ and $r_{\mathrm{Lor}}(x)$ are the flow of the linear system given by the Equation (3.9) and the flow (return) time to the cross-section Σ given by Equation 5.3, respectively. To prove exponential mixing for the geometrical Lorenz flow certain regularity in the stable foliation is required; that is, we need the stable foliation to be $C^{1+\alpha}$ and satisfying a uniform non-integrability condition.

We take advantage of these techniques and construct a modification of the geometrical Lorenz flow, which we will call modified geometrical neutral Lorenz flow. This modified version is obtained by considering in a neighbourhood of the origin, one of the vector fields give by Equation (4.1), (8.1) or (8.11) instead of the linearised vector field. In this way, we obtained the modified Poincaré map $P_{\mathrm{Neu}}(x) = \mathrm{N}_{r_{\mathrm{Neu}}(x)}(x)$, where $N_t : \Lambda_{\mathrm{N}} \to \Lambda_{\mathrm{N}}$ and $r_{\mathrm{Neu}}(x)$ are the neutral flow given by Equation (4.7) or (8.5) and the new flow time to the cross-section given by Equation (5.11). We prove that the stable foliation of this modified version of the flow still fulfils the same regularity; that is, the foliation is $C^{1+\alpha}$ and satisfies the uniform non-integrability condition. This modification yields to a slower flow time that will ultimately allow us to deduce the polynomial decay of correlations.

Chapter 1

Basic concepts in continuous dynamical systems

1.1 Toolbox for Flows

In this section we will give some of the basic notions of flows. Most of the content of this Chapter is taken from [3], [10] and [31]. For a more detailed exposition of the material the reader is encouraged to see the references.

1.1.1 Notation. *A compact manifold M without boundary will be called **closed** manifold. For the purpose of this work we will consider C^2 manifolds.*

The manifold M will be endowed with some Riemannian metric ρ which induces a distance on M and an associated Riemannian volume which we will denote as Leb and we will take it to be normalized; that is, $\mathrm{Leb}(M) = 1$.

Given a C^r vector field X on M ($r \geq 1$) since X is defined in all M and X is bounded (since M is compact), then for every $t \in \mathbb{R}$ the associated global flow $(X^t)_{t\in\mathbb{R}}$ is well defined. The flow $(X^t)_{t\in\mathbb{R}}$ (which will be denoted as X^t for simplicity) is a family of C^r diffeomorphisms which satisfy the following:

1.- $X^0 = \mathrm{Id} : M \to M$ is the identity in M;

2.- $X^{t+s} = X^t \circ X^s$ for every $t, s \in \mathbb{R}$;

and it is generated by the vector field X if

3.- $\frac{d}{dt}X^t(q)|_{t=t_0} = X(X^{t_0}(q))$ for every $q \in M$ and $t_0 \in \mathbb{R}$.

Reciprocally, a C^{r+1} flow $(X^t)_{t\in\mathbb{R}}$ determines a unique C^r vector field X with associated flow $(X^t)_{t\in\mathbb{R}}$.

1.1.2 Notation. *The vector space of all C^r vector fields on M equipped with the C^r topology will be denoted by $\mathfrak{X}^r(M)$ and by $\mathfrak{F}^r(M)$ the space of C^r flows with the C^r topology.*

The derivatives of the flow and the vector field with respect to the variable q will be denoted by $D_qX^t = DX^t(q)$ and $D_qX = DX(q)$, respectively.

1.1.3 Definition. *Given a vector field X a **singularity** or **equilibrium** for X is a point $q \in M$ such that $X^t(q) = q$ for every $t \in \mathbb{R}$ which corresponds to the zeros of X; that is, $X(q) = 0$. Any point p for which $X(p) \neq 0$ is a **regular** point for X. The set of all singularities will be denoted by* $\mathrm{S}(X)$.

*The **orbit of a point** $q \in M$ is the set $\mathrm{Orb}_X(q) = \{X^t(q) \mid t \in \mathbb{R}\}$ or simply $\mathrm{Orb}(q)$ if there is no confusion with the flow or vector field we are working with. A **periodic orbit** is an orbit $\mathrm{Orb}(p)$ with $X^T(p) = p$ for a minimal $T > 0$. The set of all periodic points will be denoted by $\mathrm{Per}(X)$.*

1.1.4 Definition. *A point $q \in M$ will be called **non-wandering** for the vector field X if for every open neighbourhood U of q and every $T > 0$ there is $t > T$ such that $X^t(U) \cap U \neq \emptyset$. We will denote the set of non-wandering points by $\Omega(X)$.*

*The **omega limit set** of a point q is the set of accumulation points of the positive orbit of q ($\{X^t \mid t > 0\}$) and will be denoted by $\omega_X(q)$ or simply $\omega(q)$ if no confusion is raised. Likewise, we define the **alpha limit** set of q as the set of accumulation points of the backward orbit of q by $\alpha_X(q) = \omega_{-X}(q)$, where $-X$ is the time reversed vector field X. We have the inclusion $\omega(q) \cup \alpha(q) \subset \Omega(X)$.*

*A subset Λ of M is called $X-$**invariant** if $X^t(\Lambda) = \Lambda$ for every $t \in \mathbb{R}$. We have that $\Omega(X)$, $\omega(q)$ and $\alpha(q)$ are X-invariant.*

1.1.5 Definition. *Let M be a closed manifold, $X \in \mathfrak{X}^r(M)$ and Λ a compact X-invariant subset of M. We define the **stable set** of Λ as*

$$W^s_X(\Lambda) = \{q \in M \mid \omega_X(q) \subset \Lambda\}$$

and the ***unstable set*** *as*

$$W^u_X(\Lambda) = \{q \in M \mid \alpha_X(q) \subset \Lambda\}.$$

When no confusion is raised we will denote them as $W^s(\Lambda)$ *and* $W^u(\Lambda)$ *for short.*

1.1.6 Definition. *Consider* M *a closed manifold,* $X \in \mathfrak{X}^r(M)$ *and* Λ *a compact* X*-invariant subset of* M*. We will say that* Λ *is* ***isolated*** *(or* ***maximal****) if there exist a neighbourhood* U *of* Λ *such that*

$$\Lambda = \bigcap_{t\in\mathbb{R}} X^t(U) = \bigcap_{t\in\mathbb{R}} Cl(X^t(U)),$$

where $Cl(\cdot)$ *denotes the closure on* M*.*

Λ *will be called* ***transitive*** *if there is* $q \in \Lambda$ *such that* $\omega_X(q) = \Lambda$ *and* ***attracting*** *if* $\Lambda(U) = \bigcap_{t>0} X^t(U) = \Lambda$ *for some neighbourhood* U *of* Λ *with* $Cl(X^t(U)) \subset U$ *for all* $t > 0$*.* U *is called* ***isolating neighbourhood*** *of* Λ*.*

An ***attractor*** *of* X *is a transitive attracting set of* X *and a* ***repeller*** *will be an attractor for* $-X$*.*

We make the observation that in general $\Lambda(U)$ is different from $\bigcap_{t\in\mathbb{R}} X^t(U)$, but for an attracting set the condition $Cl(X^t(U)) \subset U$ for all $t > 0$ guarantees that $X^{-t}(U) \supset U$ and thus

$$\Lambda \supset \bigcap_{t\in\mathbb{R}} X^t(U) = \bigcap_{t\leq 0} X^t(U) \cap \bigcap_{t\geq 0} X^t(U) \supset \Lambda \cap U = \Lambda.$$

Therefore, every attracting set is isolated.

1.1.7 Definition. *Let* M *be a closed manifold and* $X \in \mathfrak{X}^r(M)$*. A* ***sink*** *of* X *is a trivial attractor and a* ***source*** *is a trivial repeller of* X*.*

A singularity q *is called* ***hyperbolic*** *if the real part of the eigenvalues of* D_qX *are different from zero. Particularly, sources and sinks are hyperbolic since all the eigenvalues of the former have positive real part and those of the later are negative. A periodic orbit* $\mathrm{Orb}(p)$ *is hyperbolic if all the eigenvalues of* $D^T_pX : T_pM \to T_pM$*, where* $T > 0$ *is the period of* p*, are distinct from* 1*.*

The geometric interpretation of hyperbolic singularities is that their stable and unstable sets have the structure of an embedded manifold and are called **stable** and **unstable manifold**. This comes as a consequence of the Stable Manifold Theorem 1.1.9. Before stating this Theorem we give the necessary definitions. The reader can find the proof of the Stable Manifold Theorem in Robinson's book [40].

1.1.8 Definition. *Let M be a closed manifold and $X \in \mathfrak{X}^r(M)$ and Λ a compact $X-$invariant subset of M. Denote* $\mathrm{m}(T) = \inf_{\|v\|=1} \|T(v)\|$ *the minimum norm of a linear operator T. We will say that Λ is **hyperbolic** if every $q \in \Lambda$ is a hyperbolic singularity for X. Therefore, there are $\lambda \in (0,1)$, $C > 0$, and families of subspaces E^s_q, $E^u_q, E^X_q \in T_qM$ with $q \in \Lambda$, such that,*

(1) $T_qM = E^s_q \bigoplus E^u_q \bigoplus E^X_q$*, where E^X_q is the subspace generated by $X(q)$*

(2) $\left\|DqX^t|_{E^s_q})\right\| \leq C^{-1}\,\mathrm{e}^{-\lambda t}$ *for every $t \geq 0$,*

(3) $\mathrm{m}(DqX^t|_{E^u_q}) \leq C\,\mathrm{e}^{\lambda t}$ *for every $t \geq 0$,*

(4) $D_qX^t(E^i_q) = E^i(X^t(q))$ *for $i = s, u, X$ and every $t \in \mathbb{R}$ and $q \in \Lambda$.*

The sets

$$W^{s/u}_X(q) = \{p \in M \mid d(X^t(q), X^t(p)) \to 0 \text{ as } t \to \infty \text{ or } -\infty\},$$

*where d is the distance on M induced by the Riemannian metric ρ, are called **stable/unstable manifold**. See Figure 1.1*

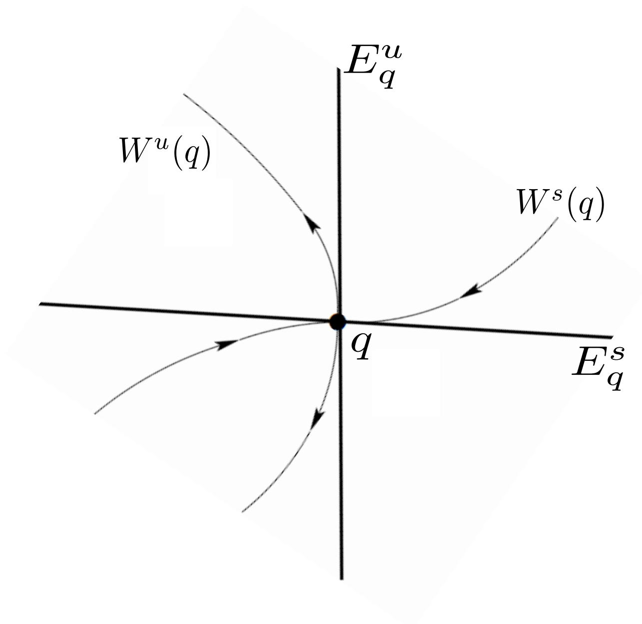

Figure 1.1: The stable and unstable manifolds.

1.1.9 Theorem. *Let M be a closed manifold, $X \in \mathfrak{X}^r(M)$ and Λ a hyperbolic set. Then the (un)stable manifold $W_X^{s/u}(q)$ are invariant C^r immersed manifolds tangent to $E_q^{s/u}$ for every $q \in \Lambda$.*

1.1.10 Definition. *Let M be an $m-$dimensional manifold, M_1 and M_2 two submanifolds of M. We say that M_1 and M_2* ***intersects transversally*** *and denoted by $M_1 \pitchfork M_2$ if and only if for any $x \in M_1 \cap M_2$ we have $T_xM = T_xM_1 \bigoplus T_xM_2$.*

1.1.11 Definition. *Let M be an $m-$manifold. An $p-$**dimensional foliation** $\mathcal{F}$ of M is a collection $\{M_i\}_{i\in\mathcal{I}}$, where $\mathcal{I}$ is an index set, of pairwise-disjoint, connected, immersed $p-$dimensional submanifolds of M, called the **leaves** of the foliation, such that for every $x \in M$, there is a chart (U, ϕ) with U homeomorphic to $\mathbb{R}^n$ containing x such that every leaf, M_i, meets U in either the empty set or a countable collection of subspaces whose images under ϕ in $\phi(M_i \cap U)$ are $p-$dimensional affine subspaces whose first $m-p$ coordinates are constant.*

The following theorem is a powerful tool known as the Hartman-Grobman

Theorem and its proof can be found in any book concerning continuous dynamical systems. For example in [31], [10] or [40].

1.1.12 Theorem. *Let $X \in \mathfrak{X}^r$ and $p \in M$ be a hyperbolic singularity of X. Let $Y = DX^0 : T_pM \to T_pM$ be the linear vector field on T_pM given by the linear transformation DX^0. Then there exists an open neighbourhood U of p in M, a neighbourhood V of 0 in T_pM and a homeomorphism $h : U \to V$ such that $X|_U$ is topologically conjugate to $Y|_V$.*

1.2 Anosov and almost Anosov diffeomorphisms and flows

In the early 60's Stephen Smale constructed the so-called Smale horseshoe, a structurally stable dynamical system given by a diffeomorphism of the two-dimensional sphere and having an infinite set of periodic points giving way to an unexpected breakthrough in the theory of dynamical systems. With this discovery, new aspects in the problem of describing the structurally stable systems emerged. Anosov met Smale in the Symposium on non-linear oscillations at Kiev in 1961, Smale posed some difficult unsolved problems. Particularly, the problem of geodesic flows on closed manifolds of negative curvature and the problem of structural stability of hyperbolic automorphisms on the torus. Anosov started working on these problems and he solved them as particular cases in his investigation of the U-systems, now called Anosov systems in [4]. The development on Smale's discovery done by Anosov marked the beginning of the 'hyperbolic revolution' in mathematics. After this brief introduction on Anosov diffeomorphism we proceed to give its formal definition.

1.2.1 Definition. *Let M be an $m-$dimensional manifold and $f : M \to M$ be a C^1 diffeomorphism. A compact, completely invariant subset $\Lambda \subset M$ is called **hyperbolic** if there are $\lambda \in (0,1)$, $C > 0$, and families of subspaces $E^s(x)$, $E^u(x) \in T_xM$ with $x \in \Lambda$, such that for every $x \in \Lambda$,*

(1) $T_xM = E^s(x) \bigoplus E^u(x)$,

(2) $\|df_x^n(v^s)\| \leq C\lambda^n \|v^s\|$ *for every* $v^s \in E^s(x)$ *and* $n \geq 0$,

(3) $\|df_x^{-n}(v^u)\| \leq C\lambda^n \|v^u\|$ *for every* $v^u \in E^u(x)$ *and* $n \geq 0$,

(4) $df_x E^s(x) = E^s(f(x))$ and $df_x E^u(x) = E^u(f(x))$.

*The subspace $E^s(x)$ (respectively, $E^u(x)$) is called the **stable (unstable) manifold** at x, and the family $\{E^s(x)\}_{x\in\Lambda}$ ($\{E^u(x)\}_{x\in\Lambda}$) is called the **stable (unstable) distribution** of $f|_\Lambda$.*

*If $M = \Lambda$, then f is called **Anosov diffeomorphism**.*

The simplest and most popular example of an Anosov diffeomorphism on $\mathbb{T}^2$ is the well-known Arnold's cat map given in Example 1.2.2

1.2.2 Example. *The cat map given by*

$$f(x) = \begin{pmatrix} 2 & 1 \\ 1 & 1 \end{pmatrix} \cdot x \bmod 1,$$

the matrix has eigenvalues $\lambda_{1,2} = \frac{3\pm\sqrt{5}}{2}$, which means that f is an Anosov map.

If instead of considering a diffeomorphism f we consider a flow $\phi^t : M \times \mathbb{R} \to M$ from a closed differentiable manifold, then we obtain the same notion for the flow; that is, if in Definition 1.2.1 we replace f by ϕ^t, then we obtain the following definition.

1.2.3 Definition. *Let M be an $m-$dimensional closed manifold (closed here means compact and without boundary) and $\phi^t : M \times \mathbb{R} \to M$ a C^1 flow on M. We will call the flow ϕ_t **Anosov** if there exists a continuous mutually transversal splitting of the tangent bundle $TM = E^c \bigoplus E^s \bigoplus E^u$ and constants a and b such that:*

(1) $\|D\phi^t(v^s)\| \leq b\,\mathrm{e}^{-at}\,\|v^s\|$ for every $v^s \in E^s(x)$ and $t > 0$,

(2) $\|D\phi^t(v^u)\| \leq b\,\mathrm{e}^{-at}\,\|v^u\|$ for every $v^u \in E^u(x)$ and $t < 0$,

(3) $D\phi^t E^s = E^s$, $D\phi^t E^u = E^u$ and $D\phi^t E^c = E^c$,

where E^c is the neutral flow direction, E^s the hyperbolically stable direction and E^u the hyperbolically unstable direction.

The concept of almost Anosov diffeomorphism was first introduced in the work of Hu and Young [32, 33], where they worked with diffeomorphisms in the two-dimensional torus. Their goal was to give an answer to the question, does a system $f : M \to M$ admit and SRB-measure if hyperbolicity fails at a fixed points?. They showed that existence of a finite or infinite SRB measure for an almost Anosov diffeomorphism on the two-dimensional torus depends on the local dynamics near the neutral fixed point. We give now the formal definition of an almost Anosov diffeomorphism.

1.2.4 Definition. *[32] We will say that a diffeomorphism $f : M \to M$ from a closed m-dimensional manifold M to itself is **almost Anosov** if there exists two continuous families of non-trivial cones $x \to \mathrm{C}_x^s, \mathrm{C}_x^u$ such that the following hold except for a finite set S of periodic points*

(1) $Df_x \mathrm{C}_x^u \subseteq \mathrm{C}_{f(x)}^u$ *and* $Df_x \mathrm{C}_x^s \supseteq \mathrm{C}_{f(x)}^s$,

(2) $\|Df(v^s)\| < \|v^s\|$ *for every* $0 \neq v^s \in \mathrm{C}_x^s$,

(3) $\|Df(v^u)\| > \|v^u\|$ *for every* $0 \neq v^u \in \mathrm{C}_x^u$.

Likewise, if in Definition 1.2.4 we substitute the diffeomorphism f by a flow $\phi^t : M \times \mathbb{R} \to M$ from a closed differentiable manifold, we get the concept of almost Anosov flow, so we get the following:

1.2.5 Definition. *We will say that a flow $\phi^t : M \times \mathbb{R} \to M$ on a closed m-dimensional manifold M is **almost Anosov** if there exists a continuous splitting of the tangent bundle $TM = E^c \bigoplus E^s \bigoplus E^u$ (where E^c is the one dimension flow direction) such that the following hold except for a finite number of periodic orbits:*

(1) $\|D\phi^t(v^s)\| < \|v^s\|$ *for every* $0 \neq v^s \in E^s(x)$ *and* $t > 0$,

(2) $\|D\phi^t(v^u)\| > \|v^u\|$ *for every* $0 \neq v^u \in E^u(x)$ *and* $t > 0$,

(3) $D\phi^t E^s = E^s$, $D\phi^t E^u = E^u$ *and* $D\phi^t E^c = E^c$.

We can think of almost Anosov diffeomorphisms (flows) as locally perturbed Anosov diffeomorphisms (flows), where the perturbation is around a finite set S (finite periodic orbits).

Chapter 2

Ergodic theory concepts and results

We will take Chapter 3 from [22] since it contains all the necessary ergodic concepts we will need through this work. Naturally, these definitions and facts can be found in text books on ergodic theory, such as the ones by Walters, Petersen and Boyarski & Gora, see [49], [37] and [15], respectively.

2.0.1 Definition. *[22] We will call a measure μ* ***absolutely continuous*** *with respect to a measure λ, if $\lambda(A) = 0$ implies $\mu(A) = 0$ and we will denote it by $\mu \ll \lambda$. If both $\mu \ll \lambda$ and $\lambda \ll \mu$ then μ and λ are called* ***equivalent****.*

2.0.2 Definition. *[22] Let $T : (X, \mathcal{A}, \lambda) \to (X', \mathcal{A}', \lambda')$ be a measurable function: Then T is called* ***measurable preserving*** *(m.p) if $\lambda \circ T^{-1} = \lambda'$.*

2.0.3 Definition. *[22] $(X, \mathcal{A}, \mu, T)$ will be called a* ***measure preserving system*** *if T is a measure preserving function from $(X, \mathcal{A}, \mu)$ to itself and will say that the measure μ is* ***T-invariant***

The following Theorem is known as the Radon-Nikodym theorem for a more detailed explanation see for example [45].

2.0.4 Remark. *We denote by $L^1(\nu)$ the space of integrable functions with respect to ν.*

2.0.5 Theorem. *If μ is a probability measure and $\mu \ll \nu$ then there is a function $h \in L^1(\nu)$ such that $\mu(A) = \int_A h(x)d\nu(x)$ for every measurable set*

*A, h is called **Radon-Nikodym density**. Sometimes we use the notation $h = \frac{d\mu}{d\nu}$.*

Let $(X, \mathcal{A}, \mu, T)$ be a measure preserving system. If $T^{-1}A = A$ for some $A \in \mathcal{A}$, then $T^{-1}A^{\mathsf{c}} = A^{\mathsf{c}}$. Thus we can split the study of T into two parts: $T|_A$ and $T|_{A^{\mathsf{c}}}$. Then we have the concept of *indecomposability* for measure preserving functions, so that if T has this indecomposable property then the study of T cannot be split into separate parts. This property is called *ergodicity*.

2.0.6 Definition. *[22] A measure preserving transformation $T : (X, \mathcal{A}, \mu) \to (X, \mathcal{A}, \mu)$ will be called **ergodic** if for any $A \in \mathcal{A}$, such that $T^{-1}A = A$, $\mu(A) = 0$ or $\mu(A^{\mathsf{c}}) = 0$. We define $\mathcal{I}(T) = \{A \in \mathcal{A};\ T^{-1}A = A\}$.*

The following results are well known and can be found in any book of ergodic theory. We will not give a proof, for more details please see for example [15] or [49]

2.0.7 Definition. *[22] Let $T : (X, \mathcal{A}, \mu) \to (X, \mathcal{A}, \mu)$ be a measure preserving function. Then T is **weakly mixing** if for all A, $B \in \mathcal{A}$*

$$\frac{1}{n}\sum_{k=0}^{n-1} |\mu(T^{-k}(A) \cap B) - \mu(A)\mu(B)| \to 0 \text{ as } n \to \infty.$$

*T will be called **strongly mixing or mixing** if for all A, $B \in \mathcal{A}$,*

$$\mu(T^{-n}(A) \cap B) \to \mu(A)\mu(B) \text{ as } n \to \infty.$$

2.0.8 Proposition. *[22] Let $(X, \mathcal{A}, \mu, T)$ be a measure preserving dynamical system. Then, T is mixing if and only if*

$$\int_X v \cdot w \circ T^n d\mu \to \int_X v d\mu \int_X w d\mu,$$

for every $v \in \mathrm{L}^1(\mu)$ and $w \in \mathrm{L}^\infty(\mu)$.

2.0.9 Observation. *[22] Mixing characterizes how the statistical correlations between subsets A and B or observables v and w evolve with time. Mixing means that the correlations decay with time; that is, they are asymptotically independent*

2.0.10 Definition. *[22] We define the **decay of correlations** as*

$$\rho_n(v,w) = \left| \int v \cdot w \circ T^n d\mu - \int v d\mu \int w d\mu \right|,$$

for discrete map T, v and w as above. For the continuous version; that is, for a flow T_t we define it as

$$\rho_t(v,w) = \left| \int v \cdot w \circ T_t d\mu - \int v d\mu \int w d\mu \right|,$$

for suitable observables v and w.

2.0.11 Definition. *[22] Let $T : (X, \mathcal{A}, \mu) \to (X, \mathcal{A}, \mu)$ be a measure preserving map. Then T is **exact** if the tail σ-algebra $\mathfrak{T}(\mathcal{A}) = \bigcap_{k \geq 0} T^{-k}\mathcal{A}$ consists of the sets of measure 0 or 1; i.e., for every $A \in \mathfrak{T}(\mathcal{A})$ we have that $\mu(A) = 0$ or $\mu(A^{\mathsf{c}}) = 0$.*

2.0.12 Proposition. *[22] We have the following implications:*

exact $\implies$ mixing $\implies$ weakly mixing $\implies$ ergodic.

We now define what a Young tower is and its continuous equivalent the suspension flow.

2.0.13 Definition. *Let $f : X \to X$ be a measurable transformation on a metric space (X, d). We say that f can be modelled by a **Young tower** if there exists $Y \subset X$ possessing a good hyperbolic structure, a countable measurable partition $\{Y_j\}_{j \geq 0}$ of Y and a return time $\tau : Y \to \mathbb{Z}^+$ constant on partition elements, such that the return map $F = f^\tau : Y \to Y$ is uniformly hyperbolic and smooth with invariant (SRB) measure μ_Y. We define the **Young tower** as $\Delta = \{(y, \ell) \in Y \times \mathbb{Z}^+ \mid 0 \leq \ell < \tau(x)\}/\sim$, where $(x, \ell(x)) \sim (F(x), 0)$. The tower map $T : \Delta \to \Delta$ is given by $T(x, \ell) = (x, \ell + 1)$ computed modulo identifications with ergodic invariant probability measure $\mu = \mu_Y \times \mathrm{count}/\bar{\tau}$, where count is the counting measure and $\bar{\tau} = \int_Y \tau d\mu_Y$ (provided $\tau \in \mathrm{L}^1(Y)$).*

2.0.14 Definition. *Let (Σ, ν) be a probability space and $P : \Sigma \to \Sigma$ an ergodic measure-preserving transformation. Let $r : \Sigma \to \mathbb{R}^+$ be a measurable (Hölder continuous) roof function. We define the **suspension space** as $\Sigma^r = \{(x, u) \in \Sigma \times [0, r(x)]\}/\sim$, where $(x, r(x)) \sim (P(x), 0)$. The **suspension flow** $f_t : \Sigma^r \to \Sigma^r$ is given by $f_t(x, u) = (x, u + t)$ computed modulo* *identifications and the measure $\mu = \nu \times \lambda$, where λ is the Lebesgue measure, is ergodic and f_t-invariant. In the finite measure case, we normalise by $\bar{r} = \int_\Sigma r d\mu$ so that $\mu = \frac{\nu \times \lambda}{\bar{r}}$ is a probability measure.*

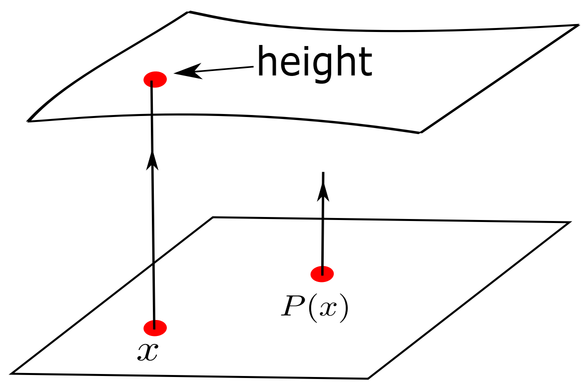

Figure 2.1: The suspension flow of P. Start at (x, u) following the suspension flow we go until $u + t = r(x)$ then we jump to $(P(x), 0)$.

2.0.15 Definition. *Let M be an $m-$dimensional closed manifold, $f^t : M \times \mathbb{R} \to M$ a C^1 flow on M and μ a flow invariant probability measure. We define the **ergodic basin** of μ by*

$$\mathrm{B}(\mu) = \left\{ x \in M \;\middle|\; \int_M \varphi d\mu = \lim_{T\to\infty} \frac{1}{T} \int_0^T \varphi(f^t x) dt \text{ for continuous observable } \varphi : M \to \mathbb{R} \right\}.$$

*A flow invariant probability measure μ is called **SRB-measure** (or **physical**) if the ergodic basin $\mathrm{B}(\mu)$ has positive Lebesgue measure.*

2.1 Functions of bounded variation

Let $[a, b] \subset \mathbb{R}$ be a bounded interval and let λ denote Lebesgue measure on $[a, b]$. For any sequence of points $a = a_0 < a_1 < \ldots < a_n = b$, $n \geq 1$, we define a partition $\mathcal{P} = \{I_i = [a_{i-1}, a_i);\; i = 1, \ldots, n\}$ of $[a, b]$. The points $\{a_0, \ldots, a_n\}$ are called *endpoints of the partition* $\mathcal{P}$.

2.1.1 Definition. *[22] Let $f : [a, b] \to \mathbb{R}$ and let $\mathcal{P}$ be a partition of $[a, b]$. If there exists a positive number M such that*

$$\sum_{k=1}^{n} |f(a_k) - f(a_{k-1})| \leq M$$

*for all partitions $\mathcal{P}$, then T is said to be of **bounded variation** on $[a, b]$.*

If f is increasing or if it satisfies the Lipschitz condition

$$|f(x) - f(y)| < K|x - y|,$$

then it is of bounded variation.

2.1.2 Definition. *[22] The number*

$$\mathrm{V}_{[a,b]}\, f = \sup_{\mathcal{P}} \left\{ \sum_{k=1}^{n} |f(a_k) - f(a_{k-1})| \right\}$$

*is called the **total variation** of f on $[a, b]$, where $f : [a, b] \to \mathbb{R}$ is a function of bounded variation.*

2.1.3 Proposition. *[22] Let f be a function of bounded variation such that $\|f\|_1 < \infty$. Then*

$$|f(x)| \leq \mathrm{V}_{[a,b]}\, f + \frac{\|f\|_1}{b - a}$$

for all $x \in [a, b]$.

Proof. We claim that there exists $y \in [a, b]$ such that $|f(y)| \leq \frac{\|f\|_1}{b-a}$. If not, then for any $x \in [a, b]$

$$(b - a)|f(x)| > \|f\|_1 .$$

Hence,

$$\|f\|_1 = \int_a^b |f(x)| d\lambda(x) > \int_a^b \frac{\|f\|_1}{b - a} d\lambda(x) = \|f\|_1$$

and we have a contradiction.

Since $|f(x)| \le |f(x) - f(y)| + |f(y)|$ we have

$$|f(x)| \le \mathrm{V}_{[a,b]} f + \frac{\|f\|_1}{b-a}.$$

$\square$

We present a result due to E. Helly that we will use later. For a proof of the theorem please see [36] page 220.

2.1.4 Theorem. *Let an infinite family of functions $\mathcal{F}$ be defined on an interval $[a,b]$. If all functions of the family and the variation of all functions of the family are bounded by a single number, i.e., $|f(x)| \le K$, $\mathrm{V}_{[a,b]} f \le K$ for every $f \in \mathcal{F}$, then there exists a sequence $\{f_n\}_{n\ge1} \subset \mathcal{F}$ that converges pointwise to some function f^* of bounded variation and $\mathrm{V}_{[a,b]} f^* \le K$.*

We now make the space of functions of bounded variation into a Banach space. Let

$$\mathrm{BV}([a,b]) = \{f \in \mathrm{L}^1(\lambda);\ \inf_{f_1 = f \text{ a.e}} \mathrm{V}_{[a,b]} f_1 < \infty\}.$$

Note that the infimum is taken over all functions a.e equal to f. For example the function

$$f(x) = \begin{cases} n, & \text{if } x = \frac{1}{n},\ n = 1, 2 \dots \\ 0, & \text{otherwise,} \end{cases}$$

clearly has infinite variation but $f \in \mathrm{BV}([0,1])$ since $f_1 = 0$ is a.e equal to f and $\mathrm{V}_{[0,1]} f_1 = 0$.

We define a norm on $\mathrm{BV}([a,b])$ as follows: For $f \in \mathrm{BV}([a,b])$,

$$\|f\|_{\mathrm{BV}} = \|f\|_1 + \inf_{f_1 = f \text{ a.e.}} \mathrm{V}_{[a,b]} f_1$$

Without $\mathrm{L}^1(\lambda)$-norm, $\|\cdot\|_{\mathrm{BV}}$ would not be a norm, since a function that is not 0 λ a.e. could have 0 variation. Now we give some properties of the space $\mathrm{BV}([a,b])$, all proofs can be found in [15].

2.1.5 Proposition. $\mathrm{BV}([a,b])$ *is dense in* $\mathrm{L}^1(\lambda)$.

Proof. Since $C^1([a,b])$ is dense in $L^1(\lambda)$ (Stone-Weierstrass Theorem) and since $C^1([a,b]) \subset BV([a,b])$ the result follows. $\square$

The following Theorem makes a connection between weakly convergence and norm convergence in $L^1(\lambda)$.

2.1.6 Theorem. *If $f_n \to f$ weakly in $L^1(\lambda)$ and almost everywhere, then $f_n \to f$ strongly in $L^1(\lambda)$*

2.1.7 Proposition. *A bounded set in $BV([a,b])$ is relatively compact in $L^1(\lambda)$;i.e., every sequence in such bounded set has a convergent subsequence*

Proof. If $\{f_i\}_{i\in\mathcal{J}} \subset BV([a,b])$ is bounded, there is $K_1 < \infty$ such that $\|f_i\|_{BV} \leq K_1$ for every $i \in \mathcal{J}$.

From the definition of $\|\cdot\|_{BV}$ if follows that $\{f_i\}_{i\in\mathcal{J}}$ is uniformly bounded; *i.e.*, there is $K_2 < \infty$ such that $|f_i(x)| \leq K_2$ for every $i \in \mathcal{J}$. Let $K = \max(K_1, K_2)$. By Helly's Theorem 2.1.4, there exists a subsequence $\{f_{i_j}\}$ such that $f_{i_j} \to f^*$ everywhere. Since $\{f_i\}_{i\in\mathcal{J}}$ is weakly compact (it is uniformly bounded) and $f_{i_j} \to f^*$, Theorem 2.1.6 implies that $f_{i_j} \to f^*$ in $L^1(\lambda)$. Hence $\{f_i\}_{i\in\mathcal{J}}$ is strongly compact in $L^1(\lambda)$. $\square$

2.2 The Frobenius-Perron operator

The following definitions, results and ideas are taken from the work of Boyarsky and Góra, for more details please consult [15].

We start by defining the Frobenius-Perron operator which enable us to study the time evolution of densities in the phase space. The spectral theory for this operator is a great tool that allow us to deduce ergodic properties of our system such as ergodicity and mixing.

2.2.1 Definition. *[22] Let $(I, \mathcal{A}, \lambda, T)$ with λ the normalized Lebesgue measure on I. We define the **Frobenius-Perron operator** $P_T : L^1(\lambda) \to L^1(\lambda)$ as follows: For any $f \in L^1(\lambda)$, $P_T f$ is the unique (up to a.e equivalence) function in $L^1(\lambda)$ such that for any $A \in \mathcal{A}$*

$$\int_A P_T f d\lambda = \int_{T^{-1}A} f d\lambda.$$

The validity of this definition, i.e., the existence and the uniqueness of $\mathrm{P}_T f$*, follows by the Radon-Nikodym Theorem 2.0.5.*

Let $\mathcal{T}(I)$ be the class of functions $T : I \to I$ that satisfy the following conditions:

1 T is *piecewise expanding*, *i.e*, there exists a partition $\mathcal{P} = \{I_i = [a_{i-1}, a_i]$ $i = 1, \ldots, q\}$ of I such that $T|_{I_i}$ is $\mathbf{C}^1$, and $|T_i'(x)| \geq \alpha > 1$ for any i and for all $x \in (a_{i-1}, a_i)$, where $T_i = T|_{I_i}$;

2 $g(x) = \frac{1}{|T'(x)|}$ is a function of bounded variation, where $T'(x)$ is the appropriate one-sided derivative at the endpoints of $\mathcal{P}$.

For each $n \geq 1$, we define the partition $\mathcal{P}^{(n)}$ as follows:

$$\mathcal{P}^{(n)} = \bigvee_{k=0}^{n-1} T^{-k}(\mathcal{P}) = \{I_{i_0} \cap T^{-1} I_{i_1} \cap \cdots \cap T^{-n+1} I_{i_n};\ I_{i_j} \in \mathcal{P}\}.$$

It follows that T^n is piecewise expanding on $\mathcal{P}^n$ if T is piecewise expanding on $\mathcal{P}$.

2.2.2 Example. *The doubling map* $T : [0,1] \to [0,1]$ *given by* $Tx = 2x \mod 1$*. Figure 2.2 shows the graph of the doubling map.*

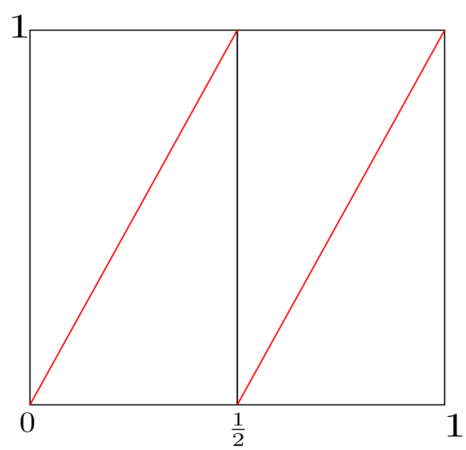

Figure 2.2: Doubling map

2.2.3 Theorem. *Let $T \in \mathcal{T}(I)$. Then it admits an absolutely continuous invariant measure whose density is of bounded variation.*

Consider two complex Banch spaces $(\mathcal{X}, |||\cdot|||)$ and $(\mathcal{L}, \|\cdot\|)$ with $\mathcal{X} \subset \mathcal{L}$. A linear operator $\mathrm{P} : \mathcal{X} \to \mathcal{X}$ is bounded with respect to both $|||\cdot|||$ and $\|\cdot\|_{\mathcal{X}}$, where

$$\|\mathrm{P}\|_{\mathcal{X}} = \sup\left\{\frac{\|\mathrm{P}\, f\|}{\|f\|_{\mathcal{X}}}, f \in \mathcal{X}, f \neq 0\right\}.$$

Assume that

1) If $f_n \in \mathcal{X}$, $f \in \mathcal{L}$, $\lim_{n\to\infty} \|f_n - f\| = 0$, and $|||f_n||| \leq C$ for all n, then $f \in \mathcal{X}$ and $|||f||| \leq C$;
2) $H = \sup_{n\geq 0} \|\mathrm{P}^n\|_{\mathcal{X}} < \infty$;
3) There exists $k \geq 1$, $0 < r < 1$, and $R < \infty$ such that for $f \in \mathcal{X}$,
$$\left|\left|\left|\mathrm{P}^k\, f\right|\right|\right| \leq r|||f||| + R\,\|f\|\,; \tag{2.1}$$
4) If $\mathcal{X}_1$ is a bounded subset of $\mathcal{X}$, then the closure of $\mathrm{P}^k\, \mathcal{X}_1$ is compact in $\mathcal{L}$.

For any complex number η, let

$$D(\eta) = \{f \in \mathcal{X};\ \mathrm{P}\, f = \eta f, f \neq 0 \text{ a.e}\},$$

that is: η is an eigenvalue of P if and only if $D(\eta) \neq \emptyset$.

We state the Ionescu-Tulcea and Marinescu Theorem:

2.2.4 Theorem. *Under conditions* $1) - 4)$*, the intersection of the spectrum of* P *with the unit circle is a set* G *of eigenvalues of* P *of modulus* 1 *which has only a finite number of elements. For each* $\eta \in G$*,* $D(\eta)$ *is finite-dimensional. Furthermore, there exist bounded linear operators* Q_η *and* S *on* $\mathcal{X}$ *such that*

$$\mathrm{P}^n = \sum_{\eta\in G} \eta^n\, \mathrm{Q}_\eta + \mathrm{S}^n, \tag{2.2}$$

$$\mathrm{Q}_\eta\, \mathrm{Q}_{\eta'} = 0 \ \textit{if}\ \eta \neq \eta',\ \mathrm{Q}_\eta^2 = \mathrm{Q}_\eta, \tag{2.3}$$

$$Q_\eta \, S = S \, Q_\eta = 0, \tag{2.4}$$

$$Q_\eta \, \mathcal{X} = D(\eta), \tag{2.5}$$

$$\rho(S) < 1, \tag{2.6}$$

where $\rho(\mathrm{S}) = \lim_{n\to\infty} \|\mathrm{S}^n\|^{\frac{1}{n}}$ *is the spectral radius of* S.

The properties (2.3) – (2.7) of P constitute one of equivalent definitions of a **quasi-compact operator**.

The following Theorem (a generalization of Theorem 2.2.4) is a sufficient criterion for quasi–compactness. For the proof please consult [29].

2.2.5 Theorem. *[29] Suppose* $(\mathcal{L}, |||\cdot|||)$ *is a Banach space and* $\mathrm{P} : \mathcal{L} \to \mathcal{L}$ *is a bounded linear operator with spectral radius* $\rho(\mathrm{P})$. *Assume that there exist a (semi)norm* $\|\cdot\|$ *with the following properties:*

1.- ***Continuity****.* $\|\cdot\|$ *is continuous in* $\mathcal{L}$*; that is,* $\|\cdot\| \leq |||\cdot|||$.

2.- ***Pre-compactness****. For any sequence* $f_n \in \mathcal{L}$*, if* $\sup_n |||f_n||| < \infty$ *then there exist a subsequence* $(n_k)_{k\in\mathbb{N}}$ *and* $f \in \mathcal{L}$ *such that* $\|\mathrm{P}\, f_{n_k} - f\| \to 0$ *as* $k \to \infty$.

3.- ***Boundness****. There is* $M > 0$ *such that* $\|\mathrm{P}\, f\| \leq M \,\|f\|$ *for every* $f \in \mathcal{L}$.

4.- ***Doeblin-Fortet inequality****. There are* $k \geq 1$, $0 < r < \rho(\mathrm{P})$ *and* $R > 0$ *such that*

$$\left|\left|\left|\mathrm{P}^k\, f\right|\right|\right| \leq r^k |||f||| + R\, \|f\| \,.$$

Then $\mathrm{P} : \mathcal{L} \to \mathcal{L}$ *is quasi-compact.*

We shall use Theorem 2.2.5 in the following setting: $\mathcal{L} = \mathrm{BV}(I)$, $|||\cdot||| = \|\cdot\|_{\mathrm{BV}}$, $\|\cdot\| = \|\cdot\|_1$ and $\mathrm{P} = \mathrm{P}_T$ is the Frobenius-Perron operator. Since we know that the Frobenius-Perron operetor P_T is $\|\cdot\|_1$ –continuous, then we have the Boundness property. We also know that $\|\cdot\|_1 \leq \|\cdot\|_{\mathrm{BV}}$; that is, the continuity property is fufilled. The pre-compactness propertie is equivalent to prove that the unit closed ball in $\mathrm{BV}(I)$ is relatively compact in $\mathrm{L}^1(\lambda)$

which follows form Proposition 2.1.7. Finally, the Doeblin-Fortet inequality follows from Lemma 2.2.6 bellow and its proof can be found in [15].

2.2.6 Lemma. *Let $T \in \mathcal{T}(I)$. Then there exists constants $0 < r < 1$, $C > 0$ and $R > 0$ such that for any $f \in \mathrm{BV}(I)$ and any $n \geq 1$,*

$$\|\mathrm{P}_T^n f\|_{\mathrm{BV}} \leq Cr^n \|f\|_{\mathrm{BV}} + R \|f\|_1 .$$

All together gives us the next Theorem.

2.2.7 Theorem. *Let $T \in \mathcal{T}(I)$. Then the Frobenius-Perron operator P_T is quasi-compact on the space $\mathrm{BV}(I)$. In particular,*

1) *T has a finite number of ergodic absolutely continuous invariant measures: $\mu_1 = f_1\lambda, \cdots, \mu_n = f_n\lambda$, where $f_1, \cdots, f_n \in \mathrm{BV}(I)$.*

2) *For each $1 \leq i \leq n$, there exists a finite collection of disjoint sets $\{A_j^{(i)}\}_{j=1}^{n(i)}$ such that $\sup \mu_i = \bigcup_{k=1}^{n(i)} A_k^{(i)}$, and such that for $f_j^{(i)} = f_i \mathbb{1}_{A_j^{(i)}}$, $j = 1, 2, \cdots, n(i)$,*

$$\mathrm{P}_T\, f_j^{(i)} = f_{j+1}^{(i)},$$

   and the dynamical system $(A_j^{(i)}, T^{n(i)}, f_j^{(i)}\lambda)$ is exact.

Now we state a Theorem which connects our ergodic concepts like mixing and erodicity with the Frobenius-Perron operator. For a proof of the Theorem see [15]. Let $\mathcal{D}((X, \mathcal{A}, \mu))$ denote the space of probability density functions on the measure space $(X, \mathcal{A}, \mu)$

2.2.8 Theorem. *[15] Let $T : (I, \mathcal{A}, \mu) \to (I, \mathcal{A}, \mu)$ be a measure preserving system. Let $\mathsf{1}$ denote the constant function equal to 1 everywhere. Then,*

1) *T is ergodic if and only if for any $f \in \mathcal{D}((I, \mathcal{A}, \mu))$*

$$\frac{1}{n}\sum_{k=0}^{n-1} \mathrm{P}_T^n f \to \mathsf{1},$$

   weakly in $\mathrm{L}^1(\mu)$ as $n \to \infty$;

2) *T is weakly mixing if and only if for any $f \in \mathcal{D}((I, \mathcal{A}, \mu))$*

$$\frac{1}{n}\sum_{k=0}^{n-1} |\,\mathrm{P}_T^n f - \mathsf{1}| \to 0,$$

weakly in $\mathrm{L}^1(\mu)$ *as* $n \to \infty$*;*

3) T is mixing if and only if for any $f \in \mathcal{D}((I, \mathcal{A}, \mu))$

$$\mathrm{P}_T^n f \to 1,$$

weakly in $\mathrm{L}^1(\mu)$ *as* $n \to \infty$*;*

4) T is exact if and only if for any $f \in \mathcal{D}((I, \mathcal{A}, \mu))$

$$\mathrm{P}_T^n f \to 1,$$

in the $\mathrm{L}^1(\mu)$*-norm as* $n \to \infty$*.*

Chapter 3

Lorenz flow

In this chapter we introduce what is probably the most famous system of all chaotic differential equations, the Lorenz system from meteorology. It was first formulated by Edward N. Lorenz in 1963 [35], as he was attempting to set up a system of differential equations that could explain some of the unpredictable weather behaviour. As a result, he obtained a simplified model of atmospheric convection. Convection occurs when a fluid located near the surface is heated faster than the cold fluid located higher. As a consequence of this irregular heating, the warmer fluid rises above the cooler one that sinks since it is heavier. This creates a large circular flow of fluid or air which rises as it gets warmer and descends as it is cooled down. Convection also occurs on smaller scales, for example in cups of hot coffee.

More exactly, Lorenz studied a two-dimensional fluid cell that was cooled from above and heated from below. The systems that can describe the motion of the fluid is a system of differential equations with infinitely many variables. Lorenz makes the assumption that all but three of these variables remained constant. Roughly speaking, these independent variables estimate the distortion of the vertical temperature profile from its equilibrium, the difference in temperature between ascending and descending fluid elements (z and y, respectively) and the rate of the circulatory fluid flow velocity (x, clockwise if $x > 0$). The analysed motion leads to a three-dimensional system of differential equations that involves three parameters: the Rayleigh number r, the Prandtl number σ, and a parameter b which relates the physical size of the system. By making all these simplifications, the system of differential equations presents only two nonlinear terms and is given by:

$$\begin{aligned} \dot{x} &= \sigma(y-x) \\ \dot{y} &= rx - y - xz \ . \\ \dot{z} &= xy - bz \end{aligned} \tag{3.1}$$

All three parameters are assumed to be positive and $\sigma > b+1$. We will denote the vector field generated by this system as $\mathrm{L}(x,y,z)$.

3.1 The Lorenz flow in a nutshell

In this section we will give an analysis of the Lorenz flow and its most prominent properties. For a more detailed analysis and proof of the following results the reader is encourage to check for example [3], [31] or [10].

Clearly, the Lorenz system exhibits a symmetry. If we perform the reflection $(x,y,z) \to (-x,-y,z)$, then the equations are unchanged. Thus, if $(x(t),y(t),z(t))$ is a solution then so is $(-x(t),-y(t),z(t))$. When $x=0$ and $y=0$, we have that $\dot{x}=0$, $\dot{y}=0$ and $\dot{z}=-bz$. Therefore, the $z-$axis is invariant. Thus, on the $z-$axis all solutions tend to the origin. As a matter of fact, when $r<1$ the solution through any point in $\mathbb{R}^3$ tends to the origin.

The equilibria are the origin $\bar{0}=(0,0,0)$ (which does not depend on the parameters) and $p_{\pm} = (\pm\sqrt{b(r-1)}, \pm\sqrt{b(r-1)}, r-1)$. A simple calculation shows that

$$D\,\mathrm{L} = \begin{pmatrix} -\sigma & \sigma & 0 \\ r-z & -1 & -x \\ y & x & -b \end{pmatrix}. \tag{3.2}$$

The eigenvalues of $D_{\bar{0}}\,\mathrm{L}$ are $\lambda_1 = -b$ and $\lambda_{\pm} = \frac{1}{2}(-(\sigma+1) \pm$
$\pm \sqrt{(\sigma+1)^2 - 4\sigma(1-r)})$. Observe that $\lambda_{\pm}$ are negative for $0 \leq r < 1$ making the origin a sink. With the help of the Lyapunov function

$$\mathcal{L}(x,y,z) = \frac{1}{2}(x^2 + \sigma y^2 + \sigma z^2) \tag{3.3}$$

we can see the global asymptotic stability of the origin. Moreover, we have the following proposition (the proof can be found in [31] page 307-324).

3.1.1 Proposition. *[31] Suppose $r < 1$. Then all solutions of the Lorenz system tend to the origin.*

As r increases through 1, the eigenvalue λ_+ becomes positive and thus the origin becomes a saddle point with 2−dimensional stable surface and 1−dimensional unstable curve. When $r = 1$ the new two equilibria $p_\pm$ are born and giving a pitchfork bifurcation they move away from the origin as r increases. In [31] the following property of the new equilibria is proven.

3.1.2 Proposition. *[31] The equilibrium $p_\pm$ are sinks provided*

$$1 < r < r_H = \sigma\Big(\frac{\sigma + b + 3}{\sigma - b - 1}\Big). \tag{3.4}$$

A Hopf bifurcation occurs when $r = r_H$. We remark that when $r > 1$, not all solutions tend to the origin, but solutions that start far from the origin at least move closer in. To be precise, if we consider the modified Lyapunov function

$$\mathcal{V}(x, y, z) = \frac{1}{2}(rx^2 + \sigma y^2 + \sigma(z - 2r)^2) \tag{3.5}$$

and the ellipsoid centered at $(0, 0, 2r)$

$$E_v = \{(x, y, z) \in \mathbb{R}^3 \mid \mathcal{V}(x, y, z) = v, v > 0\},$$

the following holds:

3.1.3 Proposition. *[31] There exists v_1 such that any solution starting outside E_{v_1} eventually enters the ellipsoid and remains trapped there for all future time.*

Consequently, if we denote as Λ the set of points whose solutions remain in the ellipsoid for all backward and forward time. Then the $\omega-$limit set of any solution must lie in Λ. In theory, Λ could be a big set. However, if we take a look at the divergence of the vector field we notice that is negative as Equation 3.6 shows.

$$\mathrm{Div}(\mathrm{L}) = \nabla \cdot \mathrm{L} = \sum_{i=1}^{3} \frac{\partial\, \mathrm{L}_i}{\partial x_i} = \mathrm{Trace}(D\,\mathrm{L}) = -(\sigma + 1 + b). \tag{3.6}$$

Since the divergence measures the rate of change of volumes under the flow L^t of the vector field L. Let B be a region with smooth boundary and write $B(t) = \mathrm{L}^t(B)$, the image of the region under the flow at time t and let $V(t)$ denote the volume of $B(t)$. Then Liouville's Theorem gives

$$\dot{V}(t) = \int_{B(t)} \mathrm{Div}(\mathrm{L})\; dx\; dy\; dz, \tag{3.7}$$

which means $\dot{V}(t) = -(\sigma + 1 + b)V(t)$ and thus by solving the differential equation we get that $V(t) = \mathrm{e}^{-(\sigma+1+b)}\, V(0)$. From this we see that volumes shrink exponentially fast to 0. Therefore, we can conclude that the volume of Λ is zero.

3.2 The Lorenz Attractor

The behaviour of the Lorenz system as r increases is of great interest since it exhibits many interesting dynamical behaviours. Although the Lorenz system has physical relevance only for values of r near to 1, we will describe the dynamics for values bigger than 1. In this section we will fix $\sigma = 10$ and $b = \frac{8}{3}$ and describe the dynamics when varying r, but always taking $r > 1$.

The equilibria of the system for this fixed values are the origin $\bar{0}$ and $p_{\pm} = (\pm(\frac{8(r-1)}{3})^{\frac{1}{2}}, \pm(\frac{8(r-1)}{3})^{\frac{1}{2}}, r-1)$. As shown in the previous section, the eigenvalues of $D_{\bar{0}}\,\mathrm{L}$ are all real two negative and one positive. We have

$$\begin{aligned}
\lambda_u &= -\frac{11}{2} + \frac{(121 + 40(r-1))^{\frac{1}{2}}}{2} \\
\lambda_{ss} &= -\frac{11}{2} - \frac{(121 + 40(r-1))^{\frac{1}{2}}}{2} \\
\lambda_s &= -\frac{8}{3}.
\end{aligned}$$

Note that $0 < -\lambda_s < \lambda_u < -\lambda_{ss}$. Any singularity with eigenvalues satisfying the above condition will be called **Lorenz-like singularity**

As observed earlier, the unstable manifold of the origin $W^u(\bar{0})^{\pm}$ is 1-dimensional and has two branches (we use the symbol $\pm$ to denote the branches of the unstable manifold). By the symmetry of the system discussed before, the two branches are related to one another. When r takes small values, the positive branch $W^u(\bar{0})^+$ remains on one side of the stable manifold $W^s(\bar{0})$ and goes to p_+ (See Figure 3.1). By symmetry, the negative branch behaves in a similar way and moving to p_-.

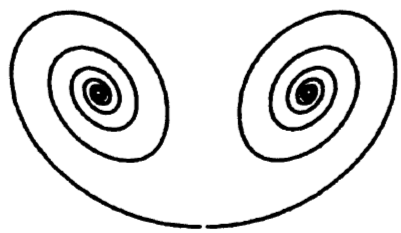

Figure 3.1: Unstable manifold of the origin for $1 < r < r_0$ (Image taken from [40]).

When r takes the value $r_0 \approx 13.93$, the unstable manifold of the origin connects with the stable manifold of the origin and giving birth to a homoclinic loop, $W^u(\bar{0}) \subset W^s(\bar{0})$ as shown in Figure 3.2.

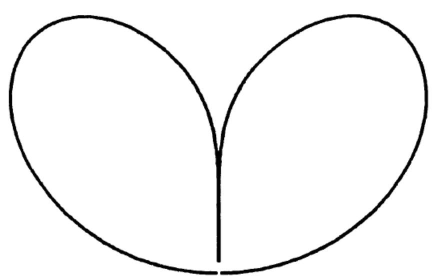

Figure 3.2: Unstable manifold of the origin forming an homoclinic loop when $r = r_0$ (Image taken from [40]).

For $r > r_0$ each branch of the unstable manifold of the origin $W^u(\bar{0})^{\pm}$ goes from one side of $W^s(\bar{0})$ to the other side (see Figure 3.3).

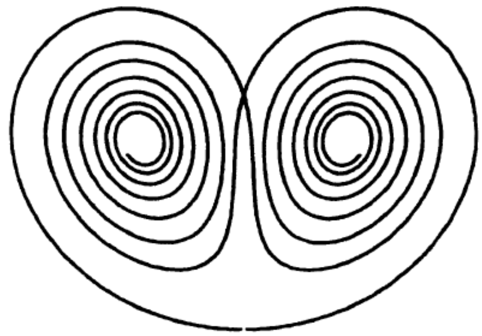

Figure 3.3: Unstable manifold of the origin forming an homoclinic loop when $r_0 < r < r_H$ (Image taken from [40]).

When r is near r_0 we have that $W^u(\bar{0})^+$ drops into $W^s(p_-)$ and $W^u(\bar{0})^-$ into $W^s(p_+)$. For values of r greater than $r_H \approx 24.74$ this is no longer the case and this will be discussed in the following paragraphs.

We will focus now on the behaviour of the equilibria $p_\pm$. We are interested in the stability type of this points. By doing some computations we can see that the characteristic equation for $p_\pm$ is

$$p(\lambda) = \lambda^3 + \frac{41}{3}\lambda^2 + \frac{8}{3}(r+10)\lambda + \frac{160}{3}(r-1) = 0. \tag{3.8}$$

By Proposition 3.1.2, we see that $p_\pm$ are stable for the values $1 < r < r_H$ and they become unstable at r_H. Actually, a Hopf bifurcation takes place when $r = r_H$; it is a subcritical bifurcation where two unstable periodic orbits disappear at r_H. When $r < r_H$, the equilibria $p_\pm$ are sinks, while for $r > r_H$, these equilibria push outward in a 2-dimensional space. Since two of the eigenvalues are complex with positive real part, then the trajectories spiral around in the 2-dimensional surface as they move outward. As a result of the existence of this expanding 2-dimensional subspace the unstable manifold $W^u(\bar{0})^\pm$ is pushed away from $p_\pm$. In fact, when $r = 28$ $W^u(\bar{0})^+$ goes from one side of $W^s(\bar{0})$ to the other and back again as shown in Figure 3.4. Lorenz originally worked with the parameter $r = 28$ and the picture displayed in Figure 3.4 it is what nowadays it is known as the Lorenz attractor. For $r = 28$, the eigenvalues are $\lambda_u \approx 11.83$, $\lambda_{ss} \approx -22.83$, $\lambda_s \approx -2.67$ and $r_H \approx 24.74$

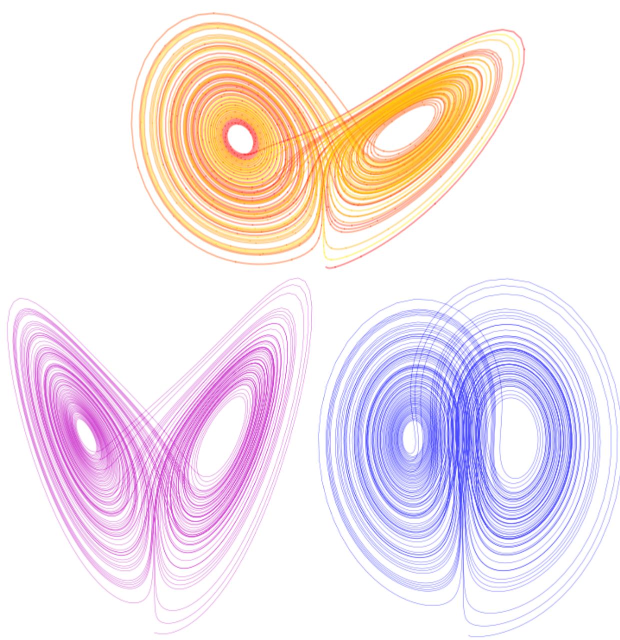

Figure 3.4: Unstable manifold of the origin for $r = 28$. The Lorenz Attractor

Figure 3.5 exhibits the local invariant manifolds and therefore the local dynamics near the equilibria.

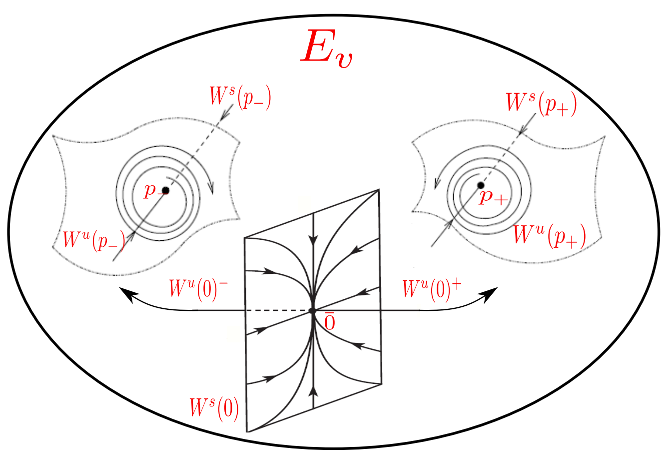

Figure 3.5: Local stable and unstable manifolds near the equilipria $\bar{0}$ and $p_{\pm}$.

As discussed in the previous section, by Proposition 3.1.3 there exists an ellipsoid E_v such that any solution starting outside the ellipsoid eventually enters it and remains trapped there for all future time. Let U be the open region bounded by this ellipsoid, then U is a trapping region for L; that is, $\mathrm{L}^t(U) \subset U$ for all $t > 0$. Note that this trapping region contains only the origin and not the other equilibria. Since $Cl(U)$ is compact, the maximal positively invariant set $\Lambda = \bigcap_{t>0} Cl(\mathrm{L}^t(U))$ is an attracting set where the trajectories of the flow accumulate when t increases. In this way, we define the **Lorenz Attractor** Λ (see Figure 3.4).

3.3 Geometric model for the Lorenz attractor

In this section we will discuss a geometric model for the Lorenz attractor proposed independently by Guckenheimer, Williams [28] and by Afraimovich, Bykov, Shilnikov [1,2]. The reader is also encouraged to check [3,10] and [31] for more details.

By Hartman-Grobman Theorem 1.1.12, the Lorenz system is locally conjugate to the linear system

$$\begin{aligned} \dot{x} &= \lambda_1 x \\ \dot{y} &= -\lambda_2 y \ , \\ \dot{z} &= -\lambda_3 z \end{aligned} \tag{3.9}$$

in a neighbourhood of the origin. Thus, we have that the flow of the linear system is

$$\mathrm{X}^t(x_0, y_0, z_0) = (x_0\, \mathrm{e}^{\lambda_1 t}, y_0\, \mathrm{e}^{\lambda_2 t}, z_0\, \mathrm{e}^{\lambda_3 t}), \tag{3.10}$$

where $(x_0, y_0, z_0) \in \mathbb{R}^3$ is an arbitrary point near to the origin. In order to make computations simpler, we chose $\lambda_1 = \lambda_u = 2$, $\lambda_2 = -\lambda_{ss} = 4$, $\lambda_3 = -\lambda_s = 1$. This eigenvalues are obtained when we take $\sigma = 1$, $r = 9$, and $b = 1$. Note that $0 < \lambda_3 < \lambda_1 < \lambda_2$.

The idea is to follow the solutions as they flow from the time when $z(t)$ is equal to some constant z_1 until $x(t)$ equals to some constant $\pm x_1$. So we consider $\Sigma^* = \{(x, y, 1) \in \mathbb{R}^3 \mid |x| \leq 1, |y| \leq 1\}$,

$$\Sigma^- = \{(x,y,1)\in\Sigma^* \mid x<0\},\quad \Sigma^+ = \{(x,y,1)\in\Sigma^* \mid x>0\},$$

$$\Sigma = \Sigma^+\cup\Sigma^- = \Sigma^*\setminus\Gamma,\ \text{where}\quad \Gamma = \{(x,y,1)\in\Sigma^* \mid x=0,\},$$

$$S^{\pm}\{(\pm1,y,z)\in\mathbb{R}^3\}\ \text{and}\qquad S = S^+\cup S^-.$$

We assume that Σ^* is a section transversal to the flow and every trajectory eventually crosses Σ^* in the direction of the negative axis z. Then for each $(x,y,1)\in\Sigma$, the time τ'_{Lor} such that $\mathrm{X}^{\tau'_{\text{Lor}}}(x,y,1)\in S$ is determined by $\mathrm{e}^{\lambda_1\tau}\,x=\pm1$. Then we have

$$\tau'_{\text{Lor}}(x) = -\frac{1}{\lambda_1}\ln|x|. \tag{3.11}$$

Observe that this time only depends on $x\in\Sigma$ and is such that $\tau(x)\to+\infty$ as $x\to0$. Let $P_1:\Sigma\to S$ be the map given by

$$\begin{aligned} P_1(x,y,1) &= \mathrm{X}^{\tau'_{\text{Lor}}(x)}(x,y,1)\\ &= (1, y(\tau'_{\text{Lor}}), z(\tau'_{\text{Lor}}))\\ &= (1, y|x|^{\beta}, |x|^{\alpha}), \end{aligned}$$

where $\alpha=\frac{\lambda_3}{\lambda_1}$ and $\beta=\frac{\lambda_2}{\lambda_1}$. Note that $0<\alpha<1<\beta$ (In our particular choice of eigenvalues we have that $\alpha=\frac{1}{2}$ and $\beta=2$). We could also forget the constant entry and write P_1 as a function of two variables. Moreover, to avoid to deal later on with a contraction in the $y-$direction, we will just divide by two the x variable to reduce the size of the cusps. The division by 2 is convenient for us because of the particular choice of the eigenvalues we are working with, but dividing by any other positive number also works. Thus, P_1 is given by $P_1(x,y)=(y|\frac{x}{2}|^{\beta},|\frac{x}{2}|^{\alpha})$. Its derivative in the first quadrant is given by

$$D_{(x,y)}P_1 = \begin{pmatrix} \beta2^{-\beta}yx^{\beta-1} & 2^{-\beta}x^{\beta}\\ \alpha2^{-\alpha}x^{\alpha-1} & 0 \end{pmatrix}. \tag{3.12}$$

We make the following observations:

3.3.1 Observation. *1.- $P_1(\Sigma^{\pm})$ has the shape of a cusp at $(\pm 1, 0, 0)$ and (making abuse of notation) we will denote this images as $S^{\pm}$ and $S = S^{+} \cup S^{-}$.*

2.- If we denote by $\ell_v(c) = \{(x, y, 1) \in \Sigma \mid x = c\}$, where c is a constant, the vertical line segments in Σ and by $\ell_h(c) = \{(\pm 1, y, z) \in S \mid z = c\}$, where c is a constant, the horizontal line segments in S. Then we clearly have that $P_1(\ell_v(c_0)) = \ell_h(c_1)$; that is, the map P_1 takes the vertical line segments in Σ to the horizontal line segments in S as illustrated in Figure 3.6.

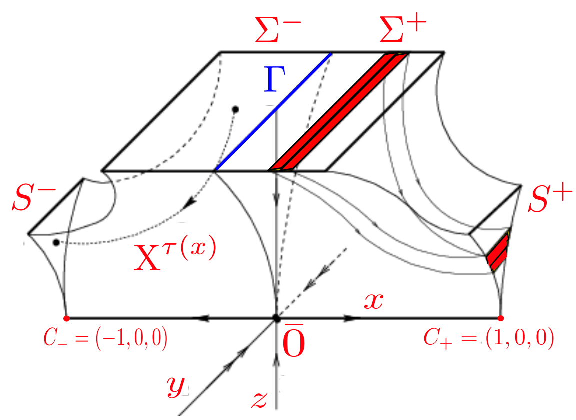

Figure 3.6: Image of Σ under P_1 (Image taken from [10]).

Since we are aiming to construct the (Poincaré map) return map to the cross-section Σ, we have to describe the return of the cusps S back to Σ. In other words, we have to describe the global dynamics; that is, what happens outside the neighbourhood of the origin. We also want the global dynamics to be as close as possible to the dynamics of the Lorenz system. This will be accomplished by composing a suitable rotation R_θ by an angle of θ, an expansion E_a by a factor of a and a translation T. In order to obtain the butterfly shape for the flow, the rotation will be around $W^s(p_{\pm})$ and we will assume that $p_{\pm} = (\pm 1, \mp\frac{1}{2}, 1)$. Therefore, the rotation axis will be the boundaries of the cross-section Σ; that is, the vertical line segments $\ell_v(\pm 1)$ which are parallel to the $y-$axis. Furthermore, we will also assume that the horizontal line segments $\ell_h(c_0)$ are taken into the vertical ones $\ell_v(c_1)$, as depicted in Figure 3.7.

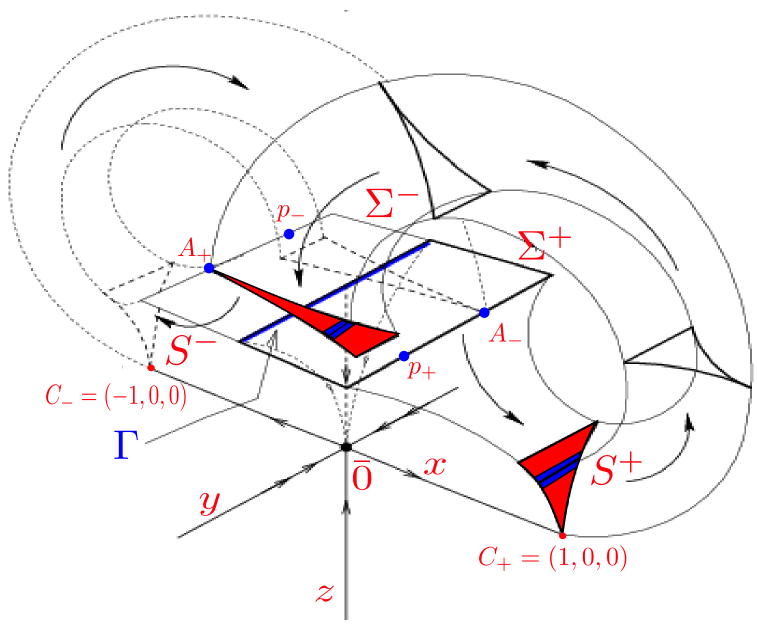

Figure 3.7: Return to Σ under P_2 (Image taken from [10]).

Recall that since the origin is hyperbolic and by the Stable Manifold Theorem (Theorem 1.1.9), the stable $W^s(0)$ and unstable $W^u(0)$ manifolds are well defined. Also note that $W^u(0) \setminus \{0\}$ is made of two connected component which we denote by $W^{\pm u}(0)$ and $W^u(0) = W^{+u}(0) \cup \{0\} \cup W^{-u}(0)$.

The rotation we mentioned above will be a rotation of 270 degrees ($\theta = \frac{3\pi}{2}$) its matrix form is given by

$$R_\theta = \begin{pmatrix} 0 & 0 & 1 \\ 0 & 1 & 0 \\ -1 & 0 & 0 \end{pmatrix}.$$

The expansion occurs only along the $x-$direction, so its matrix is

$$E_a = \begin{pmatrix} a & 0 & 0 \\ 0 & 1 & 0 \\ 0 & 0 & 1 \end{pmatrix},$$

with $a < 2^{\alpha+1} = 2\sqrt{2}$. It is worth noting that this particular bound is good for the case we are dealing with; that is, with the particular choice of eigenvalues that we have and because of the contraction we did in the map P_1 by dividing by 2 the x variable. If this division were done by another quantity this would be reflected in the bound of a.

Finally, the translation T is such that the unstable direction which starts from the origin is sent to the boundary of Σ and the image of both cusps S are disjoint. More precisely, we want to send the cusps points $C_\pm = (\pm 1, 0, 0)$ to $A_\pm = (\mp 1, \mp\frac{1}{2}, 1)$ (see Figure 3.7). Therefore the map $P_2 : S \to \Sigma$ is given by composing the rotation, expansion and translation mentioned above; that is, $P_2 = T \circ E_a \circ R_\theta$. Like in the case of P_1, we can express P_2 as a function of two variables in this case y and z; *i.e.*, $P_2(y, z) = (az \mp 1, y \mp \frac{1}{2})$ the minus/plus sign depends whether we are in S^+ or S^-, respectively. Its derivative is given by

$$D_{(y,z)} P_2 = \begin{pmatrix} 0 & a \\ 1 & 0 \end{pmatrix}. \tag{3.13}$$

The above construction allows us to describe for $t \in \mathbb{R}^+$ the orbit $\mathrm{X}^t(\bar{x})$ of each $\bar{x} \in \Sigma$. The orbit will start flowing with the linear field until $S^\pm$ and then it will follow the returning field back to Σ and so on. We denote by $W = \{\mathrm{X}^t(\bar{x}) \mid \bar{x} \in \Sigma,\ t \in \mathbb{R}^+\}$ the set where the described flow acts. The **geometric Lorenz flow** is the couple (W, X^t_W).

The return map to Σ (the Poincaré map) $P : \Sigma \to \Sigma$ will be $P = P_2 \circ P_1$ and its expression is given by

$$P(x, y) = \begin{cases} \left(a \left| \dfrac{x}{2} \right|^\alpha - 1,\ y \left| \dfrac{x}{2} \right|^\beta - \dfrac{1}{2} \right), & \text{if } x \in (0, 1]; \\ \left(1 - a \left| \dfrac{x}{2} \right|^\alpha,\ \dfrac{1}{2} - y \left| \dfrac{x}{2} \right|^\beta \right), & \text{if } x \in [-1, 0), \end{cases} \tag{3.14}$$

where we take $a = \sqrt{2}$. Its derivative is $DP = DP_2 \cdot DP_1$ and is given by

$$DP = \begin{pmatrix} a\alpha 2^{-\alpha} x^{\alpha-1} & 0 \\ \beta 2^{-\beta} y x^{\beta-1} & 2^{-\beta} x^{\beta} \end{pmatrix}. \tag{3.15}$$

Observe that the first entry of P is a function that just depends on x. This suggests that we can quotient out the stable foliation formed by the vertical line segments $\ell_v(c)$ as we will see later. Figure 3.8 shows the images of $\Sigma\pm$ under the action of P.

Note that for our choice of eigenvalues and the expansion constant $a = \sqrt{2}$ we have the following:

$$P(x,y) = \begin{cases} \left(\sqrt{2}\left|\frac{x}{2}\right|^{\frac{1}{2}} - 1,\ y\left|\frac{x}{2}\right|^{2} - \frac{1}{2}\right), & \text{if } x \in (0,1]; \\ \left(\sqrt{2}\left|\frac{x}{2}\right|^{\frac{1}{2}} + 1,\ y\left|\frac{x}{2}\right|^{2} + \frac{1}{2}\right), & \text{if } x \in [-1,0), \end{cases}$$

and

$$DP = \begin{pmatrix} \dfrac{1}{2\sqrt{x}} & 0 \\ \dfrac{xy}{2} & \dfrac{x^2}{4} \end{pmatrix}. \tag{3.16}$$

The matrix DP has eigenvalues $\lambda_1' = \dfrac{1}{2\sqrt{x}}$ and $\lambda_2' = \dfrac{x^2}{4}$. Observe that $\lambda_1' \to \infty$ as $x \to 0$. More precisely, we have that if $\frac{1}{4} \leq |x| \leq 1$ then $\lambda_1' \leq 1$ and if $|x| < \frac{1}{4}$ then $\lambda_1' > 1$. For the other eigenvalue we have that $\lambda_2' \leq \frac{1}{4}$ for $|x| \leq 1$. Thus we have that the Poincaré map P is hyperbolic when x approaches the origin.

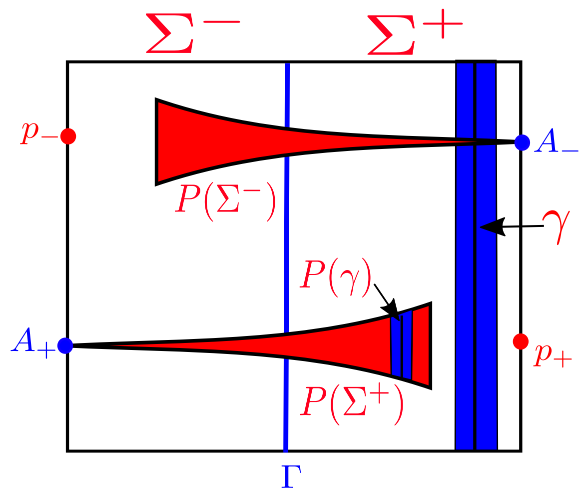

Figure 3.8: The Poncaré map P acting on $\Sigma^{\pm}$.

As we previously mentioned it, the foliation given by the vertical lines $\ell_v(c)$ is invariant under the map P; that is, given any leaf γ of this foliation its image $P(\gamma)$ is contained in a leaf of the same foliation (See Figure 3.8). Therefore, we can express P as $P(x, y) = (f(x), g(x, y))$ for some functions $f : I \setminus \{0\} \to I$ and $g : (I \setminus \{0\}) \times I \to I$, where $I = [-1, 1]$.

Now, to conclude this section we will state without proof some properties of the maps $f(x)$ and $g(x, y)$ and how the dynamics of f determines the dynamics of P. For a more detailed exposition of this properties the reader could check [1], [10], [28], [40] and [31].

First, let us state the properties of $g(x, y)$.

g1.- The map g is piecewise C^2 and for fixed x_0, the map $g(x_0, y)$ is a contraction in the $y-$direction. Meaning

$$d(g(x_0, y_1), g(x_0, y_2)) \leq cd(y_1, y_2),$$

for $0 < c < 1$.

g2.- Equation 3.15 provides the following bound on its partial derivatives:

a) For all $(x, y) \in \Sigma$ with $x > 0$ we have $\partial_y g(x, y) = 2^{-\beta} x^{\beta}$. Since $\beta > 1$ and $|x| \leq 1$, there is $0 < \eta < 1$ such that

$$|\partial_y g(x,y)| < \eta,$$

and the same bound holds for $x < 0$

b) For $(x,y) \in \Sigma$ with $x \neq 0$ we have $\partial_x g(x,y) = \beta 2^{-\beta} y x^{\beta-1}$. Since $\beta - 1 > 0$ and $|y|,\ |x| \leq 1$ we get that $|\partial_x g(x,y)| < \infty$.

g3.- From g2.a) above, the uniform contraction of the foliation given by the vertical lines $\ell_v(c)$ follows; in other words, there is $C > 0$ such that, for any given leaf γ of the foliation and for $y_1,\ y_2 \in \gamma$, then

$$d(P^n(y_1), P^n(y_2)) \leq C\eta^n d(y_1, y_2),$$

when $n \to \infty$.

For $p \in \Sigma$ we denote by $\gamma(p)$ the stable leaf which contains the point p; that is, the vertical line segment $\ell_v(c)$ which contains p. As we have mentioned before, we have that $\gamma(p)$ is taken into another such line segment $\gamma(P(p))$. We make an equivalence class of points in Σ that lie on the same $\gamma(p)$. If we collapse equivalence classes to points, we obtain a map $\pi : \Sigma \to [-1, 1]$ given by $\pi(p) = x$, where $p = (x, y)$. Since P takes equivalence classes into equivalence classes, P and π induces the map $f : I \setminus \{0\} \to I$, whose graph is depicted in Figure 3.9. The map f is called **Lorenz map**. The following properties hold for the Lorenz map:

f1.- The symmetry of the Lorenz equations implies $f(-x) = -f(x)$.

f2.- f has a single discontinuity at $x = 0$ with lateral limits $\lim_{x\to 0^-} f(x) = 1$ and $\lim_{x\to 0^+} f(x) = -1$, since P is not defined at Γ because $\Gamma \subset W^s(\bar{0})$.

f3.- f is differentiable on $I \setminus \{0\}$ and $f'(x) \geq \sigma > 1$.

f4.- The lateral limits of f' at $x = 0$ are $\lim_{x\to 0^-} f'(x) = \infty$ and $\lim_{x\to 0^+} f'(x) = -\infty$.

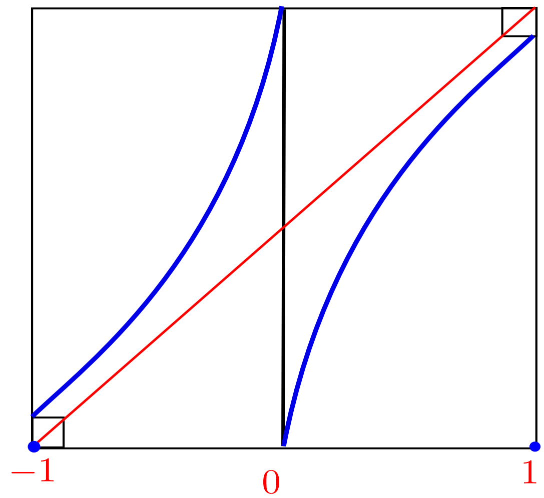

Figure 3.9: The graph of the one dimensional map f.

The proofs of the following statements about the map f can be found in Section 7.11.1 in [40].

3.3.2 Definition. *Let $I \subset \mathbb{R}$ be an interval and $f : I \to I$ be a continuous map. f is called **locally eventually onto** if for any nonempty open interval $K \subset I$, there is an $n > 0$ such that $f^n(K) \supset I$. If f is locally eventually onto, then it is transitive on I.*

3.3.3 Theorem. *[40, Theorem 11.2] Assume that $f : I \setminus \{0\} \to I$ satisfies assumptions f1-f4 given above. Then*

a) Then f is locally eventually onto for the interval $(-1, 1)$,

b) Therefore f is transitive on $(-1, 1)$ and $\Omega(f) = [-1, 1]$.

3.3.4 Theorem. *[40, Theorem 11.3] There is a one to one correspondence between the periodic points of f and the periodic points of P. Let $\Lambda_P = \bigcap_{n \geq 0} P^n(\Sigma)$. Then $\Lambda_P = \Omega(P)$.*

Hence the study of the 3−dimensional flow (W, X_W^t) can be reduced to the study of the 2−dimensional Poincaré map P on Σ and, furthermore, the dynamics of the later can be reduced to a 1−dimensional map f on the interval I, since we have an invariant stable foliation which enables us to identify two points on the same leaf.

3.4 a.c.i.p and decay of correlations for the Lorenz map

All the results presented in this section are given without proof and are taken from the notes of Viana. For a complete presentation and the proofs please refer to [48]. The main tool used in the proofs is the fact that the Frobenius-Perron operator P_f is quasi-compact on the space of functions of bounded variation $\mathrm{BV}(I)$ (Theorem 2.2.7).

In this section, f will denote a map from an interval $I = [a, b]$ to itself. The maps considered in [48] are required to have the following properties:

(C1) **Regularity**. There exists a partition $\mathcal{P} = \{\alpha = (a_{i-1}, a_i) \mid a = a_0 < a_1 < \cdots < a_r = b\}$ such that $f|_{\alpha_i}$ is of class C^1 with $|Df(x)| > 0$ for all $x \in \alpha_i$ and all $i = 1, \ldots, r$. Moreover, the function $g_{\alpha_i} = \dfrac{1}{|Df|_{\alpha_i}|}$ has bounded variation for every i.

Particularly, $f|_{\alpha_i}$ and g_{α_i} admit continuous extensions to $\bar{\alpha}_i = [a_{i-1}, a_i]$. Since the modification on the values of a map over a finite set of points does not alter its statistical properties, we can assume that f is right-continuous or left-continuous (or both) at a_i for any i. We let $\mathcal{P}^1$ be some partition of I into intervals α with $\alpha_i \subset \alpha \subset \bar{\alpha}_i$ for some i and $f|_\alpha$ is continuous. Furthermore, for $m \geq 1$ we let $\mathcal{P}^m$ be the partition of I such that $\mathcal{P}^m(x) = \mathcal{P}^m(y)$ if and only if $\mathcal{P}^1(f^j(x)) = \mathcal{P}^1(f^j(y))$ for every $0 \leq j < m$. For $\alpha \in \mathcal{P}^m$, we denote $g_\alpha^m = \dfrac{1}{|Df^m|_\alpha|}$.

(C2) **Expansivity**. There exist constants $C > 0$ and $0 < \lambda < 1$ such that $\sup g_\alpha^m \leq C\lambda^m$ for every $\alpha \in \mathcal{P}^m$ and every $m \geq 1$.

By Theorem 2.2.7 we know that f admits a finite number of ergodic absolutely continuous invariant measures whose densities have bounded variation. In order to guarantee uniqueness of the absolutely continuous invariant measure as well as the mixing properties we want to study, the following assumption on the expanding map f is required:

(C3) **Topological mixing**. There exists an interval $J \subset I$ such that $f(J) = J$, every orbit $f^n(x)$ eventually goes into J, with $x \in I$, and $f|_J$ is topologically mixing.

3.4.1 Theorem. *[48, Corollary 3.6] If f satisfies conditions (C1)-(C3) then it admits a unique a.c.i.p. $\mu = \varphi m$ with $\varphi \in \mathrm{BV}(I)$, where m denotes the Lebesgue measure. Moreover, μ is ergodic.*

By the properties of the Lorenz map f1-f4 and by Theorem 3.3.3 in the previous section we have that the Lorenz map f fulfils the assumptions (C1)-(C3) above. Thus, by Theorem 3.4.1 we know that f has an ergodic and unique a.c.i.p. $\mu = \varphi m$ with $\varphi \in \mathrm{BV}(I)$.

Proving the decay of correlations requires a main ingredient, namely, showing that the spectrum of the Frobenius-Perron operator ($\mathrm{spec}(\mathrm{P}_f)$) acting on the space of functions of bounded variation $\mathrm{BV}(I)$ can be decomposed

$$\mathrm{spec}(\mathrm{P}_f) = \{1\} \cup \Sigma_0 \ \text{ with } \Sigma_0 \ \text{ contained in a disc of radius } \ \rho < 1.$$

A direct consequence of quasi-compactness is that (f, μ) has exponential decay of correlations, with rate of decay no bigger than ρ. In order to have such decomposition exactness of the measure μ is required. Thus, we have the following result

3.4.2 Proposition. *[48, Proposition 3.13] If f is a piecewise expanding map satisfying (C1)-(C3), then the a.c.i.p. μ is exact, and thus mixing for f.*

Exactness is the last ingredient needed to prove exponential decay of correlations. Hence, we have the following result.

3.4.3 Theorem. *[48, Corollary 3.10] If f is a piecewise expanding map satisfying (C1)-(C3), then f has exponential decay of correlations; that is, given $v \in \mathrm{BV}(I)$ and $w \in \mathrm{L}^1(\mu)$ there are constants $C(v, w) = C > 0$ and $0 < \Theta < 1$ such that*

$$\rho_n(v, w) = \left| \int v \cdot w \circ f^n d\mu - \int v d\mu \int w d\mu \right| \leq C \rho^n \left\| v \right\|_{\mathrm{BV}} \left\| w \right\|_1 .$$

We even have the Central Limit Theorem (CLT):

3.4.4 Theorem. *[48, Corollary 3.11] If f is a piecewise expanding map satisfying (C1)-(C3), then f satisfies CLT; that is, given $v \in \mathrm{BV}(I)$ and $\sigma^2 = \int w^2 d\mu + 2\sum_{j=1}^{\infty} \int w(w \circ f^j) d\mu$, where $w = v - \int v d\mu$. Then σ is well-defined and $\sigma = 0$ if and only if $w = u \circ f - u$ for some $u \in \mathrm{L}^2(\mu)$. If $\sigma > 0$ then for every interval A*

$$\mu(\{x \in I \mid \frac{1}{\sqrt{n}} \sum_{j=0}^{n-1} w(f^j(x)) \in A\}) \to \int_A \frac{1}{\sigma\sqrt{2\pi}} \mathrm{e}^{-\frac{t^2}{2\sigma^2}}\, dt \text{ as } n \to \infty.$$

By Proposition 3.4.2, we know that the a.c.i.p. μ of the Lorenz map f is exact and by Theorem 3.4.3 and Theorem 3.4.4, f has exponential decay of correlations and satisfy CLT.

Chapter 4

Neutralizing the Lorenz origin

In this chapter we will apply local surgery in a neighbourhood of the hyperbolic saddle equilibrium of the geometrical Lorenz model, namely the origin, and transform it into a neutral equilibrium. We will investigate the effects of this change in the dynamics of the model. We do this because we aim to slow down the time that orbits take to flow from the cross-section Σ to the cusps S and see the changes this new motion produces in the decay of correlations. The flow obtained from this modification will be an almost Anosov flow. Existence of a finite or infinite SRB measure for two dimensional almost Anosov diffeomorphisms was already proven in [32,33]. A recent paper of Hu and Zhang [34] provides polynomial mixing rates in the finite measure setting with bounds on the exponent within a parameter range. To obtain such rates they made use of the existence of a Markov partition, quotient dynamics by factoring out the stable direction, a first return inducing scheme and renewal theory. Later, Bruin and Terhesiu in [20] proved mixing rates in the infinite SRB measure setting for almost Anosov diffeomorphism using different methods. They used anisotropic Banach spaces of distributions where the transfer operator of the induced map acts and established the required spectral properties to obtain optimal rates of mixing. Furthermore, they gave more precise tail estimates for the inducing scheme. We will take advantage of these methods and results and use them to deduce the rates of mixing of the almost Anosov flow we will construct. Before jumping directly to the local surgery of the geometrical Lorenz model, we will first describe the framework we will use.

4.1 The Framework

4.1.1 Notation. *Through this Chapter we use the same notation of [17] and write* $a_n = O(b_n)$ *or* $a_n \ll b_n$ *if there is a constant* $C > 0$ *such that* $a_n \leq Cb_n$ *for all* $n \geq 1$*, and* $a_n \sim b_n$ *if* $\lim_{n\to\infty} \frac{a_n}{b_n} = 1$.

We will begin with the set-up of [17], [20] and [21], where the starting point is an almost Anosov flow $\phi^t : M \times \mathbb{R} \to M$ on a closed 3-dimensional differentiable manifold M (recall Definition 1.2.5), in this setting we will just consider a single neutral periodic orbit $\Gamma \simeq \{(0,0,0)\}$, near to this orbit the flow has the following form in local Euclidean coordinates; that is, in a neighbourhood U of the orbit Γ the flow has the form:

$$\begin{pmatrix} \dot{x} \\ \dot{y} \\ \dot{z} \end{pmatrix} = F \begin{pmatrix} x \\ y \\ z \end{pmatrix} = \begin{pmatrix} x(a_0x^2 + a_1y^2 + a_2z^2) \\ -\ell y \\ -z(b_0x^2 + b_1y^2 + b_2z^2) \end{pmatrix} + \mathcal{O}(4), \tag{4.1}$$

where the parameters satisfy $a_0, a_1, a_2, b_0, b_1, b_2 \geq 0$ with $\Delta := a_2b_0 - a_0b_2 \neq 0$, $\ell > 0$ and $a_1^2 < 4a_0a_2$, $b_1^2 < 4b_0b_2$. The latter condition implies the first component in (4.1) is non-negative and the 2nd non-positive for $x,\ z \geq 0$, $\mathcal{O}(4)$ refers to terms of order four or higher, under the condition that they are of the form $x^2\mathcal{O}(2)$ near the yz-plane and $z^2\mathcal{O}(2)$ near the xy-plane. The vector field is cubic in the transversal direction to Γ, but this is the only source of non-hyperbolicity.

Note that the divergence $\mathrm{Div}(F) = (3a_0 - b_0)x^2 + (a_1 - b_1)y^2 + (a_2 - 3b_2)z^2 - \ell$. Since we are aiming for a flow that shrinks volumes exponentially fast, like the Lorenz flow, we need that $\mathrm{Div}(F) = -c < 0$, where c is a positive constant. Then by Liouville's theorem, we will have that $\frac{dV}{dt} = \int_{D(t)} \mathrm{Div}(F)dxdydz$, where $D(t)$ is a region in the Euclidean space. Therefore, $V(t) = \mathrm{e}^{-ct}V(0)$ which means that the flow shrinks volumes exponentially fast. In order to achieve that, we let ℓ be big enough such that $(3a_0 - b_0)x^2 + (a_1 - b_1)y^2 + (a_2 - 3b_2)z^2 < \ell$ for all x, y and z in U.

A quick computation shows that

$$DF|_{\bar{0}} = \begin{pmatrix} 0 & 0 & 0 \\ 0 & -\ell & 0 \\ 0 & 0 & 0 \end{pmatrix},$$

where $\bar{0} = (0,0,0)$. $DF|_{\bar{0}}$ has eigenvalues $\lambda_{1,3} = 0$, $\lambda_2 = -\ell$ with associated eigenvectors $(1,0,0)$, $(0,1,0)$ and $(0,0,1)$.

If we solve for y in Equation (4.1); *i.e.*, $y(t) = y_0 \, \mathrm{e}^{-\ell t}$ we obtain the following non autonomous system of differential equations:

$$\begin{pmatrix} \dot{x} \\ \dot{z} \end{pmatrix} = F_{hor} \begin{pmatrix} x \\ z \end{pmatrix} = \begin{pmatrix} x(a_0 x^2 + \bar{a}_1 \, \mathrm{e}^{-2\ell t} + a_2 z^2) \\ -z(b_0 x^2 + \bar{b}_1 \, \mathrm{e}^{-2\ell t} + b_2 z^2) \end{pmatrix} + \mathcal{O}(4), \tag{4.2}$$

where $\bar{a}_1 = a_1 y_0^2 = \bar{b}_1 = b_1 y_0^2$, $\bar{0}$ is the fixed point of F_{hor}. An easy computation shows that

$$DF_{hor}|_{\bar{0}} = \begin{pmatrix} \bar{a}_1 \, \mathrm{e}^{-2\ell t} & 0 \\ 0 & -\bar{a}_1 \, \mathrm{e}^{-2\ell t} \end{pmatrix},$$

thus $\bar{0}$ is a hyperbolic saddle fixed point for negative values of t. When t tends to infinity then the fixed point changes to a neutral fixed point nature since $\mathrm{e}^{-2\ell t}$ goes to zero or for values large enough of ℓ the fixed point is neutral.

We will assume that ℓ is large enough that the time-1 map f_{hor} of the flow ϕ^t_{hor} of F_{hor} is a smooth almost Anosov map with a single neutral fixed point $p = (0,0)$. Since f_{hor} is an almost Anosov map (a local perturbation of an Anosov diffeomorphism on $\mathbb{T}^2$) we can suppose there exists a Markov partition $\{P_i\}_{i=0}^k$ for f_{hor} and assume p is in the interior of P_0. The vertical and horizontal axes are the stable and unstable manifolds of p respectively. We also make the assumption that the element $P_0 \subset U$ is a small rectangle such that $Cl(f_{hor}^{-1}(P_0) \cup P_0 \cup f_{hor}(P_0)) \subset U$, where U is the neighbourhood mentioned at the beginning of this section. Due to the symmetry $(x,z) \to (\pm x, \pm z)$, we only need to do the analysis in the first quadrant $Q = [0, x_0] \times [0, z_0]$ of P_0 (Figure 4.1). Without loss of generality (consult [20] Lemma 2.1) we can regard $[0, x_0] \times \{z_0\}$ as a local unstable leaf and $\{x_0\} \times [0, z_0]$ as a local stable leaf of the global diffeomorphism.

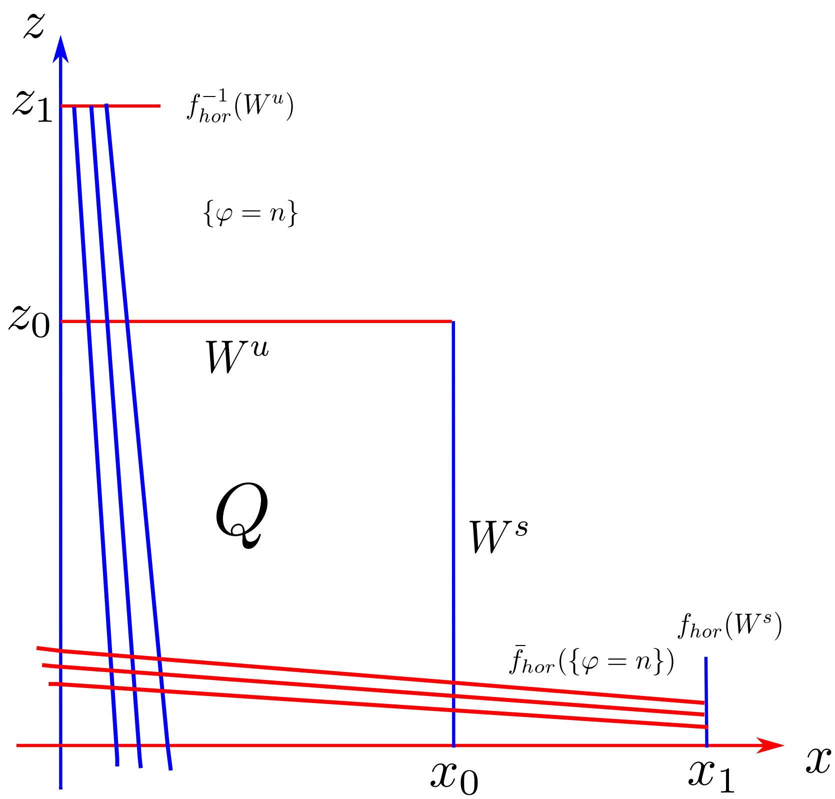

Figure 4.1: First quadrant Q, with stable and unstable foliations.

We consider an induced map $\bar{f}_{hor} = f_{hor}^{\varphi} : Y \to Y$ for $Y = \mathbb{T}^2 \setminus P_0$, where $\varphi(z) = \min\{n \geq 1 \mid f_{hor}^n(z) \notin P_0\}$ is the first return time to Y. We notice that $\bar{f}_{hor}$ is invertible because f_{hor} is. In the first quadrant of $U \setminus P_0$, $\{\varphi = n\} = \{z \in f_{hor}^{-1}(Q) \setminus Q \mid \varphi(z) = n\}$, $n \geq 2$, are vertical stripes adjacent to the local unstable leaf $[0, x_0] \times \{z_0\}$ and converging to $\{0\} \times [z_0, z_1]$ as $n \to \infty$. The images $\bar{f}_{hor}(\{\varphi = n\})$ are horizontal stripes adjacent to the local stable leaf $\{x_0\} \times [0, z_0]$ and converging to $[x_0, x_1] \times \{0\}$ as $n \to \infty$, see Figure 4.1.

Contrary to f_{hor}, the induced map $\bar{f}_{hor}$ is uniformly hyperbolic, but only piecewise continuous. Indeed, the continuity does not hold at the boundaries of the stripes $\{\varphi = n\}$, $n \geq 2$ ($\bar{f}_{hor}$ is undefined on $W^s(p)$), but these boundaries are local unstable and stable leaves, and it is possible to create a countable Markov partition $\{P_i\}_{i=1}^k$ of Y for $\bar{f}_{hor}$ where all $\{\varphi = n\}$ are partition elements.

The function $\bar{f}_{hor}$ preserves an SRB-measure μ (see [33, Lemma 5.2]).

The goal is to give estimates of the tails since they will give us the speed of the decay of correlations.

$$\mu(\varphi > n) = \mu(\{z \in f_{hor}^{-1}(Q) \setminus Q \mid \varphi(z) > n\}). \tag{4.3}$$

4.2 Estimates of $\mu(\varphi > n)$

We will start by considering the system given by Equation 4.2 without the $\mathcal{O}(4)$ terms and we also let the exponential terms be absorbed by $\mathcal{O}(4)$; *i.e.*, we consider

$$\begin{pmatrix} \dot{x} \\ \dot{z} \end{pmatrix} = F_{hor} \begin{pmatrix} x \\ z \end{pmatrix} = \begin{pmatrix} x(a_0x^2 + a_2z^2) \\ -z(b_0x^2 + b_2z^2) \end{pmatrix}, \tag{4.4}$$

where the parameters a_0, a_2, b_0 and b_2 satisfies the same restrictions as before. The approach we will take closely follows [17], [20] and [21]. Let $u, v \in \mathbb{R}$ the solutions of of the linear system

$$\left\{ \begin{array}{l} (u+2)a_0 = vb_0 \\ (v+2)b_2 = ua_2, \end{array} \right. \text{ that is : } \left\{ \begin{array}{l} u = \dfrac{2b_2c_0}{\Delta} \\ v = \dfrac{2a_0c_2}{\Delta}, \end{array} \right. \tag{4.5}$$

where $c_i = a_i + b_i$ for $i \in \{0, 2\}$.

Let $f_{hor}^{-1}(0, z_0) = (0, z_1)$. Given $q = (x, z) \in f_{hor}^{-1}(Q)$; that is; $z \in [z_0, z_1]$ and $0 < x < x_0$, we define the **exit time** $t(x, z)$ by

$$f_{hor}^{t(x,z)}(q) = f_{hor}^{t(x,z)}(x, z) = (x_0, \omega(z, t)) \in \partial Q, \tag{4.6}$$

see Figure 4.2. For fixed z, by inverting this relation we obtain the asymptotic behaviour of $x(z, t)$ and $\omega(z, t)$ as $t \to \infty$, because for integer values $t = n$ and $t = n - 1$, the curves $z \longmapsto x(z, t)$ parametrise the vertical boundaries of the strips $\{\varphi = n\}$.

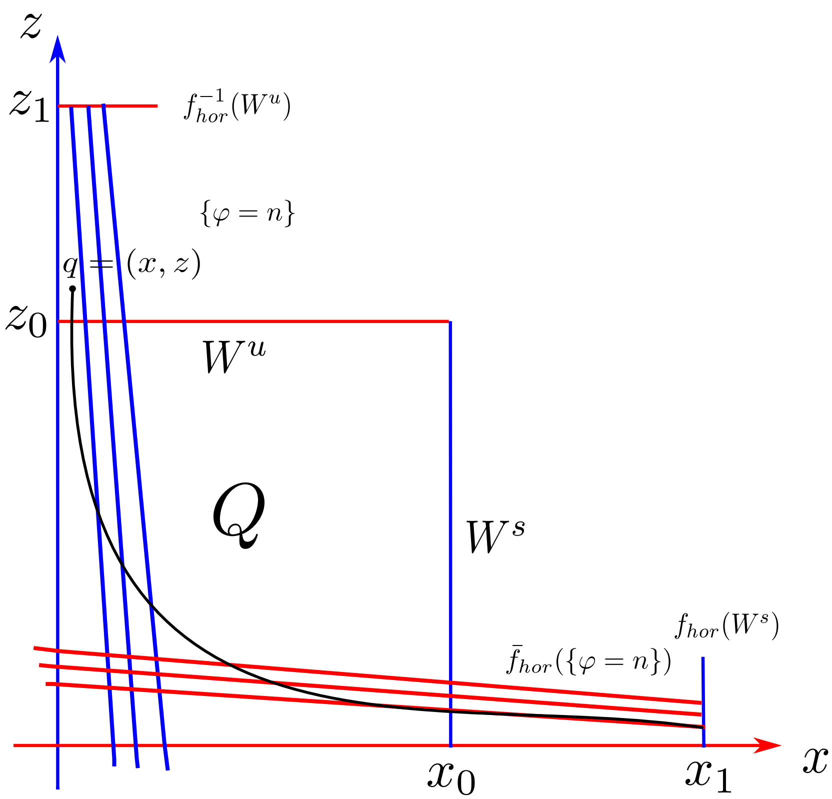

Figure 4.2: The exit time of a point $q = (x, z) \in f_{hor}^{-1}(Q)$.

For the vector field in Equation (4.4), we want to give accurate estimates for $x(z, t)$ and $\omega(z, t)$. In the choice of coordinates that we are taking $\{x_0\} \times [0, z_0]$ is a local stable leaf and thus also the curves $W_T := (x(z, t), z)$ are local stable leaves, since $f_{hor}^t(W_T) \subset \{1\} \times [0, z_0]$.

The next proposition gives a first integral for Equation (4.4) and its proof can be found in [17] or [20].

4.2.1 Proposition. *The function*

$$I(x, z) = \begin{cases} x^u z^u (\frac{a_0}{v} x^2 + \frac{b_2}{u} z^2), & \text{if } \Delta > 0; \\ \\ x^{-u} z^{-u} (\frac{a_0}{v} x^2 + \frac{b_2}{u} z^2)^{-1} & \text{if } \Delta < 0; \end{cases}$$

is a first integral of (4.4).

Bruin in [17] and [20] provides us with the following results concerning the estimates for the tails of $\mu(\varphi > n)$ and the Dulac map, where the Dulac map is the transition map from a transverse section at its stable separatrix $W^s(x_0, 0)$ to a transverse section at its unstable separatrix $W^u(0, y_0)$; that is, the Dulac map $D : W^u(0, y_0) \to W^s(x_0, 0)$ $p = D(q)$, shown in Figure 4.3, assigns the firs intersection $\phi^T(x, y_0)$ of the integral curve through (x, y_0) with the stable leaf $W^s(x_0, 0)$, where $x \in W^u(0, y_0)$ and T is the flow time; that is, the exit time (see Equation (4.6)).

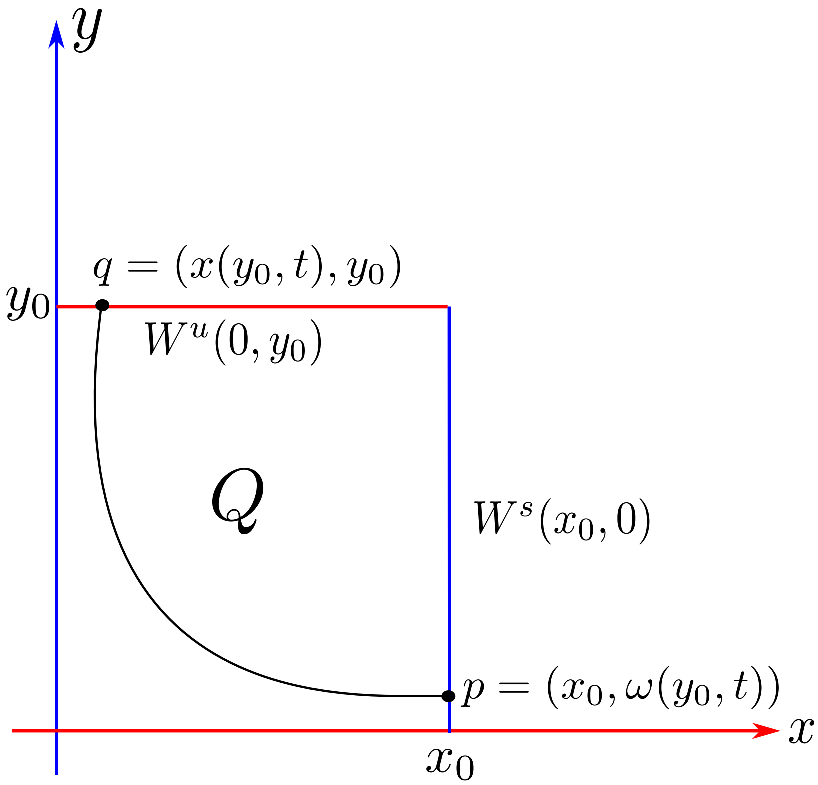

Figure 4.3: The Dulac map $D : W^u(0, y_0) \to W^s(x_0, 0)$.

4.2.2 Theorem. *Consider a C^3 vector field of local form 4.4 with parameters satisfying the same restrictions as before. Define $\beta_0 = \frac{a_0+b_0}{2a_0}$ and $\beta_2 = \frac{a_2+b_2}{2b_2}$. Then $x(z, t)$ and $\omega(z, t)$ are regularly varying of order β_2 and β_0, respectively. In order words, there are functions $\xi_0(z)$ and $\omega_0(z)$ independent of t such that*

$$x(z,t) = \xi_0(z)t^{-\beta_2}(1 + \mathcal{O}(t^{-2\beta_2}))$$

and

$$\omega(z,t) = \omega_0(z)t^{-\beta_0}(1 + \mathcal{O}(t^{-2\beta_0})).$$

Moreover, the Dulac map $D : W^u(0,z) \to W^s(x_0,0)$ *has the form:*

$$\omega = D(x) = \omega_0(z)\xi_0(z)^{-\frac{\beta_0}{\beta_2}} x^{\frac{\beta_0}{\beta_2}}(1 + \mathcal{O}(x^{\frac{1}{2\beta_2}})),$$

as $x \to 0$.

4.2.3 Theorem. *Let* $\beta^* = \frac{1}{2}\min\{1, \frac{a_2}{b_2}, \frac{b_0}{a_0}\}$, *then there exist* $C_0 > 0$ *constant such that* $\mu(\varphi > n) = \mu(\{z \in f_{hor}^{-1}(Q)\backslash Q \mid \varphi(z) > n\}) = C_0 n^{-\beta_2}(1+\mathcal{O}(n^{-\beta^*}))$.

4.3 The Poincaré map revisited

In Section 3.3 we studied the Lorenz geometrical model and constructed the return (Poincaré) map P to the cross-section Σ. The construction of the map P was given by considering two maps P_1 and P_2. The former describes the local dynamics in a neighbourhood of the origin by flowing points in Σ through the linearised Lorenz flow and the later gives the global dynamics conformed by a rotation, expansion and translation which takes the cusps S back to Σ.

In this section, we will investigate what happens if instead of considering the linearised Lorenz flow we consider the flow obtained from Equation (4.1).

Note that Equation (4.2) is non-autonomous and it was obtained by solving the $y-$component from Equation (4.1). Since the terms involving the time variable t in the x and $z-$component in Equation (4.2) decrease exponentially fast as t increases, we will consider their contribution negligible and put them together with the higher order terms $\mathcal{O}(4)$. We will make use of the estimates of the Dulac map (See Section 4.2).

Let us denote by N^t the flow obtained from Equation (4.1). By Equation (4.6) and the estimates of the Dulac map given in Theorem 4.2.2 we get the following expression:

$$
\begin{aligned}
N^{t(x,z)}(x,y,z) &= (x_0,\ y\,\mathrm{e}^{-\ell t(x,z)},\ z\omega(z,t(x,z))\ ) \\
&= (x_0,\ y\,\mathrm{e}^{-\ell|x|^{-\frac{1}{\beta_2}}},\ |x|^{\frac{\beta_0}{\beta_2}}).
\end{aligned} \tag{4.7}
$$

We will take the same cross-section as in Chapter 3; that is, we will consider

$$
\Sigma^- = \{(x,y,1) \in \Sigma^* \mid x < 0\}, \quad \Sigma^+ = \{(x,y,1) \in \Sigma^* \mid x > 0\},
$$

$$
\Sigma = \Sigma^+ \cup \Sigma^- = \Sigma^* \setminus \Gamma,\ \text{where} \quad \Gamma = \{(x,y,1) \in \Sigma^* \mid x = 0\}.
$$

The last equality in Equation (4.7) holds true because z will be consider as a constant, since we are taking points in Σ. Therefore, the time $t(x,z)$ becomes a function of the variable x and by reversing the estimates in Theorem 4.2.2 we get the result. Hence we consider the map $N : \Sigma \to S$

$$
\begin{aligned}
N(x,y,1) &= \mathrm{N}^{t(x)}(x,y,1) \\
&= \left(1, y\,\mathrm{e}^{-\ell|\frac{x}{2}|^{-\frac{1}{\beta_2}}}, \left|\frac{x}{2}\right|^{\frac{\beta_0}{\beta_2}}\right).
\end{aligned} \tag{4.8}
$$

We can assume that $x_0 = 1$ so we can restrict the local dynamics to the unit cube and like in the case of the map P_1 (See Section 3.3) we divide x by 2 to adjust the hight of the images of Σ under N. Its derivative is given by

$$
D_{(x,y)}N = \begin{pmatrix} \frac{\ell}{\beta_2} 2^{-\frac{1}{\beta_2}} y x^{-(2+\frac{1}{\beta_2})}\,\mathrm{e}^{-\ell(\frac{x}{2})^{-\frac{1}{\beta_2}}} & \mathrm{e}^{-\ell(\frac{x}{2})^{-\frac{1}{\beta_2}}} \\ \frac{\beta_0}{\beta_2} 2^{-\frac{\beta_0}{\beta_2}} x^{\frac{\beta_0}{\beta_2}-1} & 0 \end{pmatrix}. \tag{4.9}
$$

Note that the y component of N can be written as a function of the z component; that is, if we denote the z and y component of N by $\tilde{z}$ and $\tilde{y}$, respectively. Then,

$$
\tilde{y}(\tilde{z}) = \tilde{y}\,\mathrm{e}^{-\ell\tilde{z}^{-\frac{1}{\beta_0}}}\ . \tag{4.10}
$$

We make the following observations:

1.- $N(\Sigma^{\pm})$ has a cusp-like shape, since by Equation (4.10), N maps lines $y = c$ to curves of the form $\tilde{y}(\tilde{z})$. Each of these image curves meets the $xy-$plane perpendicularly at $(1, 0, 0)$. The cusp-like shapes vary as we vary $\frac{1}{2} < \beta_0 < 2$. When we take $1 \leq \ell < 4$ the shapes start to look more like the cusps we obtained from the Lorenz flow as depicted in Figure 4.4, but for $\ell > 4$ we obtain a degenerate case namely, the sides of the cusp collapse to a line. We will denote $N(\Sigma^{\pm})$ by $S^{\pm}$ and $S = S^+ \cup S^-$.

We would also like to remark that what is depicted in Figures 3.6, 3.7 and 3.8 remains true since the only changes are the new map N and the shape of the cusps which now are deformed from the original ones but the descriptions in the images remains true.

2.- Like the map P_1, the map N takes the vertical line segments in Σ to the horizontal line segments in S, where the vertical lines in Σ are given by making the x coordinate constant and the horizontal lines in S by making z constant; *i.e.*, $N(\ell_v(c_0)) = \ell_h(c_1)$ as illustrated in Figure 3.6.

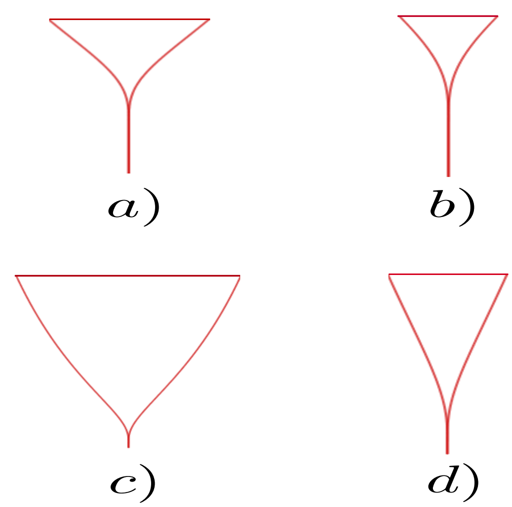

Figure 4.4: Examples of the cusp-like shapes: For a) and b) we have $\beta_0 = \frac{3}{2}$ and $\ell = 1$ and $\ell = 2$, respectively. For c and d we have $\beta_0 = \frac{5}{7}$ and $\ell = 1$ and $\ell = 2$, respectively.

To complete the return to Σ we proceed as in Chapter 3 and use the map P_2 to send the cusp-like shapes back to the cross-section. Therefore this time, the modified return map $P_{\text{Neu}} : \Sigma \to \Sigma$ is given by $P_{\text{Neu}} = P_2 \circ N$; that is,

$$P_{\text{Neu}}(x,y) = \begin{cases} \left(a\left|\dfrac{x}{2}\right|^{\frac{\beta_0}{\beta_2}} - 1,\ y\,\mathrm{e}^{-\ell\left|\frac{x}{2}\right|^{-\frac{1}{\beta_2}}} - \dfrac{1}{2}\right), & \text{if } x \in (0,1]; \\ \left(1 - a\left|\dfrac{x}{2}\right|^{\frac{\beta_0}{\beta_2}},\ y\,\mathrm{e}^{-\ell\left|\frac{x}{2}\right|^{-\frac{1}{\beta_2}}} + \dfrac{1}{2}\right), & \text{if } x \in [-1,0), \end{cases} \tag{4.11}$$

and its derivative is $DP_{\text{Neu}} = DP_2 \cdot DN$ and is given by

$$DP_{\text{Neu}} = \begin{pmatrix} a\frac{\beta_0}{\beta_2}2^{-\frac{\beta_0}{\beta_2}}x^{\frac{\beta_0}{\beta_2}-1} & 0 \\ \frac{\ell}{\beta_2}2^{-\frac{1}{\beta_2}}yx^{-(1+\frac{1}{\beta_2})}\,\mathrm{e}^{-\ell(\frac{x}{2})^{-\frac{1}{\beta_2}}} & \mathrm{e}^{-\ell(\frac{x}{2})^{-\frac{1}{\beta_2}}} \end{pmatrix}. \tag{4.12}$$

The matrix DP_{Neu} has eigenvalues $\lambda_1 = a\frac{\beta_0}{\beta_2}2^{-\frac{\beta_0}{\beta_2}}x^{\frac{\beta_0}{\beta_2}-1}$ and $\lambda_2 = \mathrm{e}^{-\ell(\frac{x}{2})^{-\frac{1}{\beta_2}}}$. Note that if we let $\beta_2 > 2$, then $\dfrac{\beta_0}{\beta_2} < 1$ (since we are taking $\frac{1}{2} < \beta_0 < 2$ in order to have nice cusp shapes) and then we will have that $\lambda_1 \to \infty$ as $x \to 0$. For the other eigenvalue we have that $\lambda_2 < 1$ and $\lambda_2 \to 0$ as x goes to 0 since $\left|\dfrac{x}{2}\right|^{-\frac{1}{\beta_2}} \to \infty$ as x goes to 0. Thus the modified Poincaré map P_{Neu} is hyperbolic when x approaches the origin.

Some properties we saw in Chapter 3 remain true for the modified return map P_{Neu} like the invariance of the stable foliation given by the vertical lines $\ell_v(c)$ under the map P_{Neu}. Therefore, given any leaf γ of this foliation, its image $P_{\text{Neu}}(\gamma)$ is contained in a leaf of the same foliation (See Figure 3.8). Hence, we can express again P_{Neu} as $P_{\text{Neu}}(x,y) = (f_{\text{Neu}}(x), g_{\text{Neu}}(x,y))$ for some functions $f_{\text{Neu}} : I \setminus \{0\} \to I$ and $g_{\text{Neu}} : (I \setminus \{0\}) \times I \to I$, where $I = [-1,1]$.

Let us state the properties of $g_{\text{Neu}}(x,y)$, which are similar to the properties stated in Chapter 3.

g1.- The map g_{Neu} is piecewise C^2 and for fixed x_0, the map $g_{\text{Neu}}(x_0,y)$ is a contraction in the $y-$direction. Meaning

$$d(g_{\text{Neu}}(x_0,y_1), g_{\text{Neu}}(x_0,y_2)) \le cd(y_1,y_2),$$

for $0 < c < 1$.

g2.- Equation (4.12) provides the following bound on its partial derivatives:

a) For all $(x, y) \in \Sigma$ we have $\partial_y g_{\mathrm{Neu}}(x, y) = \mathrm{e}^{-\ell(\frac{x}{2})^{-\frac{1}{\beta_2}}}$. Since $\beta_2 > 2$ and $|x| \leq 1$, there is $0 < \eta < 1$ such that

$$|\partial_y g_{\mathrm{Neu}}(x, y)| < \eta.$$

b) For $(x, y) \in \Sigma$ with $x \neq 0$ we have $\partial_x g_{\mathrm{Neu}}(x, y) = \frac{\ell}{\beta_2} 2^{-\frac{1}{\beta_2}} y x^{-(1+\frac{1}{\beta_2})}$ $\mathrm{e}^{-\ell(\frac{x}{2})^{-\frac{1}{\beta_2}}}$. Since $1 < 1 + \dfrac{1}{\beta_2} < \dfrac{3}{2}$ and $|y|,\ |x| \leq 1$ we get that $|\partial_x g_{\mathrm{Neu}}(x, y)|$ is bounded. In fact, it tends to zero exponentially fast as x approaches the origin.

g3.- From g2.a) above follows the uniform contraction of the foliation given by the vertical lines $\ell_v(c)$; in other words, there is $C > 0$ such that, for any given leaf γ of the foliation and for $y_1,\ y_2 \in \gamma$, we have

$$d(P^n_{\mathrm{Neu}}(y_1), P^n_{\mathrm{Neu}}(y_2)) \leq C\eta^n d(y_1, y_2),$$

when $n \to \infty$.

As before, $\gamma(p)$ denotes the stable leaf which contains the point $p \in \Sigma$ and we make again an equivalence class of points in Σ that lie on the same $\gamma(p)$. If we collapse equivalence classes to points, we obtain a map $\pi : \Sigma \to [-1, 1]$ given by $\pi(p) = x$, where $p = (x, y)$. Since P_{Neu} takes equivalence classes into equivalence classes, P_{Neu} and π induces the map $f : I \setminus \{0\} \to I$, whose graph is depicted in Figure 4.5. The new map f is a slight modification of the Lorenz map f_{Lor} obtained in Chapter 3 and all the properties mentioned there also hold for the new version f. We will fix notation and denote this modification of the Lorenz map by f_{Neu} and is given by:

$$f_{\mathrm{Neu}}(x) = \begin{cases} ax^{\beta} - 1, & \text{if } x \in (0, 1]; \\ \\ 1 - a|x|^{\beta}, & \text{if } x \in [-1, 0), \end{cases} \tag{4.13}$$

where $\beta = \dfrac{\beta_0}{\beta_2} \in (0, 1)$.

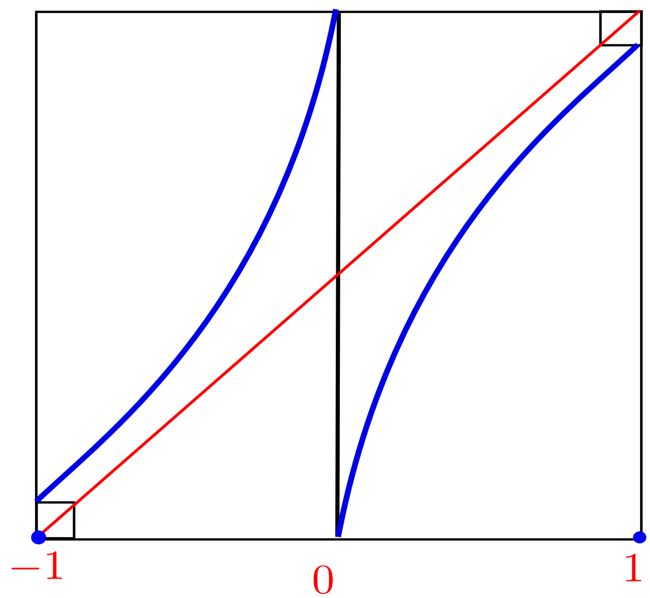

Figure 4.5: The graph of the one dimensional map f_{Neu}.

As we saw in Section 3.4 the one dimensional Lorenz map f_{Lor} admits a unique exact a.c.i.p measure $\mu_{\mathrm{Lor}} = \varphi_{\mathrm{Lor}} m$ with $\varphi_{\mathrm{Lor}} \in \mathrm{BV}(I)$, where m is the Lebesgue measure. Since f_{Neu} has the same properties as f_{Lor}, following the same argumentation stated in Section 3.4 we can deduce that f_{Neu} also admits a unique exact a.c.i.p measure $\mu_{\mathrm{Neu}} = \varphi_{\mathrm{Neu}} m$ with $\varphi_{\mathrm{Neu}} \in \mathrm{BV}(I)$. Furthermore, μ_{Neu} has exponential decay of correlations for observables in $\mathrm{BV}(I)$ and satisfies the CLT by Theorem 3.4.3 and Theorem 3.4.4, respectively.

Chapter 5

Stable foliation

In this chapter we will deal with the stable foliation of the neutral Lorenz flow. In the first section we will recall the construction of the Geometrical Lorenz flow and we will talk about its stable foliation. The main references for this section are the books of Shub [43], Araújo and Pacifico [10] and the work of Araujo *et al.* [7].

5.1 Geometrical Lorenz case

Recall that the Lorenz attractor is given by $\Lambda = \bigcap_{t>0} Cl(\mathrm{L}^t(O))$ (See section 3.2), where O is a trapping region for L; that is, $\mathrm{L}^t(O) \subset O$ for all $t > 0$. In Section 3.3, the construction of the Geometrical model of the Lorenz attractor was given by analysing the dynamics at the origin and then imitating the effect of the pair of saddles in the original Lorenz flow. This was achieved by considering the Poincaré section Σ which is transversal to the flow and the Poincaré map $P_{\mathrm{Lor}} : \Sigma \to \Sigma$, where $\Sigma = \{(x, y, 1) \in \mathbb{R}^3 \mid |x|, |y| < 1 \text{ and } x, y \neq 0\}$. The return map P_{Lor} is decomposed in two parts. The first one of which, denoted by P_1, deals with the local behaviour near the origin and is obtained by considering a linear system in a neighbourhood of the origin, where Σ is also contained, and flowing points in Σ until time τ, where τ is the time it takes a point in Σ to hit a plane S transversal to the $x-$axis under the linearised flow.

More accurately, we considered the flow of the linear system given by the

Equation (3.9); that is,

$$\mathrm{L}^t(x_0, y_0, z_0) = (x_0\, \mathrm{e}^{\lambda_s t}, y_0\, \mathrm{e}^{\lambda_s t}, z_0\, \mathrm{e}^{\lambda_{ss} t}), \tag{5.1}$$

where the inequalities for the eigenvalues λ_u, λ_s and λ_{ss} will be specified later (see Equation (5.7)).

Then for each $(x, y, 1) \in \Sigma$, the time τ_{Lor} such that $\mathrm{L}^{\tau_{\mathrm{Lor}}}(x, y, 1) \in S$ is determined by

$$\tau'_{\mathrm{Lor}}(x) = -\lambda_u^{-1} \ln(|x|) \tag{5.2}$$

and only depends on $x \in \Sigma$. Therefore the Poincaré map has the form $P_1(x, y) = (y|\frac{x}{2}|^\beta, |\frac{x}{2}|^\alpha)$, where $\alpha = \frac{\lambda_{ss}}{\lambda_u}$ and $\beta = \frac{\lambda_s}{\lambda_u}$. Note that $0 < \alpha < 1 < \beta$.

The second one considers the return of points in S to the cross-section Σ and simulates the random turns of a regular orbit around the origin and describes a butterfly-like shape. It is described by an appropriate composition of a rotation, expansion and translation denoted by P_2. Note that P_2 is a diffeomorphism, therefore the hitting time $\tau_2(x)$ from S to Σ is C^ϵ. Thus, if we denote by $r_{\mathrm{Lor}}(x)$ the full return time of the Poincaré map P_{Lor} we notice that

$$r_{\mathrm{Lor}}(x) = \tau'_{\mathrm{Lor}}(x) + \tau_2(x). \tag{5.3}$$

The Poincaré map is given by

$$P_{\mathrm{Lor}}(x) = P_2 \circ P_1(x) = \begin{cases} \left(a|x|^\alpha - 1,\ y|x|^\beta - \dfrac{1}{2}\right), & \text{if } x \in (0, 1]; \\ \left(1 - a|x|^\alpha,\ \dfrac{1}{2} - y|x|^\beta\right), & \text{if } x \in [-1, 0). \end{cases}$$

There we saw that the vertical lines denoted by $\ell_v(c)$ in the cross-section Σ form the stable foliation which is invariant under the return map P_{Lor}; that is, given any leaf γ of this foliation, its image $P_{Lor}(\gamma)$ is contained in a leaf of the same foliation (See Figure 3.8). Thus by quotienting out the stable direction we can rewrite the Poincaré map as a skew-product; that is, $P_{\text{Lor}}(x,y) = (f_{\text{Lor}}(x), g_{\text{Lor}}(x,y))$.

Before stating the results concerning the stable foliation for the Lorenz flow we give first the necessary definitions.

5.1.1 Definition. *Let Λ be a compact invariant set of $X \in \mathfrak{X}^r(M)$, $c > 0$ and $0 < \lambda < 1$. We say that Λ has a $(c,\lambda)-$**dominated splitting** if the bundle $T_\Lambda M$ has a DX_t-invariant splitting of sub-bundles*

$$T_\Lambda M = E^1 \oplus E^2,$$

such that for all $t > 0$ and $x \in \Lambda$, we have

$$\left\| DX_t|_{E^1_x} \right\| \cdot \left\| DX_{-t}|_{E^2_{X_t(x)}} \right\| < c \cdot \lambda^t. \tag{5.4}$$

*We say that Λ is **partially hyperbolic** if it has a $(c,\lambda)-$dominated splitting such that E^1 is uniformly contracting; that is, for some $c > 0$ and all $t > 0$ and every $x \in \Lambda$ it holds*

$$\left\| DX_t|_{E^1_x} \right\| < c \cdot \lambda^t. \tag{5.5}$$

In this case we will denote E^1 by E^s and we will refer to it as the contracting direction. E^2 will be denoted by E^{cu} and refer as the center-unstable direction.

5.1.2 Observation.

1. *If the inequality in Equation* (5.4) *holds we will refer it as Domination of the splitting.*
2. *If the inequality in Equation* (5.5) *holds then the splitting will be refer as uniformly contracting.*

For $x \in \Lambda$ and $t \in \mathbb{R}$, $\mathrm{J}^{cu}_t(x)$ will denote the absolute value of the determinant of $DX_t|_{E^{cu}_x} : E^{cu}_x \to E^{cu}_{X_t(x)}$. We say that E^{cu}_Λ is **area expanding** if for any $x \in \Lambda$ and $t \geq 0$ there are constants $c > 0$ and $0 < \lambda < 1$ such that

$$\mathrm{J}^{cu}_t(x) \geq c \cdot \lambda^{-t}. \tag{5.6}$$

Note that this condition is weaker than the uniform expansion along the central-unstable direction.

5.1.3 Definition. *Let Λ be a compact invariant set of $X \in \mathfrak{X}^r(M)$. We say that Λ is **singular hyperbolic set** for X if all the equilibria of Λ are hyperbolic and Λ is partially hyperbolic with area expanding central direction. If Λ is also an attractor we will say that it is a **singular hyperbolic attractor**.*

The following result due to [7] is a restatement of Theorem IV.1 in [43].

5.1.4 Theorem. *[7, Theorem 6] Let X be a C^2 flow and Λ be a compact X-invariant singular hyperbolic attractor having a dominated splitting*

$$T_\Lambda M = E^s \oplus E^{cu}.$$

There are $\epsilon > 0$ and $0 < \lambda < 1$ such that for any $x \in \Lambda$ there are two embedded disks $W^{ss}_\epsilon(x)$ and $W^{cu}_\epsilon(x)$ tangent to E^s_x and E^{cu}_x at x, respectively, such that for any $t > 0$ the following holds:

1.- Let $d(\cdot,\cdot)$ be the distance induced by the Riemannian metric. $W^{ss}_\epsilon(x)$ is a C^2 embedded disk and is given by

$$W^{ss}_\epsilon(x) = \{y \in M \mid d(X_t(x), X_t(y)) \leq \epsilon \text{ and } \lim_{t\to\infty} \frac{d(X_t(x), X_t(y))}{\lambda^t} = 0\}$$

2.- $X_t(W^{ss}_\epsilon(x)) \subset W^{ss}_\epsilon(X_t(x))$.

3.- The embedding $W^{ss}_\epsilon(x)$ varies continuously on x in the following sense: There is a neighbourhood B of x and a continuous map $\Phi : B \to \mathrm{Emb}^2(\mathbb{I}, M)$ such that $\Phi(x)(0) = x$ and $\Phi(x)(\mathbb{I}) = W^{ss}_\epsilon(x)$, where $\mathrm{Emb}^2(\mathbb{I}, M)$ is the set of embeddings from the unit interval $\mathbb{I}$ to M endowed with the C^2 distance.

4.- $X_t(W^{cu}_\epsilon(x)) \cap B_\epsilon(x) \subset W^{cu}_\epsilon(X_t(x))$, where $B_\epsilon(x)$ is the open ball of radius ϵ centred at x.

5.- The $W^{cu}_\epsilon(x)$ varies continuously on x as in 3. That is, there is a neighbourhood B of x and a continuous map $\Phi : B \to \mathrm{Emb}^2(\mathbb{D}^2, M)$ such that $\Phi(x)(0) = x$ and $\Phi(x)(\mathbb{D}^2) = W^{ss}_\epsilon(x)$, where $\mathbb{D}^2$ is the 2-dimensional unit disk.

We note that, for any $x \in \Lambda$, both $W^{ss}_\epsilon(x)$ and $W^{cu}_\epsilon(x)$ are embedded discs and hence sub-manifolds of M, and we will call them the **local strong-stable** and **local center-unstable** manifold, respectively. We also have that $W^{ss}_\epsilon(x)$ is uniquely determined since E^s is uniformly contracting.

Theorem 5.1.4 provides us with a strong-stable lamination $W^{ss}_\epsilon(x)$ through the points $x \in \Lambda$. The following result due to [7] shows us that the lamination can be extended to an invariant foliation $\mathcal{F}^{ss}(x)$ of a open neighbourhood of Λ with C^2 leaves and whose foliated charts are C^1. Moreover, the leaves are uniformly contracted by the action of the flow. Thus, we have the following result due to [7].

5.1.5 Proposition. *[7, Corollary 6] Let X_t be a C^2 flow. Then for any compact X_t-invariant subset Λ which is partially hyperbolic; that is, the conditions in Equations* (5.4) *and* (5.5) *are satisfied for the continuous DX_t-invariant splitting $T_\Lambda M = E^s \oplus E^{cu}$, where E^s is the one-dimensional stable direction, there exists a neighbourhood V of Λ in M where an extension $\mathcal{F}^{ss}(x)$ of the local stable lamination $\{W^{ss}_\epsilon(x)\}_{x\in\Lambda}$ is defined. $\mathcal{F}^{ss}(x)$ is a locally X_t-invariant foliations whose leaves are uniformly contracted by the action of X_t for any $t > 0$. Furthermore, each leaf is a C^2 one-dimensional submanifold of M.*

Now we will see how the stable foliation constructed for the cross-section Σ, mentioned at the beginning of this section (see Section 3.3 for a full definition), relates to the contracting foliation of the flow. We can assume that Σ, that is, a C^2 embedded compact disk transverse to the flow L_t at every point $x \in \Sigma$, is contained in the open neighbourhood V of Λ where the contracting foliation $\mathcal{F}^{ss}$ which extends the strong-stable lamination through every point of Λ is defined.

In this way, for $x \in \Sigma$ we define $W^{ss}(x, \Sigma)$ to be the connected component of $\mathcal{F}^{sc}(x) \cap \Sigma$, where $\mathcal{F}^{sc}(x) = \bigcup_{t\in\mathbb{R}} L_t(\mathcal{F}^{ss}(x))$ is the center-stable leaf. Since the flow $(L_t)_{t\in\mathbb{R}}$ is C^2, $W^{ss}(x, \Sigma)$ is a C^2 one-dimensional embedded curve for every $x \in \Sigma$ and their leaves form a C^1 foliation $\mathcal{F}^{ss}_\Sigma$ of Σ.

Given a pair of embedded disks D_1 and D_2 in Σ intersecting transversally a set $\{W^{ss}(x, \Sigma)\}_{x\in\Sigma}$ of stable leafs, the **holonomy map** $H : D_1 \cap W^{ss}(x, \Sigma) \to D_2 \cap W^{ss}(x, \Sigma)$ assigns to $y \in D_1 \cap W^{ss}(x, \Sigma)$ the unique point in $h(y) \in D_2 \cap W^{ss}(x, \Sigma)$, see Figure 5.1.

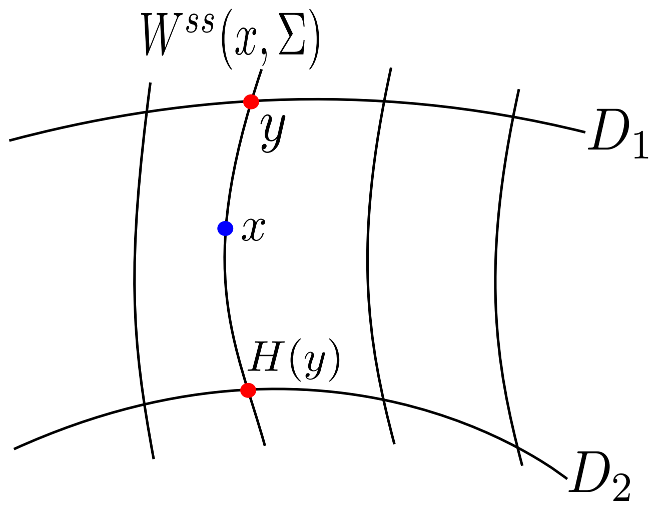

Figure 5.1: The holonomy map.

From the developments in the partially hyperbolic theory by Brin-Pesin [16] and Pugh-Shub [39] we have that the projection along leaves, also known as holonomies, between pair of transverse surfaces to $\mathcal{F}^{ss}$ have a Hölder Jacobian with respect to Lebesgue measure. This implies a similar conclusion for the holonomies transverse to $\mathcal{F}^{cs}$. It follows that the holonomy between pairs of transverse curves to $\mathcal{F}^{ss}_{\Sigma}$ along the lines of $\mathcal{F}^{ss}_{\Sigma}$ can be thought as interval maps having a Hölder Jacobian. Hence these holonomies are $C^{1+\alpha}$ for some $0 < \alpha < 1$. In this setting, the leaves $W^s s(x, \Sigma)$, with $x \in \Sigma$, determine a foliation $\mathcal{F}^{ss}_{\Sigma}$ of Σ with transversal smoothness $C^{1+\alpha}$.

Therefore, given a cross-section Σ we can assume that Σ is the image of the unit square $I \times I$ under the action of a $C^{1+\alpha}$ diffeomorphism h, for some $0 < \alpha < 1$. Furthermore, h sends vertical lines inside the leaves of $\mathcal{F}^{ss}_{\Sigma}$.

In the construction of the geometrical model given in Section 3.3 we saw that we have three eigenvalues satisfying

$$\lambda_{ss} < \lambda_s < 0 < -\lambda_s < \lambda_u < -\lambda_{ss}, \tag{5.7}$$

which corresponds to the stable, unstable and strong stable directions. Figure 3.6 shows how the linear flow (Equation (3.10)) preserves lines in the y-direction when we flow points from Σ to S. Thus, its derivative DX_t preserves planes which are orthogonal to the $y-$axis.

Furthermore, by the way the flow from S to Σ was constructed (Figure 3.7) we notice that horizontal lines in S; that is, parallel to the $y-$axis, are taken to parallel lines to the same axis in Σ. In other words, the flow from S to Σ preserves parallel lines to the $y-$axis. Since this flow is a composition of rotation, expansion and translation we can deduce that the derivative of the flow also preserves planes orthogonal to the $y-$axis. From this we can deduce that the splitting $\mathbb{R}^3 = E \oplus F$, where $E = \{0\} \times \mathbb{R} \times \{0\}$ and $F = \mathbb{R} \times \{0\} \times \mathbb{R}$, is preserved by the flow; *i.e.*, $DX_t(E) = E$ and $DX_t(F) = F$ for any t.

We observe that $\|DX_t|_{E_x}\| \leq \mathrm{e}^{\lambda_{ss} t}$ and since $\lambda_{ss} < 0$ it follows that E is uniformly contracting, and it will be called stable direction. Notice also that

$$\|DX_t|_{E_x}\| \cdot \left\| DX_{-t}|_{F_{X_t(x)}} \right\| \leq \mathrm{e}^{\lambda_{ss} - \lambda_s t} .$$

Since $\lambda_{ss} - \lambda_s < 0$ we see that the contraction along the F direction is weaker than the one along the E direction. This is true for any point $x \in \Lambda$. Since domination of the splitting and uniform contraction are satisfied (See Definition 5.1.1) we can conclude that Λ is partially hyperbolic. Furthermore, since $\mathrm{J}_t^{cu}(x) = \mathrm{e}^{(\lambda_u + \lambda_s)t}$ then the flow expands area along the F direction and hence Λ is a singular hyperbolic attractor (See Definition 5.1.3). The existence of the strong-stable $W^{ss}(x)$ and center-unstable $W^{cu}(x)$ manifolds and the strong-stable foliation $\mathcal{F}^{ss}(x)$ follows from Theorem 5.1.4 and Proposition 5.1.5, respectively. Furthermore, the strong stable foliation $\mathcal{F}^{ss}(x)$ is C^1.

The next step is to prove that the strong stable foliation $\mathcal{F}^{ss}(x)$ is not only C^1 but also $C^{1+\alpha}$, for some $0 < \alpha < 1$. This is done in the work of Araújo, Melbourne and Varandas [9], stated as Lemma 2.2. This result is a consequence of domination of the splitting (Equation 5.4), uniform contraction along the stable direction (Equation 5.5) and strong dissipativity (Definition 5.1.6 below).

5.1.6 Definition. *Let G be a C^∞ vector field on $\mathbb{R}^3$ with a Lorenz-like equilibrium; that is, the eigenvalues of DG_p are real and satisfy the inequalities in Equation 5.7. We say that G is* ***strongly dissipative*** *if the divergence of the vector field G is strictly negative; that is, there is $c > 0$ such that* $\mathrm{Div}(G)(x) \leq -c$ *for any x and the eigenvalues of the singularity at p satisfy the constraint*

$$\lambda_u + \lambda_{ss} < \lambda_s. \tag{5.8}$$

The usual parameter choice of the Lorenz model ($\lambda_{ss} \approx -22.83$, $\lambda_s = -\frac{8}{3}$ and $\lambda_u \approx 11.83$) and also the particular choice of eigenvalues taken for the construction of the geometrical model in Section 3.3 ($\lambda_{ss} = -4$, $\lambda_s = -1$ and $\lambda_u = 2$) satisfy the strong dissipative condition. In fact, from Section 3.1 we know that $\lambda_s = -b$, $\lambda_{ss} = \frac{1}{2}(-(\sigma+1) - \sqrt{(\sigma+1)^2 - 4\sigma(1-r)})$ and $\lambda_u = \frac{1}{2}(-(\sigma+1) + \sqrt{(\sigma+1)^2 - 4\sigma(1-r)})$. Therefore Equation (5.8) holds true if

$$-(\sigma+1) < -b. \tag{5.9}$$

In this way, we have shown that the strong stable foliation $\mathcal{F}^{ss}(x)$ of the geometrical Lorenz flow is $C^{1+\alpha}$.

5.2 Neutral geometrical Lorenz case

In this section we will study the properties of the strong stable foliation $\mathcal{F}^{ss}$ for the neutralized geometrical Lorenz model we built in Section 4.3. Let us first recall the construction of the model.

For the modified geometrical model of the Lorenz attractor, denoted by Λ_{N}, we consider the Lorenz attractor Λ as we did in previous section, but in an open neighbourhood U of the origin instead of considering the linearised vector field (Equation (3.9)) we consider the vector field given by Equation (4.1). More precisely, we take an open neighbourhood U in which the cross-section Σ, constructed for the geometrical Lorenz Model (see Section 3.3), is contained. Then the flow we consider from Σ to S has the form;

$$\begin{aligned} N(x,y,1) &= \mathrm{N}^{\tau_{\mathrm{Neu}}(x)}(x,y,1) \\ &= \left(1, y\,\mathrm{e}^{-\ell\left|\frac{x}{2}\right|^{-\frac{1}{\beta_2}}}, \left|\frac{x}{2}\right|^{\frac{\beta_0}{\beta_2}}\right). \end{aligned}$$

This modification yields to a different flow time form the cross-section Σ to S, in the original construction we had a logarithmic time (see Equation (5.2)): for the new flow we have a polynomial time

$$\tau'_{\mathrm{Neu}}(x) = |x|^{-\frac{1}{\beta_2}}. \tag{5.10}$$

Nevertheless, the rest of the construction remains unchanged; that is, the flow constructed from S to Σ made by a composition of expansion, rotation and translation. Therefore we have the same hitting time $\tau_2(x)$ and thus the full return time for the modified Poincaré map P_{Neu} is given by

$$r_{\mathrm{Neu}}(x) = \tau'_{\mathrm{Neu}}(x) + \tau_2(x). \tag{5.11}$$

The neutralized Poincaré map $P_{\mathrm{Neu}} : \Sigma \to \Sigma$ is given by

$$P_{\mathrm{Neu}}(x,y) = \begin{cases} \left(a|x|^{\frac{\beta_0}{\beta_2}} - 1,\ y\,\mathrm{e}^{-\ell|x|^{-\frac{1}{\beta_2}}} - \dfrac{1}{2}\right), & \text{if } x \in (0,1]; \\ \left(a|x|^{\frac{\beta_0}{\beta_2}} + 1,\ y\,\mathrm{e}^{-\ell|x|^{-\frac{1}{\beta_2}}} + \dfrac{1}{2}\right), & \text{if } x \in [-1,0). \end{cases} \tag{5.12}$$

Despite the slight modification done in the construction of the geometrical Lorenz model, the new return map $P_{\mathrm{Neu}} : \Sigma \to \Sigma$ preserves the same stable foliation as before; *i.e.*, the foliation conformed by the vertical lines $\ell_v(c)$ in the cross-section Σ thus what is shown in Figure 3.8 remains true. Once again by quotienting out the stable direction we can rewrite the modified Poincaré map as a skew-product; that is, $P_{\mathrm{Neu}}(x,y) = (f_{\mathrm{Neu}}(x), g_{\mathrm{Neu}}(x,y))$ where f_{Neu} behaves in the same manner as f_{Lor}.

We want to proceed as in the previous case. Notice that for any point x in $U \setminus \{\bar{0}\}$, where $\bar{0}$ denotes the origin, the eigenvalues of $DF|_x$ (where F is the vector field in Equation (4.1)) behave in the same fashion as the ones of the Lorenz vector field; that is, we have the situation of Equation (5.7). The origin is the only point where we have $\lambda_{ss} = -\ell$, $\lambda_s = 0$ and $\lambda_u = 0$. Nevertheless, we can still consider the same splitting as before; *i.e.*, $\mathbb{R}^3 = E \oplus F$, where $E = \{0\} \times \mathbb{R} \times \{0\}$ and $F = \mathbb{R} \times \{0\} \times \mathbb{R}$, once again this splitting is preserved by the flow ($DN_t(E) = E$ and $DN_t(F) = F$ for any t, where N_t is the flow obtained from Equation 4.1). Since we have uniform contraction along E ($\|DX_t|_{E_x}\| \leq \mathrm{e}^{\lambda_{ss}t}$ with $\lambda_{ss} = -\ell < 0$ for every $x \in U$) and domination of the splitting ($\|DX_t|_{E_x}\| \cdot \left\|DX_{-t}|_{F_{X_t(x)}}\right\| \leq \mathrm{e}^{\lambda_{ss}-\lambda_s t}$ with $\lambda_{ss} - \lambda_s < 0$ for every $x \in U$) we can conclude that U is partially hyperbolic.

It is worth noticing that the origin is the only point that spoils the singular hyperbolicity condition since $J_t^{cu}(\bar{0}) = \mathrm{e}^{(\lambda_u+\lambda_s)t} = 1$ (recall $\lambda_s = 0 = \lambda_u$); that is, we do not possess the area expansion along the subbundle F. Hence, Λ_N is a partially hyperbolic attractor.

The existence of the strong-stable $W^{ss}(x)$ and center unstable $W^{cu}(x)$ manifolds and the strong-stable foliation $\mathcal{F}^{ss}(x)$ follows from the same argument as in the previous case for every $x \in U \setminus \{\bar{0}\}$. The situation for the origin is slightly different, since the splitting of the tangent bundle is given by a one dimensional strong-stable direction E^s and a two dimensional center direction E^c. However, we are only concerned about the existence of the strong-stable manifold $W^{ss}(\bar{0})$, which follows from the theory of partial hyperbolicity (see [38] or [24]); that is, the part concerning $W^{ss}(x)$ in Theorem 5.1.4 can be restated by considering a compact partially hyperbolic invariant set instead of a singular hyperbolic set. Therefore, using the same argumentation as in previous paragraphs, we get a C^1 strong-stable foliation $\mathcal{F}^{ss}(x)$ for the flow and strong-stable foliation $\mathcal{F}^{ss}_{\Sigma}$ for the modified return map whose transversal smoothness is $C^{1+\alpha}$, with $0 < \alpha < 1$. Furthermore, Equation (5.8) remains true for the origin since we have $-\ell = \lambda_{ss} + \lambda_u < \lambda_s = 0$, hence strong dissipativity holds true. Therefore, we can conclude as before that the strong-stable foliation $\mathcal{F}^{ss}(x)$ is $C^{1+\alpha}$, for some $0 < \alpha < 1$.

Chapter 6

Uniformly nonintegrability condition (UNI)

The main goal of this chapter is to show that the stable and unstable manifolds of the modified geometrical model are jointly nonintegrable. From the work of Araújo, Butterley and Varandas [6], we know that the joint nonintegrability of the stable and unstable manifolds is equivalent to the uniformly nonintegrability condition. Therefore, in this chapter we will aim to prove the UNI condition.

In [5] and [9] Araújo *et al.* prove the UNI condition by exploiting the properties obtained by using hyperbolic times. Therefore, in the first section we will give all the relevant definitions and properties concerning hyperbolic times. In the second section, we will see without proof that the geometrical Lorenz flow satisfies the UNI condition by following the work of Araújo, Melbourne and Varandas [9] and the work of Araújo and Melbourne [8]. Finally, the third section will be devoted to prove the UNI condition for the modified geometrical Lorenz flow.

6.1 Hyperbolic times

In this section, we will give the concept of hyperbolic times that we will use in the next sections. We start by giving the definition of an exceptional set. Throughout this section $f : M \to M$ will denote a continuous map defined on a compact Riemannian manifold M with induced distance d and a normalized Riemannian volume form m which we call Lebesgue measure.

The map f is assumed to be a local diffeomorphism in M except for a compact submanifold $S \subset M$ satisfying some non-degeneracy conditions.

6.1.1 Definition. *$S \subset M$ will be called* ***non-degenerate exceptional set*** *for the map f if the following holds:*

1.- f behaves like a power of the distance to S; that is, there are constants $C > 1$ and $\beta > 0$ such that for any $x \in M \setminus S$ and any $v \in T_x M$

$$C^{-1} d(x,S)^{\beta} \leq \frac{\|Df(x)v\|}{\|v\|} \leq C d(x,S)^{-\beta}.$$

Furthermore, for every $x, y \in M \setminus S$ with $d(x,y) < \frac{d(x,S)}{2}$

2.-

$$\left|\log \left\|Df(x)^{-1}\right\| - \log \left\|Df(y)^{-1}\right\|\right| \leq \frac{C}{d(x,S)^{\beta}} d(x,y)$$

3.-

$$|\log|\det Df(x)| - \log|\det Df(y)|| \leq \frac{C}{d(x,S)^{\beta}} d(x,y)$$

The set S can be formed by critical points of the map f or points where f is not differentiable. The next definition make use of the **δ-truncated distance** from x to S given by

$$d_{\delta}(x,S) = \begin{cases} d(x,S), & \text{if } d(x,S) \leq \delta \\ 1, & \text{otherwise.} \end{cases} \tag{6.1}$$

6.1.2 Definition. *We take β as in the previous definition and fix $c > 0$ such that $c < \min\{\frac{1}{2}, \frac{1}{4\beta}\}$. Given $0 < \sigma < 1$ and $\delta > 0$, we say that n is a (σ, δ)-**hyperbolic time** for $x \in M$ if for any $1 \leq k \leq n$,*

$$\prod_{j=n-k}^{n-1} \left\|Df(f^j(x))^{-1}\right\| \leq \sigma^k \quad \text{and} \qquad d_{\delta}(f^{n-k}(x), S) \geq \sigma^{ck}. \tag{6.2}$$

6.1.3 Observation. *Condition 6.2 in Definition 6.1.2 implies the dynamical property*

$$\left\| Df^k(f^{n-k}(x))^{-1} \right\| \leq \sigma^k \quad \textit{for} \quad 1 \leq k \leq n, \tag{6.3}$$

which means that at any intermediate time k we have exponential stretching by iteration of the map f.

The following Lemma gives us some bounds for the distortion when using hyperbolic times.

6.1.4 Lemma. *[5, Lemma 4.1] Given $0 < \sigma < 1$ and $\delta > 0$, there exist δ_1, c_1 and $\kappa > 0$, which depend only on σ, δ and f such that if for any $x \in M$ and $n \geq 1$ a (σ, δ)-hyperbolic time for x, then there exist a neighbourhood $V(x)$ for which*

1.- f^n maps $V(x)$ diffeomorphically onto the ball $B_{\delta_1}(f^n(x))$.

2.- For $1 \leq k \leq n$ and $y, z \in V(x)$,

$$d(f^{n-k}(y), f^{n-k}(z)) \leq \sigma^k d(f^n(y), f^n(z)).$$

3.- For all $y, z \in V(x)$,

$$\left| \frac{\det Df^n(y)}{\det Df^n(z)} - 1 \right| \leq c_1 d(f^n(y), f^n(z)).$$

4.- $V(x) \subset B_{\kappa^n}(x)$.

6.2 UNI condition for the geometrical Lorenz model

Let $I = [-1, 1]$ and $f_{\text{Lor}} : I \to I$ be the one-dimensional Lorenz map obtained from the geometrical model (see Section 3.3). We notice that the set $\{0\}$ is an nondegenerate exceptional set for f_{Lor}. The next Theorem will give us the existence of an induce uniformly expanding Markov map and it can be found in [5].

6.2.1 Theorem. *[5, Theorem 4.3] There exist a neighbourhood $\tilde{X} = (-a, a) \subset I$ of the singularity 0, for some $0 < a < 1$, a countable Lebesgue modulo zero partition $\tilde{\mathfrak{Q}}$ of $\tilde{X}$ into subintervals, a function $\tau : \tilde{X} \to \mathbb{Z}^+$ constant on elements of $\tilde{\mathfrak{Q}}$, and constants $c > 0$, $\kappa > 1$ such that for any $\tilde{Q} \in \tilde{\mathfrak{Q}}$ and $\tau = \tau(\tilde{Q})$, the map $\tilde{F} = f_{\text{Lor}}^{\tau} : \tilde{Q} \to \tilde{X}$ is a C^2 uniformly expanding diffeomorphism with bounded distortion; that is, for every x, $y \in \tilde{Q}$*

$$\left| \frac{D\tilde{F}(x)}{D\tilde{F}(y)} - 1 \right| \leq c|\tilde{F}(x) - \tilde{F}(y)| \quad \textit{and} \qquad |\tilde{F}(x) - \tilde{F}(y)| > \kappa|x - y|.$$

Moreover, for every $\tilde{Q} \in \tilde{\mathfrak{Q}}$ there is $0 < k \leq N$ such that $n = \tau(\tilde{Q}) - k$ is a (σ, δ)-hyperbolic time for each $x \in \tilde{Q} \subset V(x)$ and $f^j(\tilde{Q}) \subset I \setminus \tilde{X}$ for any $n \leq j \leq \tau(\tilde{Q})$.

We make now some observations regarding the induce map $\tilde{F}$ obtained from the previous Theorem.

6.2.2 Observation. *The map $\tilde{F}$ is obtained by inducing f_{Lor} on the interval $\tilde{X}$, the inducing time is given by the sum of a hyperbolic time with a non-negative integer bounded by N, where N is such that $\bigcup_{i=1}^{N} (f^i)^{-1}(\{0\})$ is 2δ-dense in $\tilde{X}$. Furthermore, $\tilde{F}$ is a full branch Markov map since 0 has dense preimages under f_{Lor}.*

In addition to the bounded distortion and uniform expansion of $\tilde{F}$, we have the following inequalities for f_{Lor} as a consequence of hyperbolic times. Given $\sigma \in (0, 1)$ and $c > 0$ as in Definition 6.1.2, there is a constant $b > 0$ such that:

1.- (Backward contraction) Let $\tilde{Q}(x)$ denotes the element of the partition $\tilde{\mathfrak{Q}}$ containing x, for $y \in \tilde{Q}(x)$

$$|f_{\text{Lor}}^i(y) - f_{\text{Lor}}^i(x)| \leq b\sigma^{\tau(x)-i}|\tilde{F}(y) - \tilde{F}(x)|, \quad i = 0, \dots, \tau(x) - 1.$$

2.- (Slow recurrence to the singular point)

$$|f_{\text{Lor}}^i(x)| \leq \sigma^{c(\tau(x)-i)}, \quad i = 0, \dots, \tau(y) - 1.$$

Following [9], our next step is to construct a piecewise uniformly hyperbolic map F with infinitely many branches, which covers $\tilde{F}$. First, let $W^{ss}_{P_{\text{Lor}}}(x)$ denote the stable leaf under the Poincaré map P_{Lor} containing the point x

(see Section 5.1), $\pi : \Sigma \to I$ the projection map (see Section 3.3). We define $X = \bigcup\{W^{ss}_{P_{\mathrm{Lor}}}(x) \mid x \in \tilde{X}\}$ as the union of stable leaves along $\tilde{X}$. We also extend the induce time τ from Theorem 6.2.1 to a function on X denoted also by τ and given by $\tau(x) = \tau(\pi(x))$. Now, we construct $F : X \to X$ the Poincaré map by setting $F(x) = P_{\mathrm{Lor}}^{\tau(\pi(x))}(x)$ for $x \in X$. Furthermore, let $\mathcal{Q}$ be the measurable partition of X by taking $\bigcup\{W^{ss}_{P_{\mathrm{Lor}}}(x) \mid x \in \tilde{Q}\}$ as its elements, with $\tilde{Q} \in \tilde{\mathcal{Q}}$. We will make use of X and F when making the model of the geometrical Lorenz flow by a suspension flow.

It is standard that the map $\tilde{F}$ has a unique a.c.i.p measure $\mu_{\tilde{X}}$ on $\tilde{X}$, see Section 4.4. Furthermore, $r_{\mathrm{Lor}} \in \mathrm{L}^1(\mu_{\tilde{X}})$ and it is well-known that there exists a unique invariant measure μ_X for F, μ_Σ for P_{Lor} and μ_I for f_{Lor} (see [5] and Section 3.4 for more details) satisfying $\pi_*(\mu_X) = \mu_{\tilde{X}}$, $\pi_*(\mu_\Sigma) = \mu_I$, $\mu_\Sigma = \sum_{n\geq 1}\sum_{i=0}^{n-1}(P^i_{\mathrm{Lor}})_*(\mu_X|\{\tau\circ\pi = n\})$ and also $\mu_I = \sum_{n\geq 1}\sum_{i=0}^{n-1}(f^i_{\mathrm{Lor}})_*(\mu_{\tilde{X}}|\{\tau\circ \pi = n\})$. Moreover, $\mu_X \ll \mu_\Sigma$ and $\mu_X(X) = 1$, thus $\mu_\Sigma(X) > 0$.

Now we take the induced roof function $R : X \to \mathbb{R}^+$ given by $R(x) = \sum_{k=0}^{\tau(x)-1} r_{\mathrm{Lor}}(P^k_{\mathrm{Lor}}(x))$. Notice that R is constant along stable leaves because r_{Lor} is constant along stable leaves, we also call R the quotient induced roof function $R : \tilde{X} \to \mathbb{R}^+$.

6.2.1 Local product structure

In this subsection we present the results of [9] concerning the local product structure for the induced hyperbolic map $F : X \to X$. In Section 5.1, we saw that the Poincaré map $P_{\mathrm{Lor}} : \Sigma \to \Sigma$ has a strong stable foliation. To avoid confusion, it will be denoted by $\mathcal{F}^{ss}_{P_{\mathrm{Lor}}}$. We note that the leaves of this foliation cross Σ, hence the induced map F has a strong stable manifold $W^{ss}_F(x) = W^{ss}_{P_{\mathrm{Lor}}}(x)$ that cross X. The next result will give us local unstable manifolds of uniform size for F and defined almost everywhere. For more details consult [9].

6.2.3 Proposition. *[9, Proposition 2.4] There is a local unstable manifold $W^u_F(x) \subset W^u_{\epsilon,P_{\mathrm{Lor}}}(x)$ that crosses X, for μ_X-almost every $x \in X$. Particularly, $\pi(W^u_F(x)) = \tilde{X}$ for μ_X-almost every x.*

Using the geometric structure provided by Proposition 6.2.3 above, we get the local product structure stated in the next Proposition.

6.2.4 Proposition. *[9, Proposition 2.5] The induced map $F : X \to X$*

has local product structure; that is, for $Q \in \mathcal{Q}$ there is a measurable map $[\cdot,\cdot] : X \times Q \to Q$ defined for all $y \in Q$ and μ_X-almost every $x \in X$ such that,

$$[x, y] \in W^u_F(x) \pitchfork W^s_F(y)$$

consists of a unique point (see Figure 6.1). Furthermore, the map $[\cdot,\cdot]$ is constant along unstable manifolds in the first coordinate and in the second coordinate is constant along stable manifolds. Moreover, $[\cdot,\cdot]$ is $C^{1+\alpha}$ in the second coordinate.

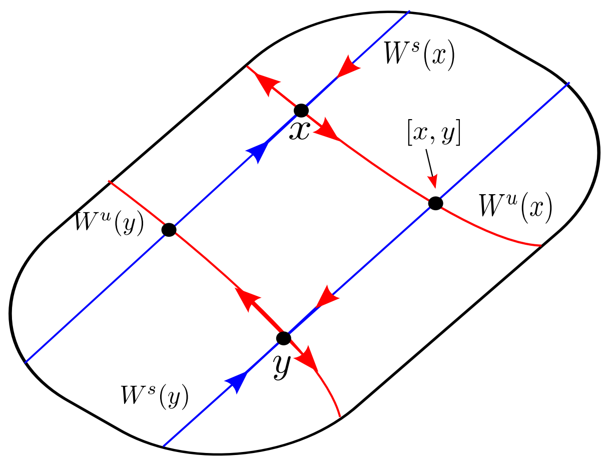

Figure 6.1: Local product structure for F.

6.2.2 Uniform bound of the derivative

In this section we give an important result that will be needed to prove the UNI condition for the geometrical Lorenz flow. For the proof and more details of these results consult [9].

6.2.5 Proposition. *[9, Section 2.5] Let $Q \in \mathcal{Q}_0$ and $\tilde{F} : Q \to \tilde{X}$ as in Theorem 6.2.1. Denote by $\mathcal{H}$ the set of all inverse branches of $\tilde{F}$. Then we have*

$$\sup_{h \in \mathcal{H}} \sup_{x \in \tilde{X}} |D(R \circ h)(x)| < \infty.$$

For $x,\ y \in \tilde{X}$ define the **separation time** $s(x, y)$ as the least integer $n \geq 0$ such that $\tilde{F}^n(x)$ and $\tilde{F}^n(y)$ are in different partition elements of $\mathcal{Q}_0$. For given $0 < \eta < 1$ define the **symbolic metric** on $\tilde{X}$ as $d_\eta(x,y) = \eta^{s(x,y)}$. Denote $r^{(k)}_{\mathrm{Lor}}(x) = \sum_{i=0}^{k-1} r_{\mathrm{Lor}}(P^i_{\mathrm{Lor}}(x))$.

6.2.6 Proposition. *[9, Lemma 2.9] There exists $B > 0$ such that for all $x,\ y \in \tilde{X}$ with $s(x,y) \geq 1$ and $0 \leq k \leq \tau(x) = \tau(y)$ we have,*

$$|r^{(k)}_{\mathrm{Lor}}(x) - r^{(k)}_{\mathrm{Lor}}(y)| \leq B|\tilde{F}(x) - \tilde{F}(y)|^\epsilon.$$

Consequently, there is $\eta \in (0,1)$ such that $|R|_\eta < \infty$, where $|R|_\eta = \sup_{x\neq y} \frac{|R(x)-R(y)|}{d_\eta(x,y)}$ denotes the Lipschitz constant of the quotient induced roof function $R : \tilde{X} \to \mathbb{R}^+$ with respect to d_η. Moreover, $|\tilde{F}(x) - \tilde{F}(y)| \leq B \cdot d_\eta(x,y)$.

6.2.3 Temporal distortion function

The geometrical Lorenz flow can be modelled as a suspension flow $S_t : \Sigma^{r_{\mathrm{Lor}}} \to \Sigma^{r_{\mathrm{Lor}}}$ over the Poincaré section Σ and with roof function r_{Lor}. Recall from Section 6.2 that we constructed X by first taking $\tilde{X} \subset I$, the domain where the induced map $\tilde{F}$ is defined, then taking the union of stable leaves along $\tilde{X}$; *i.e.*, $X = \bigcup\{W^{ss}_{P_{\mathrm{Lor}}}(x) \mid x \in \tilde{X}\}$. However, by shrinking Σ to X and taking the induced roof function R, which does not need to be the first hitting time, we get an alternative model for the geometrical Lorenz flow now as the suspension flow $S_t : X^R \to X^R$ over a uniformly hyperbolic map $F : X \to X$ and an integrable but unbounded return time $R : X \to \mathbb{R}^+$. The suspension flow is given by $S_t(x,s) = (x, s+t)$ computed modulo identifications with S_t-invariant probability measure $\mu = \mu_X \times m/\bar{R}$, where m is the Lebesgue measure and $\bar{R} = \int R d\mu_X$ (recall Definition 2.0.14).

Analogously, we have the quotient suspension semiflow $\tilde{S}_t : \tilde{X}^R \to \tilde{X}^R$ with invariant probability measure $\mu = \mu_{\tilde{X}} \times m/\bar{R}$, where $\bar{R} = \int R d\mu_{\tilde{X}}$.

Let $Q \in \mathfrak{Q}$ be a partition elements for F. The **temporal distortion function** $T : Q \times Q \to \mathbb{R}$ is defined almost everywhere by

$$
\begin{aligned}
T(x,y) &= \sum_{i=-\infty}^{\infty}[r_{\mathrm{Lor}}(P^i_{\mathrm{Lor}}(x)) - r_{\mathrm{Lor}}(P^i_{\mathrm{Lor}}([x,y])) - r_{\mathrm{Lor}}(P^i_{\mathrm{Lor}}([y,x])) \\
&+ r_{\mathrm{Lor}}(P^i_{\mathrm{Lor}})(y)] \\
&= \sum_{i=-\infty}^{-1}[r_{\mathrm{Lor}}(P^i_{\mathrm{Lor}}(x)) - r_{\mathrm{Lor}}(P^i_{\mathrm{Lor}}([x,y])) - r_{\mathrm{Lor}}(P^i_{\mathrm{Lor}}([y,x])) \\
&+ r_{\mathrm{Lor}}(P^i_{\mathrm{Lor}}(y))], \qquad (6.4)
\end{aligned}
$$

where $[x,y]$ is the local product of x and y (see Figure 6.2). The second inequality follows from the property of r_{Lor} of being constant along stable leaves.

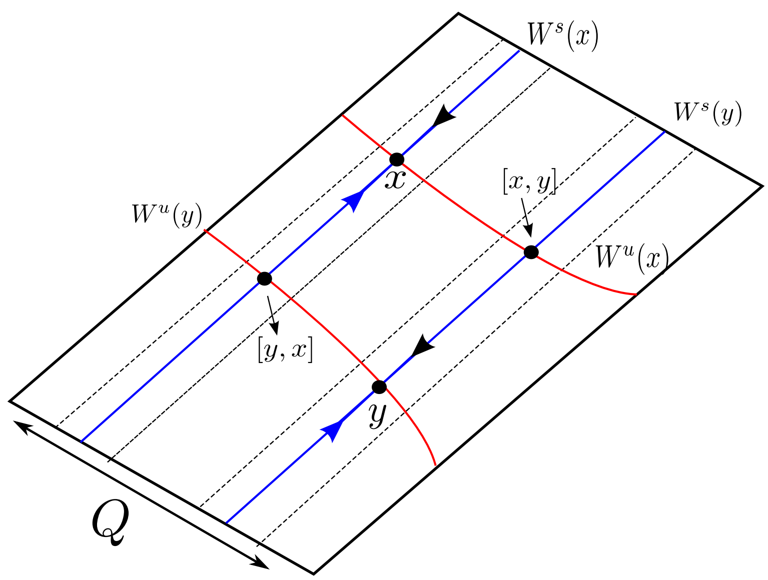

Figure 6.2: Definition of temporal distortion function T.

Now, for every $x,\ y \in X$ in the same unstable manifold for $F : X \to X$ we define

$$
T_0(x,y) = \sum_{i=1}^{\infty}[r_{\mathrm{Lor}}(P^{-i}_{\mathrm{Lor}}(x)) - r_{\mathrm{Lor}}(P^{-i}_{\mathrm{Lor}}(y))]. \qquad (6.5)
$$

The continuity and other properties of T_0 are stated in the following Proposition taken from [9].

6.2.7 Proposition. *[9, Lemma 3.1]The function T_0 is measurable and $T_0(x, y)$ is finite μ_X-almost every x and every $y \in W^u_F(x)$. Furthermore, T_0 is continuous; that is, assume $T_0(x, y)$ is well-defined and $\epsilon > 0$ is given. Then, there is $\delta > 0$ such that $|T_0(x', y') - T_0(x, y)| < \epsilon$ for any pair (x', y') satisfying:*

1. *$T_0(x', y')$ is well-defined.*
2. *$|x' - x| < \delta$ and $|y' - y| < \delta$.*
3. *$d_\eta(x', x) < \delta$ and $d_\eta(y', y) < \delta$.*

6.2.8 Observation. *We can rewrite the temporal distortion function $T(x, y)$ in terms of T_0; that is,*

$$T(x, y) = T_0(x, [x, y]) + T_0(y, [y, x]).$$

The principal result in [9] concerning the temporal distortion function is the following Theorem, which establishes the jointly nonintegrability of the stable and unstable foliations for the flow.

6.2.9 Theorem. *[9, Theorem 3.4]For any geometric Lorenz flow the temporal distortion function T is not identically zero; that is, there is $Q \in \mathcal{Q}$ and $x,\ y \in Q$ such that $T(x, y) \neq 0$.*

Proposition 6.2.10 will be of great help for the proof of Theorem 6.2.11 below.

6.2.10 Proposition. *[11, Proposition 7.4]Let $G : Y \to Y$ be a uniformly expanding Markov map with partition $\{Y^{(i)}\}_{i\geq 0}$, $r : Y \to \mathbb{R}$ be a C^1 function on each $Y^{(i)}$ with $\sup_{h\in\mathcal{H}} \|D(r \circ h)\|_{C^0} < \infty$, where $\mathcal{H}$ denotes the set of inverse branches of F as before. Then the following are equivalent:*

1.- *There exists $D > 0$ such that there is an arbitrary large n, there exist $h,\ g \in \mathcal{H}_n$, where $\mathcal{H}_n$ denotes the set of inverse branches of F^n, there is a continuous unitary vector field $x \mapsto y(x)$, such that for any $x \in Y$,*

$$|D(r^{(n)} \circ h)(x) \cdot y(x) - D(r^{(n)} \circ g)(x) \cdot y(x)| > D. \tag{6.6}$$

2.- *There exists $D > 0$ such that there is an arbitrary large n, there exist $h,\ g \in \mathcal{H}_n$, where $\mathcal{H}_n$ denotes the set of inverse branches of F^n, there* *are $x \in X$ and $y \in T_xX$ with $\|y\| = 1$ such that*

$$|D(r^{(n)} \circ h)(x) \cdot y - D(r^{(n)} \circ g)(x) \cdot y| > D. \tag{6.7}$$

3.- *It is not possible to write $r = \psi + (\phi \circ F) - \phi$ on $\bigcup_{i\geq 0} Y^{(i)}$, where $\psi : Y \to \mathbb{R}$ is constant on each $Y^{(i)}$ and $\phi \in C^1(Y)$.*

4.- *It is not possible to write $r = \psi + (\phi \circ F) - \phi$ almost everywhere, where $\psi : Y \to \mathbb{R}$ is constant on each $Y^{(i)}$ and $\phi : Y \to \mathbb{R}$ is measurable.*

Finally, the UNI condition for the geometrical Lorenz flow is stated in the following Theorem. For a better understanding, we give a sketch of the proof.

6.2.11 Theorem. *[8, Corollary 4.3] The UNI condition holds for the geometrical Lorenz flow.*

Proof. Let $Q \in \mathfrak{Q}$, $x,\ y \in Q$. By Observation 6.2.8, we can write the temporal distortion function as $T(x, y) = T_0(x, [x, y]) + T_0(y, [y, x])$. Proposition 6.2.7 gives us a sequence of partition elements $Q_i \in \mathfrak{Q}$ and points $x_i,\ y_i \in Q_i$ with $x = x_0$, $y = y_0$ and $x_{i-1} = F(x_i)$, $y_{i-1} = F(y_i)$ for $i \geq 1$, such that

$$T_0(x, y) = \sum_{i=1}^{\infty}[R(x_i) - R(y_i)].$$

Observe that the last equality holds since the points x_i and y_i are a sort of backwards iteration under the map F.

Now assume, by contradiction, that the UNI condition fails. By Proposition 6.2.10, there exists a locally constant function $\psi : X \to \mathbb{R}$, constant on each element $Q \in \mathfrak{Q}$, and a $C^1(X)$ function ϕ such that $R = \psi + (\phi \circ F) - \phi$. Moreover, it follows that ϕ is constant along stable manifolds since R is constant along stable manifolds and $\phi = \sum_{j=0}^{n-1} \psi \circ F^j + \phi \circ F^n - \sum_{j=0}^{n-1} R \circ F^j$. Substituting into the formulas for T and T_0, we get $T_0(x, y) = \phi(x) - \phi(y)$ and

$$T(x, y) = \phi(x) - \phi([x, y]) + \phi(y) - \phi([y, x]) = 0.$$

Thus, the temporal distortion function T is identically zero, a contradiction to Theorem 6.2.9. Therefore, the UNI condition holds for the geometrical Lorenz flow. $\square$

6.3 UNI condition for the modified geometrical Lorenz model

This section will be devoted to proving the UNI condition for the modified geometrical Lorenz flow. The strategy is the same presented in Section 6.2. Although some of the results stated in the previous section still hold true for the modified version, others need to be adjusted for our situation.

We keep the same notation as in Section 6.2. Let $I = [-1, 1]$ and $f_{\text{Neu}} : I \to I$ be the one-dimensional Lorenz-like map obtained from the modified geometrical model, see Section 4.3. We make the observation that f_{Neu} is essentially the same function as f_{Lor}, the only difference they have is the dependence of their exponents. Although both exponents are in $(0, 1)$, for f_{Lor} the exponent is $\alpha = \frac{\lambda_s}{\lambda_u}$, where λ_u and λ_s are the eigenvalues of the unstable and stable directions, respectively. Therefore, α depends on those eigenvalues (see Section 3.3), whereas for f_{Neu} the exponent $\beta = \frac{\beta_0}{\beta_2}$, where β_0 and β_2 depends on the coefficients of vector field in Equation (4.4), see Section 4.2. Observe that $\{0\}$ is also a nondegenerate[1] exceptional set for f_{Neu}. Applying Theorem 6.2.1 to f_{Neu}, we know there are $\tilde{X}$ a neighbourhood of the singularity 0, a countable partition $\tilde{\mathcal{Q}}$ of $\tilde{X}$ Lebesgue modulo zero into subintervals, a function $\tau : \tilde{X} \to \mathbb{Z}^+$ constant on partition elements and the induced map $\tilde{F} = f_{\text{Neu}}^{\tau} : \tilde{Q} \to \tilde{X}$ which is a C^2 uniformly expanding diffeomorphism with bounded distortion for any $\tilde{Q} \in \tilde{\mathcal{Q}}$. Furthermore, the properties and inequalities stated in Observation 6.2.2 hold true for the new induced map by replacing f_{Neu} for f_{Lor} in the statements.

Following Section 6.2, we construct now a piecewise uniformly hyperbolic map F with infinitely many branches, which covers $\tilde{F}$. As before, let $W^{ss}_{P_{\text{Neu}}}(x)$ denote the stable leaf under the modified Poincaré map P_{Neu} containing the point x (see Section 5.2), $\pi : \Sigma \to I$ the projection map. Let $X = \bigcup\{W^{ss}_{P_{\text{Neu}}}(x) \mid x \in \tilde{X}\}$ be the union of stable leaves along $\tilde{X}$. We also extend the induce time τ from Theorem 6.2.1 to a function on X denoted also by τ and given by $\tau(x) = \tau(\pi(x))$. Now, $F : X \to X$ is the Poincaré map given by $F(x) = P_{\text{Neu}}^{\tau(\pi(x))}(x)$ for $x \in X$. Furthermore, let $\mathcal{Q}$ be the measurable partition of X by taking $\bigcup\{W^{ss}_{P_{\text{Neu}}}(x) \mid x \in \tilde{Q}\}$ as its elements, with $\tilde{Q} \in \tilde{\mathcal{Q}}$.

[1]Nondegenerate here is meant for the derivative of the one dimensional map f_{Neu} and shouldn't be confused with the degeneracy at the singularity 0 concerning the eigenvalues being zero.

Let $\mu_{\tilde{X}}$ be the unique a.c.i.p measure for $\tilde{F}$ on $\tilde{X}$. Furthermore, $r_{\mathrm{Neu}} \in \mathrm{L}^1(\mu_{\tilde{X}})$ and there exists a unique invariant measure μ_X for F, μ_Σ for P_{Neu} and μ_I for f_{Neu} satisfying $\pi_*(\mu_X) = \mu_{\tilde{X}}$, $\pi_*(\mu_\Sigma) = \mu_I$, $\mu_\Sigma = \sum_{n\geq 1}\sum_{i=0}^{n-1}(P^i_{\mathrm{Neu}})_*$ $(\mu_X|\{\tau\circ\pi = n\})$ and also $\mu_I = \sum_{n\geq 1}\sum_{i=0}^{n-1}(f^i_{\mathrm{Neu}})_*(\mu_{\tilde{X}}|\{\tau\circ\pi = n\})$. Moreover, $\mu_X \ll \mu_\Sigma$ and $\mu_X(X) = 1$, thus $\mu_\Sigma(X) > 0$. We take the induced roof function $R : X \to \mathbb{R}^+$ given by $R(x) = \sum_{k=0}^{\tau(x)-1} r_{\mathrm{Neu}}(P^k_{\mathrm{Neu}}(x))$. Notice that R is constant along stable leaves because r_{neu} is constants along stable leaves. We also call R the quotient induced roof function $R : \tilde{X} \to \mathbb{R}^+$.

The local product structure discussed in Section 6.2.1 remains true for the new version of the induced uniformly hyperbolic map $F : X \to X$. From Section 5.2, we know that the modified Poincaré map $P_{\mathrm{Neu}} : \Sigma \to \Sigma$ has a strong stable foliation which will be denoted in this section by $\mathcal{F}^{ss}_{P_{\mathrm{Neu}}}$ and whose leaves cross the Poincaré section Σ and hence F has strong stable manifolds $W^{ss}_F(x) = W^{ss}_{P_{\mathrm{Neu}}}(x)$ that cross X. The existence of local unstable manifolds of uniform sizes for the new F is given by Proposition 6.2.3, since its proof remains true for our modified version of the model because it relies on the partial hyperbolicity of the attractor and the domination of the splitting on the attractor, properties that are still true for our modified model, see Section 5.2. Moreover, the local product structure of F is obtained from Proposition 6.2.4, since the proof is the same for our case because it uses Proposition 6.2.3, partial hyperbolicity of the attractor and the construction of the geometrical model.

6.3.1 Uniform bound of the derivative

Although most of the results stated in Section 6.2 are still true for the modified version of the model, the statements in Section 6.2.2 need some care. The main difference we have is the flow times; that is, recall from Section 5.1 that $r_{\mathrm{Lor}}(x) = -\lambda_u^{-1}\ln|x| + \tau_2(x)$, where $\tau_2 \in C^\epsilon(\Sigma)$, whereas the modified flow time is $r_{\mathrm{Neu}}(x) = |x|^{-\frac{1}{\beta_2}} + \tau_2(x)$. In order to prove Proposition 6.2.5 and Proposition 6.2.6, we need to adjust the proofs for the modified flow time as we show next.

6.3.1 Proposition. *Let $\tilde{Q} \in \tilde{\mathcal{Q}}$ and $\tilde{F} : \tilde{Q} \to \tilde{X}$ as above. Denote by $\mathcal{H}$ the set of all inverse branches of $\tilde{F}$. Then we have*

$$\sup_{h\in\mathcal{H}}\sup_{x\in\tilde{X}} |D(R\circ h)(x)| < \infty.$$

Proof. Let $\tilde{Q} \in \tilde{\mathfrak{Q}}$ and $h \in \mathcal{H}$; that is, $h : \tilde{X} \to \tilde{Q}$ be an inverse branch of $\tilde{F}$ with inducing time $\tau = \tau(\tilde{Q}) \geq 1$ and fix $x \in \tilde{Q}$. We first observe that

$$\begin{aligned} |D(R \circ h)(x)| &= |DR(h(x))| \cdot |Dh(x)| = \frac{|DR(h(x))|}{|D\tilde{F}(h(x))|} \\ &= \left| \sum_{i=0}^{\tau-1} \frac{(Dr_{\text{Neu}} \circ f^i_{\text{Neu}}) \cdot Df^i_{\text{Neu}}}{D\tilde{F}} \circ h(x) \right|. \end{aligned}$$

From the construction of the inducing partition using hyperbolic times, we have that backward contraction and slow recurrence to the singular point, see Observation 6.2.2; that is, there are constants $\sigma \in (0,1)$, $b_0 > 0$ and $0 < c \leq \frac{1}{2}$ such that

1.- (Backward contraction) For $y \in \tilde{Q}(x)$

$$|f^i_{\text{Neu}}(y) - f^i_{\text{Neu}}(x)| \leq b_0 \sigma^{\tau-i} |\tilde{F}(y) - \tilde{F}(x)|, \quad i = 0, \ldots, \tau - 1.$$

2.- (Slow recurrence to the singular point)

$$|f^i_{\text{Neu}}(x)| \leq \sigma^{c(\tau-i)}, \quad i = 0, \ldots, \tau - 1.$$

Notice that

$$\left| \frac{Df^i_{\text{Neu}}}{D\tilde{F}} \circ h(x) \right| = \left| \frac{1}{Df^{\tau-i}_{\text{Neu}} \circ f^i_{\text{Neu}}} \circ h(x) \right| \leq b_0 \sigma^{\tau-i} \quad i = 0, \ldots, \tau - 1, \tag{6.8}$$

where the inequality follows from the backward contraction.

Moreover, from the slow recurrence to the singularity we also get the following inequality;

$$|(Dr_{\text{Neu}} \circ f^i_{\text{Neu}}) \circ h(x)| \leq b_1 \sigma^{-c(1+\frac{1}{\beta_2})(\tau-i)} \quad i = 0, \ldots, \tau - 1, \tag{6.9}$$

for some constant $b_1 > 0$. Altogether, Equations (6.8) and (6.9) imply that

$$|D(R \circ h)(x)| \leq b \sum_{i=0}^{\tau-1} \sigma^{si}, \tag{6.10}$$

where $s = 1 - c(1 + \frac{1}{\beta_2})$. Since $0 < c \leq \frac{1}{2}$ and $\beta_2 > 2$, we have $s < 1$. Therefore the sum converges, and we have that

$$\sup_{h \in \mathcal{H}} \sup_{x \in \tilde{X}} |D(R \circ h)(x)| < \infty.$$

$\square$

Recall that for $x,\ y \in \tilde{X}$ we defined the separation time $s(x, y)$ as the least integer $n \geq 0$ such that $\tilde{F}^n(x)$ and $\tilde{F}^n(y)$ are in different partition elements of $\mathcal{Q}_0$. For given $0 < \eta < 1$ the symbolic metric was defined on $\tilde{X}$ as $d_\eta(x, y) = \eta^{s(x,y)}$. Finally, $r^{(k)}_{\mathrm{Neu}}(x) = \sum_{i=0}^{k-1} r_{\mathrm{Neu}}(P^i_{\mathrm{Neu}}(x))$

6.3.2 Proposition. *There exists $B > 0$ such that for all $x,\ y \in \tilde{X}$ with $s(x, y) \geq 1$ and $0 \leq k \leq \tau(x) = \tau(y)$ we have $|r^{(k)}_{\mathrm{Neu}}(x) - r^{(k)}_{\mathrm{Neu}}(y)| \leq B|\tilde{F}(x) - \tilde{F}(y)|^\epsilon$. Consequently, there is $\eta \in (0, 1)$ such that $|R|_\eta < \infty$, where $|R|_\eta = \sup_{x \neq y} \frac{|R(x)-R(y)|}{d_\eta(x,y)}$ denotes the Lipschitz constant of the quotient induced roof function $R : \tilde{X} \to \mathbb{R}^+$ with respect to d_η. Moreover, $|\tilde{F}(x) - \tilde{F}(y)| \leq B d_\eta(x, y)$.*

Proof. For convenience, in this proof f will denote f_{Neu}. Let $x,\ y \in \tilde{X}$ such that $s(x, y) = n \geq 1$ and $0 \leq k \leq \tau(x) = \tau(y)$. Thus $y \in \tilde{Q}^n(x)$, where $\tilde{Q}^n(x) = \bigvee_{i=0}^{n-1} (\tilde{F}^i)^{-1}(\tilde{Q}(x))$ is the nth refinement of $\tilde{Q}(x)$, and so $\tau(\tilde{F}^i(x)) = \tau(\tilde{F}^i(y))$ for $i = 0, \ldots, n-1$. Hence, by the choice of the cross-section, assuring that r_{Neu} is constant along stable leaves, and because $r_{\mathrm{Neu}}(x) = |x|^{-\frac{1}{\beta_2}} + \tau_2(x)$ we can write

$$\begin{aligned}
|R(x) - R(y)| &\leq \sum_{i=0}^{\tau(x)-1} |r_{\mathrm{Neu}}(f^i(x)) - r_{\mathrm{Neu}}(f^i(y))| \\
&\leq \sum_{i=0}^{\tau(x)-1} \left| |f^i(x)|^{-\frac{1}{\beta_2}} - |f^i(y)|^{-\frac{1}{\beta_2}} \right| + |\tau_2(f^i(x) - \tau_2(f^i(y))|.
\end{aligned}$$

Now observe that

$$\begin{aligned}
\left||f^i(x)|^{-\frac{1}{\beta_2}} - |f^i(y)|^{-\frac{1}{\beta_2}}\right| &= |f^i(x)|^{-\frac{1}{\beta_2}} \left|1 - \left(\frac{|f^i(y)|}{|f^i(x)|}\right)^{-\frac{1}{\beta_2}}\right| \\
&= |f^i(x)|^{-\frac{1}{\beta_2}} \left|1 - \left(1 + \frac{|f^i(y) - f^i(x)|}{|f^i(x)|}\right)^{-\frac{1}{\beta_2}}\right| \\
&\leq |f^i(x)|^{-\frac{1}{\beta_2}} C_0 \frac{1}{\beta_2} \frac{|f^i(y) - f^i(x)|}{|f^i(x)|} \\
&= \frac{C_0}{\beta_2} |f^i(x)|^{-(1+\frac{1}{\beta_2})} |f^i(y) - f^i(x)| \\
&\leq \frac{C_0}{\beta_2} \sigma^{1-c(1+\frac{1}{\beta_2})(\tau(x)-i)} \left|\tilde{F}(y) - \tilde{F}(x)\right|,
\end{aligned}$$

where $C > 0$ and $0 < c \leq \frac{1}{2}$. Also notice that

$$\begin{aligned}
\left|\tau_2(f^i(y)) - \tau_2(f^i(x))\right| &\leq \|\tau_2\|_\epsilon \left|f^i(y) - f^i(x)\right|^\epsilon \\
&\leq \sigma^{\epsilon(\tau(x)-i)} \|\tau_2\|_\epsilon \left|\tilde{F}^i(y) - \tilde{F}^i(x)\right|^\epsilon .
\end{aligned}$$

All these estimates lead us to

$$\begin{aligned}
|R(x) - R(y)| &\leq C \sum_{i=0}^{\tau(x)-1} [\sigma^{s(\tau(x)-i)} |\tilde{F}(y) - \tilde{F}(x)| \\
&\quad + \sigma^{\epsilon(\tau(x)-i)} \|\tau_2\|_\epsilon |\tilde{F}^i(y) - \tilde{F}^i(x)|^\epsilon] \\
&\leq B|\tilde{F}^i(y) - \tilde{F}^i(x)|^\epsilon,
\end{aligned}$$

where $s = 1 - c(1 + \frac{1}{\beta_2})$ and some constant $B > 0$. As in the previous proof, the sum converges since $\beta_2 > 2$, $0 < c \leq \frac{1}{2}$ and hence $s < 1$. This establishes what we were aiming to prove. $\square$

6.3.2 Temporal distortion function

As mentioned in Section 6.2.3, the geometrical Lorenz model can be modelled via a suspension flow. We will proceed in the same fashion for the modified version of the geometrical Lorenz model. The main difference will be the roof function, for the geometrical Lorenz model the roof function was given by r_{Lor}, whereas for the modified version the roof function will be given by r_{Neu}; that is, we take the suspension flow $S_t : \Sigma^{r_{\text{Neu}}} \to \Sigma^{r_{\text{Neu}}}$ over the Poincaré section Σ and with roof function r_{Neu}. However, by shrinking Σ to X and taking the induced roof function R, we get an alternative model for the modified geometrical Lorenz flow now as the suspension flow $S_t : X^R \to X^R$ over a uniformly hyperbolic map $F : X \to X$ and an integrable but unbounded return time $R : X \to \mathbb{R}^+$. Recall Definition 2.0.14 the suspension flow is given by $S_t(x, s) = (x, s + t)$ computed modulo identifications with S_t-invariant probability measure $\mu = \mu_X \times m/\bar{R}$, where m is the Lebesgue measure and $\bar{R} = \int Rd\mu$.

Likewise, we have the quotient suspension semiflow $\tilde{S}_t : \tilde{X}^R \to \tilde{X}^R$ with invariant probability measure $\tilde{\mu} = \mu_{\tilde{X}} \times m/\bar{R}$, where $\bar{R} = \int Rd\mu$.

Let $Q \in \mathcal{Q}$ be a partition elements for F. The temporal distortion function $T : Q \times Q \to \mathbb{R}$ is defined almost everywhere as before by

$$
\begin{aligned}
T(x,y) &= \sum_{i=-\infty}^{\infty} [r_{\text{Neu}}(P^i_{\text{Neu}}(x)) - r_{\text{Neu}}(P^i_{\text{Neu}}([x,y])) - r_{\text{Neu}}(P^i_{\text{Neu}}([y,x])) \\
&+ r_{\text{Neu}}(P^i_{\text{Neu}})(y)] \\
&= \sum_{i=-\infty}^{-1} [r_{\text{Neu}}(P^i_{\text{Neu}}(x)) - r_{\text{Neu}}(P^i_{\text{Neu}}([x,y])) - r_{\text{Neu}}(P^i_{\text{Neu}}([y,x])) \\
&+ r_{\text{Neu}}(P^i_{\text{Neu}}(y))],
\end{aligned} \tag{6.11}
$$

where $[x, y]$ is the local product of x and y (see Figure 6.2). The second inequality follows from the property of r_{Neu} of being constant along stable leaves. Now, for every $x,\ y \in X$ in the same unstable manifold for $F : X \to X$ we define

$$T_0(x,y) = \sum_{i=1}^{\infty} [r_{\text{Neu}}(P_{\text{Neu}}^{-i}(x)) - r_{\text{Neu}}(P_{\text{Neu}}^{-i}(y))]. \tag{6.12}$$

The continuity and other properties of T_0 are stated in Proposition 6.2.7 taken from [9]. Furthermore, by Observation 6.2.8 we can rewrite the temporal distortion function $T(x,y)$ in terms of T_0; that is,

$$T(x,y) = T_0(x,[x,y]) + T_0(y,[y,x]).$$

The main result in [9] concerning the temporal distortion function, and stated in Section 6.2.3, is Theorem 6.2.9, which establishes the joint nonintegrability of the stable and unstable foliations for the flow by proving that the temporal distortion function T is not identically zero, that is, there is $Q \in \mathcal{Q}$ and $x,\ y \in Q$ such that $T(x,y) \neq 0$.

In Section 6.3.1, we adjusted the proof of the uniform bound of the derivative for the modified model since we want to apply Proposition 6.2.10 in order to use the same proof in Theorem 6.2.11. Thus, we get the UNI condition for the modified geometrical Lorenz flow. For completeness we state it in the following Theorem.

6.3.3 Theorem. *The UNI condition holds for the geometrical neutral Lorenz flow.*

For fixed $x \in X$, we define the map $h : W_F^u(x) \to \mathbb{R}$ given by

$$h(y) = T(x,y) = T_0(x,[x,y]) + T_0(y,[y,x]),$$

the map h is C^1. Furthermore, there exists a nonempty open set $U \subset W_F^u(x)$ such that $h|_U$ is a C^1 diffeomorphism. For the proves of the properties of the map h see Proposition 3.6 and Corollary 4.7 in [9].

The next result will be of great help in proving the decay of correlations for the modified geometrical Lorenz flow. Before stating the result we give the necessary definitions.

6.3.4 Definition. *Let X, and F be as in the beginning of Section 6.3. A subset $Z_0 \subset X$ is called a **fine subsystem** of X if $Z_0 = \bigcap_{n\geq 0} F^{-n}Z$, where Z is the union of finitely many partition elements of X.*

Let Q_1 and $Q_2 \in \mathcal{Q}$ be to partition elements and consider $Q = Q_1 \cup Q_2$. We define the finite subsystem $Q_0 = \bigcap_{n \geq 0} F^{-n} Q$, then we have the following:

6.3.5 Proposition. *[9, Proposition 3.8]For the finite subsystem Q_0, the set $T(Q_0 \times Q_0)$ has positive lower box dimension.*

Chapter 7

Decay of correlations

Araújo and Melbourne proved in [8] that the geometrical Lorenz model, and hence the typical Lorenz model, has exponential decay of correlations. In this chapter, we prove that the modified geometrical Lorenz model we constructed has polynomial decay of correlations.

We will give in the first two Sections all the definitions and results that we will need to prove the polynomial decay of correlations for the modified model that we state in Section 3.

7.1 Gibbs-Markov semiflows and flows

All the results and the set-up of this Section are taken from [12]. Let us first describe the framework where the polynomial decay of correlations is proven. We first give the definitions of Gibbs-Markov map, semiflow and flow so we can define the concept of nonuniformly hyperbolic flow. Then we will see that under suitable conditions, nonuniformly hyperbolic flows can be modelled by Gibbs-Markov flows. Last but not least, we state the result concerning the decay of correlations

Assume that $(\tilde{X}, \mu_{\tilde{X}})$ is a probability space with measure preserving transformation $\tilde{F} : \tilde{X} \to \tilde{X}$ and countable measurable partition $\tilde{\mathfrak{Q}} = \{\tilde{Q}_i\}_{i\geq 1}$. Recall from Section 6.3.1, that a function $v : \tilde{X} \to \mathbb{R}$ is $d_\theta-$**Lipschitz** if $|v|_\theta < \infty$, where $|v|_\theta = \sup_{x\neq y} |v(x) - v(y)|/d_\theta(x, y)$ and $d_\theta(x, y)$ is the symbolic metric. We will denote the Banach space of Lipschitz functions on $\tilde{X}$

by $\mathcal{F}_\theta(\tilde{X})$ equipped with the norm $\|v\|_\theta = |v|_\infty + |v|_\theta$. We say that $v : \tilde{X} \to \mathbb{R}$ is **piecewise $d_\theta-$Lipschitz** if

$$|1_{\tilde{Q}_i} v|_\theta = \sup_{\substack{x,y \in \tilde{Q}_i \\ x \neq y}} \tfrac{|v(x)-v(y)|}{d_\theta(x,y)} < \infty,$$

for every i.

7.1.1 Definition. *A measure preserving transformation $\tilde{F} : \tilde{X} \to \tilde{X}$ as above, will be called (full branched)* ***Gibbs-Markov map*** *if*

1.- *$\tilde{F}|_{\tilde{Q}_i} : \tilde{Q}_i \to \tilde{X}$ is a measurable bijection for every i.*

2.- *Let $\nu = \frac{d\mu_{\tilde{x}}}{d\mu_{\tilde{X}} \circ \tilde{F}} : \tilde{X} \to \mathbb{R}$. There are constants $C > 0$ and $0 < \theta < 1$ such that*
$$|\log \nu(x) - \log \nu(y)| \leq C d_\theta(x,y)$$
for every x, $y \in \tilde{Q}$, with $\tilde{Q} \in \tilde{\mathcal{Q}}$.

As result of the second statement we have that there is a constant $C > 0$ such that

$$\nu(x) \leq C\mu_{\tilde{X}}(\tilde{Q}), \qquad\qquad |\nu(x) - \nu(y)| \leq C\mu_{\tilde{X}}(\tilde{Q})$$

for every x, $y \in \tilde{Q}$, and $\tilde{Q} \in \tilde{\mathcal{Q}}$.

7.1.2 Definition. *Let $\varphi : \tilde{X} \to \mathbb{R}^+$ be an integrable roof function with* $\inf \varphi > 0$. *The suspension semiflow (see Definition 2.0.14) $\tilde{F}_t : \tilde{X}^\varphi \to \tilde{X}^\varphi$ with ergodic invariant probability measure $\tilde{\mu}^\varphi$ is called* ***Gibbs-Markov semiflow*** *if it is built over a Gibbs-Markov map $\tilde{F} : \tilde{X} \to \tilde{X}$ and there are constants $C > 0$ and $\theta \in (0,1)$ such that,*

$$|1_{\tilde{Q}_i} \varphi|_\theta \leq C \inf_{\tilde{Q}_i} \varphi \qquad\qquad \textit{for all } i \geq 1. \tag{7.1}$$

Let $b \in \mathbb{R}$, we define the the operator $M_b : \mathrm{L}^\infty(\tilde{X}) \to \mathrm{L}^\infty(\tilde{X})$ by

$$M_b(v) = \mathrm{e}^{ib\varphi}\, v \circ \tilde{F},$$

where $\tilde{F}$ and φ are as above. Note that $\mathrm{L}^\infty(X)$ in this context denotes the complex-valued essentially bounded measurable functions on $\tilde{X}$.

7.1.3 Definition. *We will say that M_b has **approximate eigenfunctions** on a subsystem $Z_0 \subset X$ (see Definition 6.3.4) if for any $\beta_0 > 0$ there are constants β, $a > \beta_0$, $C > 0$, and sequences $b_k \in \mathbb{R}$ with $|b_k| \to \infty$, $\varphi_k \in (0, 2\pi]$, $u_k \in \mathcal{F}_\theta(\tilde{X})$ with $|u_k| \equiv 1$ and $|u_k|_\theta \leq C|b_k|$, such that if we set $n_k = a \ln |b_k|$ we have,*

$$|(M_{b_k}^{n_k} u_k)(x) - \mathrm{e}^{i\varphi_k} u_k(x)| \leq C|b_k|^{-\beta}, \tag{7.2}$$

for every $x \in Z_0$ and $k \geq 1$.

When we state "assume absence of approximate eigenfunctions" we will assume the existence of at least one finite subsystem Z_0 such that M_b does not have approximate eigenfunctions on Z_0.

Let (X, d) be a metric space with $\mathrm{diam}(X) \leq 1$, $F : X \to X$ be a piecewise continuous map, and μ_X the $F-$invariant probability measure. Let $\mathcal{F}^s$ be a cover by disjoint measurable subsets of X, which we call stable leaves. We also need that for every $x \in X$ $F(W^s(x)) \subset W^s(F(x))$.

We quotient out X by $\mathcal{F}^s$ and denote $\tilde{X}$ the quotient space, and $\pi_1 : X \to \tilde{X}$ the natural projection. Suppose that the quotient map $\tilde{F} : \tilde{X} \to \tilde{X}$ is Gibbs-Markov with partition $\tilde{\mathcal{Q}} = \{\tilde{Q}\}_{i\geq 1}$, and ergodic invariant probability measure $\mu_{\tilde{X}} = (\pi_1)_* \mu_{\tilde{X}}$. By taking $Q_i = \pi_1^{-1}(\tilde{Q}_i)$ we can form a partition of X, where each Q_i is the union of stable leaves. Furthermore, we assume there is a measurable subset $Y \subset X$ such that for any $x \in X$ there exists a unique point $y \in Y \cap W^s(x)$ with associated projection $\pi_2 : X \to Y$ given by $\pi_2(x) = y$. We also assume there are constants $C \geq 1$ and $\gamma \in (0, 1)$ such that for every $n \geq 0$,

$$d(F^n(x), F^n(y)) \leq C\gamma^n \qquad \text{for any } x,\ y \in X \text{ with } y \in W^s(x) \tag{7.3}$$

$$d(F^n(x), F^n(y)) \leq C\gamma^{s(x,y)-n} \qquad \text{for any } x,\ y \in Y. \tag{7.4}$$

For every $x \in X$ we define

$$\chi(x) = \sum_{k=0}^{\infty} (\varphi(F^k(\pi_2(x))) - \varphi(F^k(x))), \tag{7.5}$$

such that the series converges absolutely.

(H) a) The series in Equation (7.5) converges almost surely on X and $\chi \in \mathrm{L}^\infty(X)$,

b) there are constants $C \geq 1$ and $0 < \gamma < 1$ such that for any x, $y \in X$

$$|\chi(x) - \chi(y)| \leq C(d(x,y) + \gamma^{s(x,y)}).$$

7.1.4 Definition. *Let $\varphi : X \to \mathbb{R}^+$ be an integrable roof function with $\inf \varphi > 0$. Let $F_t : X^\varphi \to X^\varphi$ be the suspension flow built over $F : X \to X$ as above with ergodic invariant probability measure μ^φ. Furthermore, we assume that φ is constant along stable leaves, so it projects to a roof function $\varphi : \tilde{X} \to \mathbb{R}^+$. Thus the suspension flow F_t projects to a quotient suspension semiflow $\tilde{F}_t : \tilde{X}^\varphi \to \tilde{X}^\varphi$ and suppose it is a Gibbs-Markov semiflow. Then we call the suspension flow F_t a* ***skew product Gibbs-Markov flow****. We say that F_t has approximate eigenfunctions if $\tilde{F}_t$ has approximate eigenfunctions*

Notice that by increasing γ if necessary, the inequality in (7.1) holds now as,

$$|\varphi(x) - \varphi(y)| \leq C\gamma^{s(x,y)} \inf_{Q_i} \varphi \qquad \text{for all } x,\ y \in \tilde{Q}_i,\ i \geq 1. \tag{7.6}$$

Bálint *et al.* studied in [12] an enlarged class of Gibbs-Markov flows by assuming that the roof function φ is not constant on stable leaves. This class can be reduced to the class of skew product Gibbs-Markov flows by assuming the condition (H). Since the flow time r_{Neu} we work with is constant on stable leaves it is sufficient for us to work with the class of skew product Gibbs-Markov flows. Hence we will not give the details for this general class of Gibbs-Markov flows. However, we like to remark that every skew product Gibbs-Markov flow is a Gibbs-Markov flow since it satisfies the criteria established in [12]. Therefore in this work we will make no distinction between the two classes but we make the warning that the class of Gibbs-Markov flows is more general than we state here.

7.2 Nonuniformly hyperbolic flows

In this subsection we will also follow the framework of [12], and give the concept of nonuniformly hyperbolic flow. We consider a measurable transformation $f : I \to I$ on a metric space (I, d), where $\mathrm{diam}(I) \leq 1$. We assume that f is nonuniformly hyperbolic meaning it can be modelled by a Young tower, see Definition 2.0.13. We will also assume the following:

Product structure; that is, let $X \subset I$ be a measurable subset, $\mathcal{F}^s$ and $\mathcal{F}^u$ be a collection of disjoint measurable subsets of X called stable leaves and unstable leaves, respectively such that each of them covers X. For $x \in X$ given, we denote the stable and unstable leaves containing the point x by $W^s(x)$ and $W^u(x)$, respectively. For each x, $y \in X$ we have that $z = W^s(x) \cap W^u(y)$ is unique and $z \in X$. We also suppose that there is $C \geq 1$ such that for all x, $y \in X$, $z = W^s(x) \cap W^u(y)$ we have,

$$d(x, z) \leq C d(x, y). \tag{7.7}$$

Induced map Let $\{X_j\}_{j \geq 1}$ be a countable measurable partition of X such that $X = \cup_{x \in X_j} W^s(x) \cap X$ for all $j \geq 1$ and $\tau : X \to \mathbb{Z}^+$ constant on partition elements such that $f^{\tau(x)}(x) \in X$ for every $x \in X$. We define the induced map as the usual way $f^\tau = F : X \to X$ with ergodic invariant probability measure μ_X and we will also assume that $\tau \in \mathrm{L}^1(X)$. As in the previous section $F(W^s(x)) \subset W^s(F(x))$ for very $x \in X$ and denote by $\tilde{X}$ the space obtained form X after quotienting the stable leaves $\mathcal{F}^s$ with projection $\pi_1 : X \to \tilde{X}$. The quotient map $\tilde{F} : \tilde{X} \to \tilde{X}$ will be assumed to be Gibbs-Markov with ergodic invariant probability measure $\mu_{\tilde{X}} = (\pi_1)_* \mu_X$.

Contraction/expansion We suppose that there are constants $C \geq 1$ and $0 < \gamma < 1$ such that for any $n \geq 0$ and all x, $y \in X$ we have,

$$d(F^n(x), F^n(y)) \leq C\gamma^{\lambda_n(x)} d(x, y) \qquad \text{for all } y \in W^s(x), \tag{7.8}$$

$$d(F^n(x), F^n(y)) \leq C\gamma^{s(x,y) - \lambda_n(x)} \qquad \text{for all } y \in W^u(x), \tag{7.9}$$

where $\lambda_n(x) = \#\{i = 1, \ldots, n \mid F^i(x) \in X\}$ is the number of returns to X by time n.

Now let (M, d) be a metric space with $\operatorname{diam}(M) \leq 1$ and define a flow $T_t : M \to M$ on M. We fix $\eta \in (0, 1]$ and for a given observable $v : M \to \mathbb{R}$ we define

$$|v|_{C^\eta} = \sup_{x \neq y} \frac{|v(x) - v(y)|}{d(x, y)^\eta},$$

and the norm $\|v\|_{C^\eta} = |v|_\infty + |v|_{C^\eta}$. We define the Banach space of Hölder functions on M by $C^\eta(M)$; *i.e.*,

$$C^\eta(M) = \{v : M \to \mathbb{R} \mid \|v\|_{C^\eta} < \infty\}.$$

Furthermore, let

$$|v|_{C^{0,\eta}} = \sup_{\substack{x\in M \\ t>0}} \frac{|v(T_t(x)) - v(x)|}{t^\eta}$$

and define $\|v\|_{C^{0,\eta}} = |v|_\infty + |v|_{C^{0,\eta}}$. We denote the space of Hölder observables in the flow direction by

$$C^{0,\eta}(M) = \{v : M \to \mathbb{R} \mid \|v\|_{C^{0,\eta}} < \infty\}.$$

We will say that an observable $w : M \to \mathbb{R}$ is **differentiable in the flow direction** if

$$\partial_t w = \lim_{t\to 0} \frac{w \circ T_t - w}{t}$$

exist pointwise. Let $\|w\|_{C^{\eta,m}} = \sum_{k=0}^m \left\|\partial_t^k w\right\|_{C^\eta}$. We will denote the space of observables that are m-times differentiable in the flow direction by

$$C^{\eta,m}(M) = \{w : M \to \mathbb{R} \mid \|w\|_{C^{\eta,m}} < \infty\}.$$

For $X \subset M$ Borel subset we define $C^\eta(X)$ as above by using the restriction of the metric d to X.

7.2.1 Definition. *Let (M, d) be a metric space, $\Sigma \subset M$ be a Borel subset, let $T_t : M \to M$ be a flow defined on M and fix $\eta \in (0, 1]$. We will call T_t a **nonuniformy hyperbolic flow** if there is a return time $h : \Sigma \to \mathbb{R}^+$ with $h \in C^\eta(\Sigma)$ and $\inf h > 0$ such that $T_{h(x)}(x) \in \Sigma$ for every $x \in \Sigma$, and the map $f : \Sigma \to \Sigma$ given by $f(x) = T_{h(x)}(x)$ is nonuniformly hyperbolic as defined above.*

7.2.2 Observation. *Typically, the map $f : \Sigma \to \Sigma$ in Definition 7.2.1 will be the Poincaré map over a cross-section Σ. Notice that since f is nonuniformly hyperbolic, then it can be modelled by a Young tower over a induced map*

$F = f^\tau : X \to X$, where $X \subset \Sigma$ with induce time $\tau : X \to \mathbb{Z}^+$ and all the other properties described before.

We define the new induced roof function $\varphi : X \to \mathbb{R}^+$ given by $\varphi(x) = \sum_{k=0}^{\tau(x)} h(f^k(x))$. Observe that $h(x) \leq \varphi(x) \leq \tau(x)|h(x)|_\infty$, hence $\varphi \in \mathrm{L}^1(X)$ and $\inf \varphi > 0$. Thus, we define the suspension flow $F_t : X^\varphi \to X^\varphi$ as in the Definition 2.0.14.

Under suitable conditions, namely condition (H) it can be shown that the suspension flow F_t described in Observation 7.2.2 is a Gibbs-Markov flow, see [12] for more details. Therefore, the rates of mixing for nonuniformly hyperbolic flows are deduced from the corresponding results for Gibbs-Markov flows. Thus we have the following Theorem, the detailed proof can be found as Corollary 8.1 in [12].

7.2.3 Theorem. *[12, Corollary 8.1] Let (M, d) be a metric space with $\operatorname{diam}(M) \leq 1$ and $T_t : M \to M$ be a nonuniformly hyperbolic flow as in Definition 7.2.1. Assume that condition (H) holds. Then*

a) $F_t : X^\varphi \to X^\varphi$ is a Gibbs-Markov flow.

b) Assume absence of approximate eigenfunctions for F_t and suppose that $\mu_X(\varphi > t) = \mathcal{O}(t^{-\beta})$ for some $\beta > 1$. Then there exist $m \geq 1$ and $C > 0$ such that,

$$|\rho_t(v, w)| \leq C(\|v\|_{C^\eta} + \|v\|_{C^{0,\eta}}) \|w\|_{C^{\eta,m}} t^{-(\beta-1)},$$

for every $v \in C^\eta(M) \cap C^{0,\eta}(M)$, $w \in C^{\eta,m}(M)$, $t > 1$.

7.3 Modified geometrical Lorenz model

In this Section we will state the main result concerning the decay of correlations for the modified geometrical Lorenz model we constructed throughout this work. Let us begin by summarizing what we have so far.

We started by considering the construction of the geometrical Lorenz model and the geometric Lorenz flow. Roughly speaking, a geometric Lorenz flow is the natural extension of a suspension flow built over a certain type of one-dimensional expanding map f. To obtain the one-dimensional map f

we first considered the cross-section Σ which is transversal to the flow and the Poincaré map $P_{\mathrm{Lor}} : \Sigma \to \Sigma$ given by $P_{\mathrm{Lor}}(x) = \mathrm{L}_{r_{\mathrm{Lor}}(x)}(x)$, where $\mathrm{L}_t : \Lambda \to \Lambda$ and $r_{\mathrm{Lor}}(x)$ are the flow of the linear system given by the Equation (3.9) and the flow (return) time to the cross-section Σ given by Equation 5.3, respectively. The modified version was obtained by considering in a neighbourhood of the origin the vector field give by Equation (4.1) instead of the linearised vector field given by Equation (3.9), in this way we obtained the modified Poincaré map $P_{\mathrm{Neu}}(x) = \mathrm{N}_{r_{\mathrm{Neu}}(x)}(x)$, where $N_t : \Lambda_{\mathrm{N}} \to \Lambda_{\mathrm{N}}$ and $r_{\mathrm{Neu}}(x)$ are the neutral flow given by Equation (4.7) and the new flow time to the cross-section given by Equation (5.11). This modification yields to a slower flow time that will ultimately allow us to deduce the polynomial decay of correlations.

In Section 5.2 we saw that the modified Poincaré return map P_{Neu} and modified geometrical Lorenz flow N_t, have an invariant stable foliation $\mathcal{F}^s$ with $C^{1+\alpha}$ leaves with $\alpha \in (0,1)$. By quotienting out the stable direction we wrote the modified Poincaré map as a skew-product $P_{\mathrm{Neu}}(x,y) = (f_{\mathrm{Neu}}(x), g_{\mathrm{Neu}}(x,y))$, thus we obtained the one-dimensional nonuniformly hyperbolic map $f_{\mathrm{Neu}} : I \to I$, where $I = [-1,1]$. In Section 6.2, we saw that there exists an inducing scheme for f_{Neu}; that is, there are $\tilde{X} \subset I$ a neighbourhood of the singularity 0 , a countable Lebesgue modulo zero partition $\tilde{\mathcal{Q}} = \{\tilde{Q}_i\}_{i\geq 0}$ into subintervals, a function $\tau : \tilde{X} \to \mathbb{Z}^+$ constant on partition elements and the induced map $\tilde{F} = f_{\mathrm{Neu}}^{\tau} : \tilde{Q}_i \to \tilde{X}$ which is Gibbs-Markov as in Definition 7.1.1.

Then we constructed a subset $X \subset \Sigma$ with nice hyperbolic structure (see Section 6.2.1) by taking the union of stable leaves along $\tilde{X}$; that is, $X = \bigcup\{W^{ss}_{P_{\mathrm{Neu}}}(x) \mid x \in \tilde{X}\}$ with projection map along stable leaves $\pi_1 : \Sigma \to I$. By taking $\bigcup\{W^{ss}_{P_{\mathrm{Neu}}}(x) \mid x \in \tilde{Q}\}$ with $\tilde{Q} \in \tilde{\mathcal{Q}}$ we got a measurable partition $\mathcal{Q}$ of X, and we extended the induce time τ form above to $\tau : X \to \mathbb{Z}^+$ given by $\tau(x) = \tau(\pi_1(x))$ for $x \in X$. Then a Gibbs-Markov map $F : X \to X$ with infinitely many branches, which covers $\tilde{F}$ was obtained by taking $F(x) = P_{\mathrm{Neu}}^{\tau(\pi(x))}(x)$ for $x \in X$.

We also obtained unique invariant probability measures μ_Σ and μ_I for P_{Neu} and f_{Neu}, respectively, satisfying $(\pi_1)_*(\mu_\Sigma) = \mu_I$. Additionally, we got $\mu_{\tilde{X}}$ and μ_X the unique a.c.i.p measures for $\tilde{F}$ and F with $\mu_{\tilde{X}} \ll \mu_I$ and $\mu_X \ll \mu_\Sigma$, respectively, fulfilling $(\pi_1)_*(\mu_X) = \mu_{\tilde{X}}$. Moreover, we have $\mu_\Sigma = \sum_{n\geq 1}\sum_{i=0}^{n-1}(P^i_{\mathrm{Neu}})_*(\mu_X|\{\tau\circ\pi_1 = n\})$ and also

$\mu_I = \sum_{n\geq 1}\sum_{i=0}^{n-1}(f^i_{\text{Neu}})_*(\mu_{\tilde{X}}|\{\tau\circ\pi_1 = n\})$. We make the following important observation.

7.3.1 Observation. *The tails of the return time τ and the extended version also denoted by τ are exponential; i.e., there exists a constant $c > 0$ such that $\mu_{\tilde{X}}(\tau > n) = \mathcal{O}(\mathrm{e}^{-cn})$ and $\mu_X(\tau > n) = \mathcal{O}(\mathrm{e}^{-cn})$.*

The neutral geometrical Lorenz flow can be modelled as a suspension flow over the Poincaré map P_{Neu} with base the cross-section Σ and roof function r_{Neu}. However, we will use an alternative model so that we can use the results of Sections 7.1 and 7.2 to deduce the decay of correlation. The alternative model is given by taking X instead of Σ as the cross-section to the flow with induced roof function $R : X \to \mathbb{R}^+$ given by $R(x) = \sum_{k=0}^{\tau(x)-1} r_{\text{Neu}}(P^k_{\text{Neu}}(x))$. Then the suspension flow over F; that is, $F_t : X^R \to X^R$ is identical to the suspension flow $S_t : \Sigma^{r_{\text{Neu}}} \to \Sigma^{r_{\text{Neu}}}$, thus F_t is an extension of the underlying flow, namely the neutral geometrical Lorenz flow. For observables v and w let $\rho_t(v, w)$ denote the decay of correlations of the geometrical Lorenz neutral flow; that is,

$$\rho_t(v, w) = \int v \cdot w \circ N_t d\mu - \int v d\mu \int w d\mu, \tag{7.10}$$

where μ is the SRB measure of N_t. The above summary leads us to our conclusive result,

7.3.2 Theorem. *Let Λ_{N}, $N_t : \Lambda_{\text{N}} \to \Lambda_{\text{N}}$ and μ be the geometrical Lorenz neutral attractor, the geometrical Lorenz neutral flow constructed in Chapter 4 and its SRB measure, respectively. Then N_t has polynomial decay of correlations; that is, there exist $m \geq 1$ and constant $C > 0$ such that for observables $v \in C^\eta(M) \cap C^{0,\eta}(M)$, $w \in C^{\eta,m}(M)$, and time $t > 1$ we have*

$$\rho_t(v, w) \leq C(\|v\|_{C^\eta} + \|v\|_{C^{0,\eta}})\, \|w\|_{C^{\eta,m}}\, t^{-\beta_2}.$$

Proof. By the brief summary given at the beginning of this Section, we know that $N_t : \Lambda_{\text{N}} \to \Lambda_{\text{N}}$ can be written as the suspension flow $F_t : X^R \to X^R$ with roof function $R(x) = \sum_{k=0}^{\tau(x)-1} r_{\text{Neu}}(P^k_{\text{Neu}}(x))$, where X has the properties described in Section 7.2. Furthermore, since R is constant along stable leaves it projects to a quotient roof function also denoted by R. Hence the suspension flow F_t also projects to a quotient suspension semiflow $\tilde{F}_t : \tilde{X}^R \to \tilde{X}^R$, where $\tilde{X}$ is the quotient space obtained from X after quotienting out the stable leaves. Recall that $\tilde{F} : \tilde{X} \to \tilde{X}$ is a Gibbs-Markov map. Proposition 6.3.2 ensures that Inequality (7.1) holds. Therefore, we have that $\tilde{F}_t$ is a Gibbs-Markov semiflow and it follows that F_t is a Gibbs-Markov flow. We have ultimately shown that N_t is a nonuniformly hyperbolic flow as in Definition 7.2.1. Then the conclusion follows from Theorem 7.2.3.

There are still four details concerning the hypothesis in Theorem 7.2.3 that we have not mentioned yet. The first one is regarding condition (H), for us this condition holds automatically since R is constant along stable leaves. The second, concerns the absence of approximate eigenfunctions for F_t. Bálint *et al.* gave in [12] sufficient conditions for the absence of approximate eigenfunctions, namely the existence of a finite subsystem with positive lower box dimension. Hence, it follows from Proposition 6.3.5 and Lemma 8.9 in [12] that F_t has absence of approximate eigenfunctions.

The third concerns the tails of R; that is, we want to estimate $\mu_X(R > t)$. From Observation 7.3.1 we know that $\mu_X(\tau > n)$ has exponential tails; *i.e.*, there exists a constant $c_0 > 0$ such that $\mu_X(\tau > n) = \mathcal{O}(\mathrm{e}^{-c_0 n})$. Moreover, by Theorem 4.2.3 we have that $\mu_X(r_{\mathrm{Neu}} > t)$ has polynomial tails; that is, there is a constant $c_1 > 0$ such that $\mu_X(r_{\mathrm{Neu}} > t) = \mathcal{O}(c_1 t^{-\beta_2})$, where $\beta_2 = \frac{a_2+b_2}{2b_2}$. Then by Proposition 5.1 in [19] we have that $\mu_X(R > t) = \mathcal{O}((\ln t)^{\beta_2} t^{-\beta_2})$.

The fourth and last detail concerns how to improve the estimates for $\mu_X(R > t)$ and remove the logarithmic term. For this, we make use of Lemma 4.1 in [13]. There the settings is made for infinite horizon planar periodic Lorentz gases, for that setting the tails of the flow time (in this work denoted by r_{Neu}) is of order $\mathcal{O}(t^{-2})$. By replacing in Lemma 4.1 the order of the tails from $\mathcal{O}(t^{-2})$ to $\mathcal{O}(c_1 t^{-\beta_2})$ we can use the same proof to remove the logarithmic term. Hence, we have that $\mu_X(R > t) = \mathcal{O}(t^{-\beta_2})$. With this we conclude our proof. $\square$

Chapter 8

Alternative neutral forms

The goal of this chapter is to generalize the neutral form we used to construct the neutral Lorenz flow. So far, the local form near the periodic orbit $\Gamma = \{\bar{0}\}$ was a product where the y component was independent from the x and z component. Now, we will generalize this local form by allowing the y component to depend on the x and z component, and investigate the effects of this dependence on the construction of the neutral Lorenz flow.

8.1 First modified neutral form

In this section, instead of considering Equation (4.1) we will take the following neutral form, which we refer as Neutral model 2 to avoid confusion:

$$\begin{pmatrix} \dot{x} \\ \dot{y} \\ \dot{z} \end{pmatrix} = G \begin{pmatrix} x \\ y \\ z \end{pmatrix} = \begin{pmatrix} x(a_0x^2 + a_2z^2) \\ -\ell y(1 + c_0x^2 + c_2z^2) \\ -z(b_0x^2 + b_2z^2) \end{pmatrix} + \mathcal{O}(4). \tag{8.1}$$

Since we want to exploit the results of [17] and [20]; *i.e.*, we want to make use of the asymptotics given in Section 4.2, we let a_0, a_2, b_0 and b_2 satisfy the same properties stated in Section 4.1 and let c_0 and $c_2 > 0$. Recall that $\Gamma = \{(0, 0, 0)\}$ is the only neutral periodic orbit and in a neighbourhood U of Γ the flow has the form of Equation (8.1). Note as before that the vector field is cubic in the transversal direction to Γ, but this is the only source of non-hyperbolicity.

If $x = 0$ and $z = 0$, then we see that $\dot{x} = 0$, $\dot{y} = -\ell y$ and $\dot{z} = 0$. Hence, the $y-$axis is invariant and all solutions tend to the origin as in the previous model. Moreover, since $\dot{x}$ and $\dot{z}$ are decoupled from y then we have Equation (4.4) and all the asymptotic of Section 4.2 will follow. We also have that $\mathrm{Div}(F) = (3a_0 - \ell c_1 - b_0)x^2 + (a_2 - \ell c_2 - 3b_2)z^2 - \ell$. Since we want a flow that shrinks volumes exponentially fast as before, we need that $\mathrm{Div}(F) = -c < 0$, where c is some positive constant. Thus, we let ℓ to be big enough such that $\frac{(3a_0-b_0)x^2+(a_2-3b_2)z^2}{1+c_0x^2+c_2z^2} < \ell$ for all x and z.

As in Section 4.1, we have that

$$DG|_{\bar{0}} = \begin{pmatrix} 0 & 0 & 0 \\ 0 & -\ell & 0 \\ 0 & 0 & 0 \end{pmatrix},$$

where $\bar{0} = (0,0,0)$. $DG|_{\bar{0}}$ has eigenvalues $\lambda_{1,3} = 0$, $\lambda_2 = -\ell$ with associated eigenvectors $(1,0,0)$, $(0,1,0)$ and $(0,0,1)$.

As in Section 4.3, we will consider the same cross-section Σ and we will proceed to construct the Poincaré map in the same way. First, let us state an auxiliary result, known as Grönwall's Lemma, that will help us to find an explicit expression for the Poincaré map. Its proof can be found in [46, Theorem 1.12]

8.1.1 Theorem. *Let $u : [a,b] \to \mathbb{R}^+$ be non-negative and differentiable. Moreover, assume the following differential inequality holds for u:*

$$\dot{u} \leq \psi(t)u(t)$$

for almost every $t \in [a,b]$, where $\psi : [a,b] \to \mathbb{R}^+$ is continuous and non-negative. Then we have that

$$u(t) \leq u(t_0)\exp(\int_a^t \psi(s)\, ds)$$

for every $t \in [a,b]$.

Let us denote by N^t the flow obtained from Equation (8.1); that is, $N^t(x,y,z)$ $= (x(t), y(t), z(t))$. By Equation (4.6) we get the following form for the flow,

$$N^{t(x,z)}(x,y,z) = (x_0, y(t(x,z)), \omega(z, t(x,z)). \tag{8.2}$$

Note that $\dot{y} = y(-\ell(1 + c_0x^2 + c_2z^2))$. By taking $u(t) = y(t)$ and $\psi(t) = -\ell(1 + c_0x^2 + c_2z^2)$ and applying Theorem 8.1.1 we get,

$$\begin{aligned} y(t) &= y_0 \exp(-\ell \int_0^t (1 + c_0x^2 + c_2z^2)ds) \\ &= y_0 \, \mathrm{e}^{-\ell t} \exp(-\ell \int_0^t (c_0x^2 + c_2z^2)ds). \end{aligned} \tag{8.3}$$

By the estimates of the Dulac map given in Theorem 4.2.2 and since $z \in \Sigma$, we obtain that the time $t(x,z)$ becomes a function of the variable x and the integral $\int_0^t (c_0x^2 + c_2z^2)ds$ can be expressed as a function of the variable x which we denote by $q(x)$. Observe that $q(x) > 0$ for every x. Therefore we get that,

$$y(t) = y_0 \, \mathrm{e}^{-\ell t} \, \mathrm{e}^{-\ell q(x)} . \tag{8.4}$$

Hence $y(t)$ decreases exponentially fast as before but with a faster rate. All together, we get that the map $N : \Sigma \to S$ is given by

$$\begin{aligned} N(x,y,1) &= \mathrm{N}^{t(x)}(x,y,1) \\ &= \Big(1, y \, \mathrm{e}^{-\ell(|x|^{-\frac{1}{\beta_2}} + q(x))}, |x|^{\beta}\Big), \end{aligned} \tag{8.5}$$

where $\beta = \frac{\beta_0}{\beta_2}$, compare this with Equation (4.8). Its derivative is given by

$$D_{(x,y)}N = \begin{pmatrix} \ell y(\frac{1}{\beta_2} x^{-(1+\frac{1}{\beta_2})} - q'(x)) \, \mathrm{e}^{-\ell(x^{-\frac{1}{\beta_2}} + q(x))} & \mathrm{e}^{-\ell(x^{-\frac{1}{\beta_2}} + q(x))} \\ \beta x^{\beta - 1} & 0 \end{pmatrix}. \tag{8.6}$$

Note that the y component of N can be written as a function of the z component; that is, if we denote the z and y component of N by $\tilde{z}$ and $\tilde{y}$, respectively. Then,

$$\tilde{y}(\tilde{z}) = \tilde{y}\,\mathrm{e}^{-\ell(\tilde{z}^{-\frac{1}{\beta_0}}+q(\tilde{z}^{\frac{1}{\beta}}))}\,. \tag{8.7}$$

We have the same observations stated in Section 4.3; that is:

1.- $N(\Sigma^{\pm})$ has a cusp-like shape, since by Equation (8.7), N maps lines $y = c$ to curves of the form $\tilde{y}(\tilde{z})$. Each of these image curves meets the $xy-$plane perpendicularly at $(1, 0, 0)$. The cusp-like shapes vary as we vary $\frac{1}{2} < \beta_0 < 2$ and $\beta \in (0, 1)$. The shapes we obtain in this case are similar to the ones depicted in Figure 4.4. We will denote $N(\Sigma^{\pm})$ by $S^{\pm}$ and $S = S^{+} \cup S^{-}$.

2.- The map N takes again the vertical line segments in Σ to the horizontal line segments in S, where the vertical lines in Σ are given by making the x coordinate constant and the horizontal lines in S by making z constant; *i.e.*, $N(\ell_v(c_0)) = \ell_h(c_1)$ as illustrated in Figure 3.6.

To complete the return to Σ we proceed as before and use the map P_2 to send the cusp-like shapes back to the cross-section. Therefore, the modified return map $P_{\text{Neu}} : \Sigma \to \Sigma$ is given by $P_{\text{Neu}} = P_2 \circ N$; that is,

$$P_{\text{Neu}}(x, y) = \begin{cases} ax^{\beta} - 1,\ y\,\mathrm{e}^{-\ell(x^{-\frac{1}{\beta_2}}+q(x))} - \dfrac{1}{2}, & \text{if } x \in (0, 1]; \\ 1 - a|x|^{\beta},\ y\,\mathrm{e}^{-\ell(|x|^{-\frac{1}{\beta_2}}+q(x))} + \dfrac{1}{2}, & \text{if } x \in [-1, 0), \end{cases} \tag{8.8}$$

where $\beta = \frac{\beta_0}{\beta_2} \in (0, 1)$. Its derivative is $DP_{\text{Neu}} = DP_2 \cdot DN$ and is given by

$$DP_{\text{Neu}} = \begin{pmatrix} a\beta x^{\beta-1} & 0 \\ \ell y(\frac{1}{\beta_2}x^{-(1+\frac{1}{\beta_2})} - q'(x))\,\mathrm{e}^{-\ell(x^{-\frac{1}{\beta_2}}+q(x))} & \mathrm{e}^{-\ell(x^{-\frac{1}{\beta_2}}+q(x))} \end{pmatrix}. \tag{8.9}$$

The matrix DP_{Neu} has eigenvalues $\lambda_1 = a\beta x^{\beta-1}$ and $\lambda_2 = \mathrm{e}^{-\ell(x^{-\frac{1}{\beta_2}}+q(x))}$. Since $\beta \in (0, 1)$ we have that $\lambda_1 \to \infty$ as $x \to 0$. For the other eigenvalue we have that $\lambda_2 < 1$ and $\lambda_2 \to 0$ as x goes to 0 since $(|x|^{-\frac{1}{\beta_2}} + q(x)) \to \infty$ as x goes to 0. Thus the modified Poincaré map P_{Neu} is hyperbolic when x approaches the origin.

The properties stated in Chapter 4 remain true for this new modified return map P_{Neu} like the invariance of the stable foliation given by the vertical lines $\ell_v(c)$ under the map P_{Neu} (See Figure 3.8). Hence, we can express again P_{Neu} as $P_{\text{Neu}}(x,y) = (f_{\text{Neu}}(x), g_{\text{Neu}}(x,y))$ for some functions $f_{\text{Neu}} : I \setminus \{0\} \to I$ and $g_{\text{Neu}} : (I \setminus \{0\}) \times I \to I$, where $I = [-1,1]$.

The properties of $g_{\text{Neu}}(x,y)$ are the same as the ones we stated in Section 4.3. We just make the warning that the constants used in Section 4.3 will be different for the new version of $g_{\text{Neu}}(x,y)$, since in this new case we have the extra term $q(x)$, which makes the rate of contraction on the y direction stronger than the case studied in Chapter 4.

As before, $\gamma(p)$ denotes the invariant stable leaf which contains the point $p \in \Sigma$ and we make an equivalence class of points in Σ that lie on the same $\gamma(p)$. If we collapse equivalence classes to points, we obtain a map $\pi : \Sigma \to [-1,1]$ given by $\pi(p) = x$, where $p = (x,y)$. Since P_{Neu} takes equivalence classes into equivalence classes, P_{Neu} and π induces the map $f : I \setminus \{0\} \to I$, whose graph is depicted in Figure 4.5. The new map f is a slight modification of the Lorenz map f_{Lor} obtained in Chapter 3 and all the properties mentioned there also hold for the new version f. We will fix notation and denote this modification of the Lorenz map by f_{Neu} and is given by:

$$f_{\text{Neu}}(x) = \begin{cases} ax^{\beta} - 1, & \text{if } x \in (0,1]; \\ \\ 1 - a|x|^{\beta}, & \text{if } x \in [-1,0), \end{cases} \tag{8.10}$$

where $\beta = \dfrac{\beta_0}{\beta_2} \in (0,1)$.

As we saw in Chapter 4 the one-dimensional map f_{Neu} also admits a unique exact a.c.i.p measure $\mu_{\text{Neu}} = \varphi_{\text{Neu}} m$ with $\varphi_{\text{Neu}} \in \text{BV}(I)$. Furthermore, μ_{Neu} has exponential decay of correlations for observables in $\text{BV}(I)$ and satisfies the CLT by Theorem 3.4.3 and Theorem 3.4.4, respectively.

In Section 5.2 we saw that the modified geometrical Lorenz attractor Λ_N is a partially hyperbolic attractor, the existence of a $C^{1+\alpha}$ strong-stable foliation $\mathcal{F}^{ss}$ for the flow, where $0 < \alpha < 1$, and the existence of a strong-stable foliation $\mathcal{F}^{ss}_{\Sigma}$ for the modified return map whose transversal smoothness is also $C^{1+\alpha}$. Following the same arguments, we can arrive to the same conclusions for the case considered in this section since we have the same properties, namely $\lambda_{ss} = -\ell$, $\lambda_s = 0$, $\lambda_u = 0$, strong dissipativity and partially hyperbolicity of the attractor Λ_N.

The return time for the modified Poincaré map P_{Neu}, considered in this section, is the same we obtained before, see Equation (5.11); that is, we still have a polynomial return time. Moreover, the UNI condition for this new modification of the geometrical Lorenz flow can be deduced in the same way we did for the case studied in Section 6.3, since we have the same one-dimensional map f_{Neu} and we can obtain the same inducing schemes we needed to prove the UNI condition.

Finally, the polynomial decay of correlations for the case study of this section follows in the same manner as that shown in Section 7.3. For completeness, we state it as Theorem 8.1.2 and its proof is the same as that of Theorem 7.3.2

8.1.2 Theorem. *Let Λ_{N}, $N_t : \Lambda_{\mathrm{N}} \to \Lambda_{\mathrm{N}}$ be the geometrical Lorenz neutral attractor, the geometrical Lorenz neutral flow obtained from the neutral form given by Equation* (8.1)*, respectively, and μ its SRB measure. Then N_t has polynomial decay of correlations; that is, there exist $m \geq 1$ and constant $C > 0$ such that for observables $v \in C^{\eta}(M) \cap C^{0,\eta}(M)$, $w \in C^{\eta,m}(M)$, and time $t > 1$ we have*

$$\rho_t(v, w) \leq C(\|v\|_{C^{\eta}} + \|v\|_{C^{0,\eta}}) \|w\|_{C^{\eta,m}} t^{-\beta_2}.$$

8.2 Second modified neutral Form

In this section, we will go a step further form Section 8.1 and let the x and z component also depend on the y component; that is, instead of considering Equation (8.1) we will take the following neutral form, which will be referred as the Neutral model 3 to avoid confusion.

$$\begin{pmatrix} \dot{x} \\ \dot{y} \\ \dot{z} \end{pmatrix} = G \begin{pmatrix} x \\ y \\ z \end{pmatrix} = \begin{pmatrix} x(a_0x^2 + a_1y^2 + a_2z^2) \\ -\ell y(1 + c_0x^2 + c_2z^2) \\ -z(b_0x^2 + b_1y^2 + b_2z^2) \end{pmatrix} + \mathcal{O}(4). \tag{8.11}$$

We want to use the results of [17] and [20]. Specifically, we want to make use of the asymptotic given in Section 4.2. For that, we let a_0, a_2, b_0 and b_2 satisfy the same properties stated in Section 4.1 and let $a?1$, c_0 and $c_2 > 0$ as before. Recall that $\Gamma = \{(0,0,0)\}$ is the only neutral periodic orbit and in a neighbourhood U of Γ the flow has the form of Equation (8.11). Note as before that the vector field is cubic in the transversal direction to Γ, but this is the only source of non-hyperbolicity.

If $x = 0$ and $z = 0$, then we see that $\dot{x} = 0$, $\dot{y} = -\ell y$ and $\dot{z} = 0$. Hence, the $y-$axis is invariant and all solutions tend to the origin as in the previous model. Now, we have that $\mathrm{Div}(F) = (3a_0 - \ell c_1 - b_0)x^2 + (a_1 - b_1)y^2 + (a_2 - \ell c_2 - 3b_2)z^2 - \ell$. Since we want a flow that shrinks volumes exponentially fast, we need that $\mathrm{Div}(F) = -c < 0$, where c is some positive constant. Thus, we let ℓ to be big enough such that $\frac{(3a_0-b_0)x^2+(a_1-b_1)y^2+(a_2-3b_2)z^2}{1+c_0x^2+c_2z^2} < \ell$ for all x, y and z.

As in the previous models, we have that

$$DG|_{\bar{0}} = \begin{pmatrix} 0 & 0 & 0 \\ 0 & -\ell & 0 \\ 0 & 0 & 0 \end{pmatrix},$$

where $\bar{0} = (0,0,0)$. $DG|_{\bar{0}}$ has eigenvalues $\lambda_{1,3} = 0$, $\lambda_2 = -\ell$ with associated eigenvectors $(1,0,0)$, $(0,1,0)$ and $(0,0,1)$.

The next step is to construct the Poincaré map $P_{\mathrm{Neu}} : \Sigma \to \Sigma$, where Σ is the cross-section previously considered. First, we note that for values of y small enough, the dependence of the x and z components on the y component in Equation (8.11) will be small enough that it can be considered negligible. Hence, we will be in the situation considered in the previous section. Therefore, following the analysis given in Section 8.1 we can give an explicit formula for the Poincaré map and the results therein will hold.

Unfortunately, for bigger values of y finding an explicit solution for the differential equation on the y component, and hence an explicit formula for the Poincaré map, is not straightforward as in the previous cases. Now, the way we will proceed for this case is the following: We will analyse and compare, with numerical methods, the limit behaviour of the Dulac maps obtained in [17] and [20] and adapted to our framework. More precisely, we will analyse the limit behaviour of the map $N : \Sigma \to S$ (see Equation (8.5) and Equation (4.7)). This is sufficient since the Poincaré maps considered in this work are given by $P_{\mathrm{Neu}} = P_2 \circ N$, where $P2$ is a diffeomorphism (see Section 3.3) and the map N is the flow map from the cross-section Σ to the cusps S, which depends on the differential equation being considered. Therefore, the behavioural changes exhibited by the map P_{Neu} are represented by the changes of the map N.

8.2.1 Numerics of the 2−dimensional case

We will start the numerical analysis in the 2−dimensional case; that is, we consider the framework of [17] and [20]. There, the following neutral form was considered:

$$\begin{pmatrix} \dot{x} \\ \dot{y} \end{pmatrix} = F \begin{pmatrix} x \\ y \end{pmatrix} = \begin{pmatrix} x(a_0 x^{\kappa} + a_2 z^{\kappa}) \\ -y(b_0 x^{\kappa} + b_2 y^{\kappa}) \end{pmatrix} + \mathcal{O}(4), \tag{8.12}$$

where a_0, a_2, b_0 and $b_2 > 0$ and $\Delta := a_2 b_0 - a_0 b_2 \neq 0$. For simplicity we let $\kappa = 2$. For the analysis of the Dulac map close to the neutral equilibrium of Equation (8.12), recall Section 4.2, we take an unstable leaf $W^u(0, y_0)$ and a stable leaf $W^s(x_0, 0)$, then the Dulac map $D : W^u(0, y_0) \to W^s(x_0, 0)$, shown in Figure 8.1, assigns the firs intersection $\phi^T(x, y_0)$ of the integral curve through (x, y_0) with the stable leaf $W^s(x_0, 0)$, where $x \in W^u(0, y_0)$ and T is the flow time; that is, the exit time (see Equation (4.6)). Recall that the estimates for the map D given in [20] and stated in Theorem 4.2.2 are:

$$\omega = D(x) = c(y_0) x^{\beta} (1 + \mathcal{O}(x^{\frac{1}{2\beta_2}})), \tag{8.13}$$

where $\beta = \frac{\beta_0}{\beta_2}$, $\beta_0 = \frac{a_0 + b_0}{2a_0}$ and $\beta_2 = \frac{a_2 + b_2}{2b_2}$.

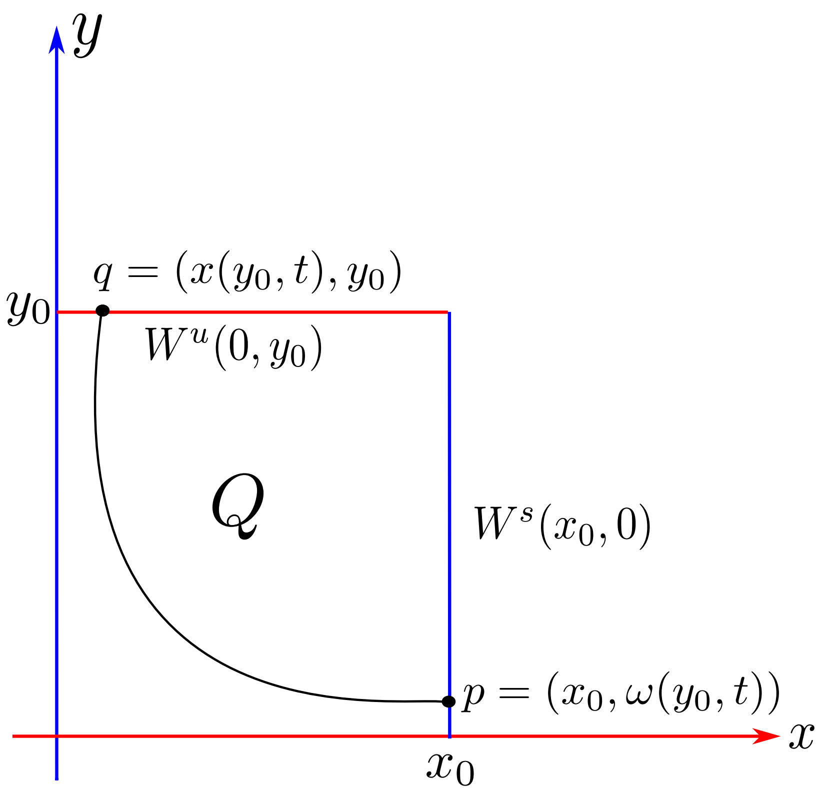

Figure 8.1: The Dulac map $D : W^u(0, y_0) \to W^s(x_0, 0)$.

For the setting considered in this work, we will perform the numerical experiments with $x_0 = 1$. In order to corroborate the estimates of the Dulac map given by Equation (8.13), we expect the numerical experiments to show us that

$$\beta \approx \frac{\ln(y)}{\ln(x)}. \tag{8.14}$$

We actually will see that

$$\beta = \frac{\ln(y)}{\ln(x)} - \frac{\ln(c(y_0))}{\ln(x)} + \mathcal{O}\Big(\frac{1}{\ln(x)}\Big). \tag{8.15}$$

From [17] and [20] we know that the constants $c(y_0)$ are given by a specific formula which is not easy to compute. For this reason, I decided to use the least-squares method to calculate the constants.

For the numerical experiments we will take different values of β and 250 points in different unstable leaves $W^u(0, y_0)$; that is, we will take 250 points $x \in [1.0 \times 10^{-5}, 1.0 \times 10^{-4}]$ and $y_0 \in \{0.5, 1.0\}$. The integration method we will use for the numerical experiments concerning this work is the so called Radau quadrature method. Since integration methods are out of the scope of this work, we encourage the reader to consult any book in numerical analysis for a detailed exposition of the Radau method, for example see [30]. Figure 8.2 *a*) and *b*) show us the approximation of β (the red graph), the adjusted approximation of β (green graph), and the theoretical value of β (blue graph). The approximation of beta is done by taking the last y value of each integral curve and divide it by the x value ranging in $[1.0 \times 10^{-5}, 1.0 \times 10^{-4}]$, the adjusted beta is calculated by using Equation (8.15). The points-axis corresponds to the 250 x values we considered starting from 1.0×10^{-4} and ending in 1.0×10^{-5}; that is, point 0 corresponds to the value $x = 1.0 \times 10^{-4}$ and point 250 corresponds to the value $x = 1.0 \times 10^{-5}$. The x points are taken from the unstable leaf at $y_0 = 1.0$ and the constant $c(y_0) = 1.2 \ln(1.1)$ for the adjusted approximation correspond to Figure 8.2 *a*), while the values taken from the unstable leaf at $y_0 = 0.5$ and the constant $c(y_0) = \ln(0.7)$ correspond to Figure 8.2 *b*). The approximations show an error that tends to decrease as we get closer to $x = 0$ as depicted in the both graphs. The value $\beta = 0.40$ is obtained by taking $a_0 = 15.0$, $a_2 = 5.0$, $b_0 = 1.0$ and $b_2 = 3.0$ in the vector field from Equation (8.12).

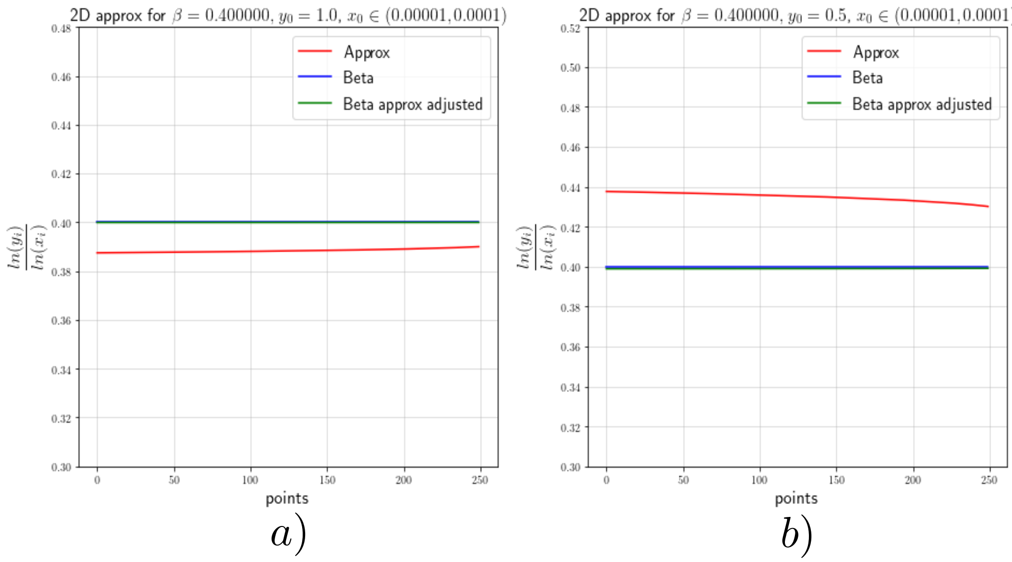

Figure 8.2: Numerical experimentation for $\beta = 0.40$

Figure 8.3 shows the same numerics performed for the value $\beta = 0.266666$, which is obtained by taking $a_0 = 15.0$, $a_2 = 6.0$, $b_0 = 1.0$ and $b_2 = 2.0$ in the vector field from Equation (8.12). For this beta value the constants for the adjusted approximations are $c(y_0) = \ln(0.8)$ and $c(y_0) = \ln(0.61)$ for Figure 8.3 a) and Figure 8.3 b), respectively. From the approximations we see, as before, that the error decreases as we approach to $x = 0$.

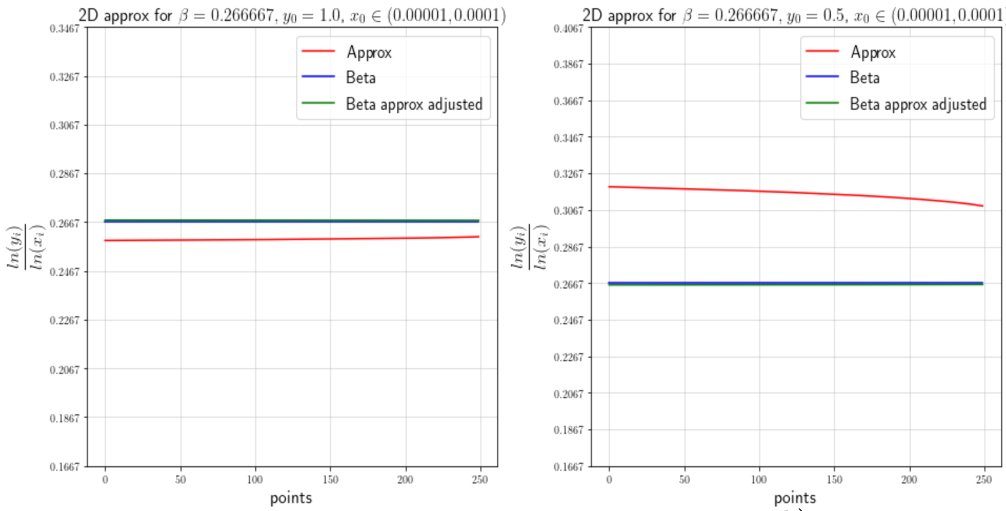

$a)$ $b)$

Figure 8.3: Numerical experimentation for $\beta = 0.266666$

Figure 8.4 shows the same numerics performed for the value $\beta = 0.741743$, which is obtained by taking the parameter values $a_0 = \sqrt{3}$, $a_2 = 6.0$, $b_0 = 3.0$ and $b_2 = \sqrt{5}$. For this case the constants for the adjusted approximations are $c(y_0) = \ln(1.32)$ and $c(y_0) = \ln(0.33)$ for Figure 8.4 $a)$ and Figure 8.4 $b)$, respectively. From the approximations we see, as before, that the error decreases as we approach to $x = 0$.

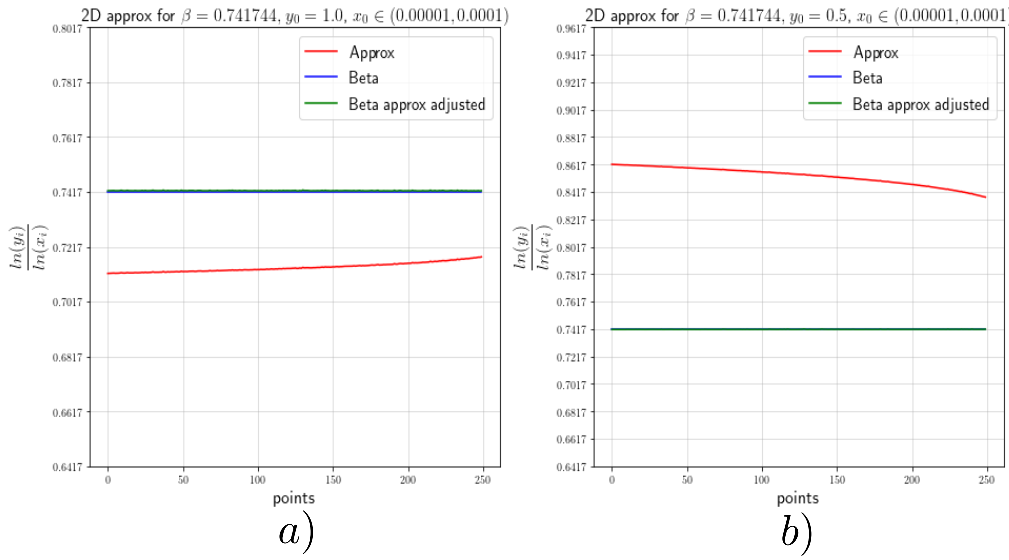

Figure 8.4: Numerical experimentation for $\beta = 0.741743$

Figure 8.5 shows the same numerics performed for the value $\beta = 0.741743$, which is obtained by taking $a_0 = 1.0$, $a_2 = 5.5$, $b_0 = 2.5$ and $b_2 = 2.0$ in the vector field from Equation (8.12). For this beta value the constants for the adjusted approximations are $c(y_0) = \ln(1.83)$ and $c(y_0) = \ln(0.31)$ for Figure 8.5 a) and Figure 8.5 b), respectively. From the approximations we see, as before, that the error decreases as we approach to $x = 0$.

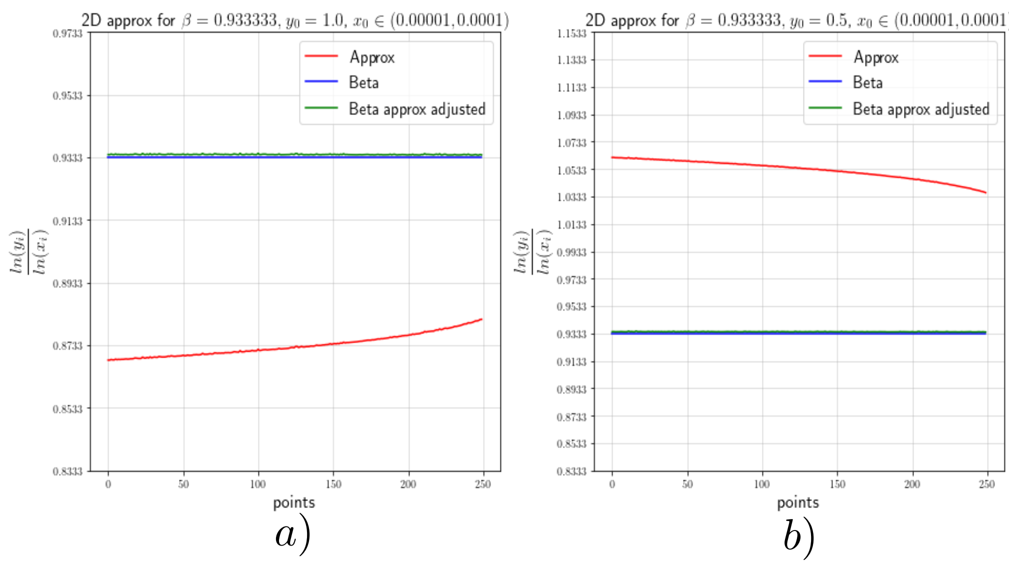

Figure 8.5: Numerical experimentation for $\beta = 0.933333$

8.2.2 Numerics of the 3−dimensional case

In this subsection we will perform the numeric experiments for the 3−dimensional models. We will start with the first Neutral model; that is, the one studied in Chapter 4, which we will refer as Neutral model. Recall that the Neutral model was given by

$$\begin{pmatrix} \dot{x} \\ \dot{y} \\ \dot{z} \end{pmatrix} = N \begin{pmatrix} x \\ y \\ z \end{pmatrix} = \begin{pmatrix} x(a_0x^2 + a_1y^2 + a_2z^2) \\ -\ell y \\ -z(b_0x^2 + b_1y^2 + b_2z^2) \end{pmatrix} + \mathcal{O}(4), \tag{8.16}$$

where $a_0,\ a_1,\ a_2,\ b_0,\ b_1,\ b_2$ and $\ell > 0$ and $\Delta := a_2b_0 - a_0b_2 \neq 0$. For the analysis of the Dulac map close to the neutral equilibrium of Equation (8.16), we will perform the numerical analysis on $N : \Sigma \to S$. For the purpose of this work, we want to show with the numeric experimentation that the x and z components behaves like the 2−dimensional model from the previous subsection regardless of the y value. To perform the numerical analysis we will take different unstable leaves $W^u(x, y_0, z_0)$ and a stable leaf $W^s(1, 0, 0)$, where $y_0 \in \{1.0, 0.5\}$ and $z_0 = 1.0$. We will just consider one value of z_0; that is, we consider just one cross-section since we want to show that the approximation of beta does not have radical changes when considering different values of y. Hence, like in the $2-$dimensional analysis we expect the numerical experiments to show us that

$$\beta \approx \frac{\ln(z)}{\ln(x)}, \tag{8.17}$$

where z is the last value of the integral curve with initial condition (x, y_0, z_0) for $x \in [1.0 \times 10^{-5}, 1.0 \times 10^{-4}]$. Again, we will actually show that

$$\beta = \frac{\ln(z)}{\ln(x)} - \frac{\ln(c(z_0))}{\ln(x)} + \mathcal{O}\Big(\frac{1}{\ln(x)}\Big). \tag{8.18}$$

As before, we will use the Radau quadrature method and take 250 points for the values of x starting from 1.0×10^{-4} and ending with 1.0×10^{-5}; that is, point 0 and point 250 correspond to $x = 1.0 \times 10^{-4}$ and $x = 1.0 \times 10^{-5}$, respectively. We will consider the same values of β we considered in the previous subsection. The approximation of beta, corresponding to the red line in all figures, is done by taking the last z value of each integral curve with initial condition (x, y_0, z_0) and divide it by the x value ranging in $[1.0 \times 10^{-5}, 1.0 \times 10^{-4}]$, the adjusted beta, ploted in green in all figures, is calculated by using Equation (8.18), and the theoretical value of β, corresponding to the blue graph in all figures, is obtained from the parameters a_0, a_2, b_0 and b_2.

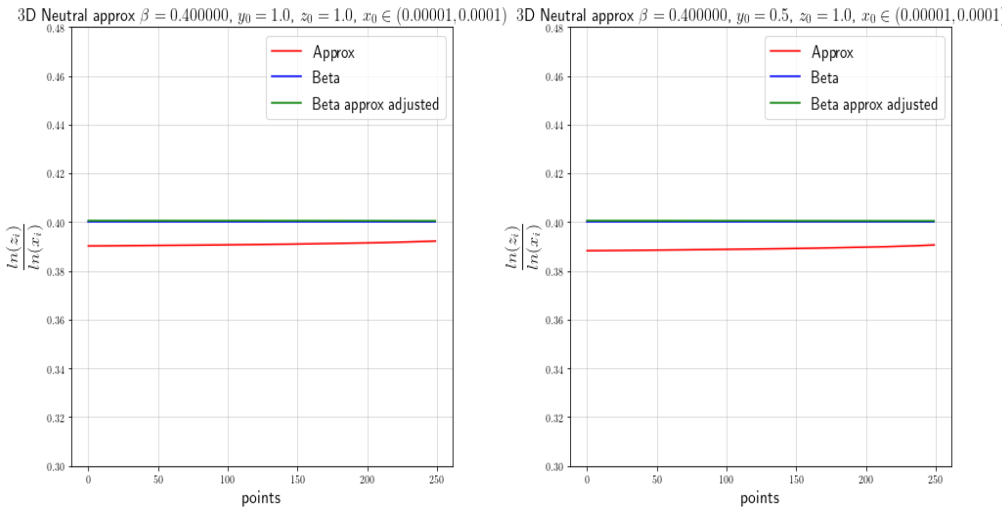

$a)$ $b)$

Figure 8.6: Numerical experimentation for the Neutral model with $\beta = 0.40$

Figure 8.6 $a)$ and $b)$ show us the the numerical approximations of the Neutral model with $\beta = 0.40$ for $y_0 = 1.0$ and $y_0 = 0.5$, respectively. We can observe in both plots, as before, that the beta approximation (red plot) approaches to the theoretical values of beta as we let x approach to 0; that is, the error made by the numerical methods tend to decrease as we get closer to the origin. Furthermore, we notice once again that the adjusted approximation of beta with constants $c(z_0) = \ln(1.1)$ and $c(z_0) = \ln(1.12)$ shown in Figure 8.6 $a)$ and $b)$, respectively, agrees with Equation (8.18). Moreover, the constant $c(z_0)$ is not affected drastically by the changes of the y values, which we expected to see since the y component decreases exponentially fast. In addition, we observe that the constants $c(z_0)$ and $c(y_0)$ from Equation (8.18) and Equation (8.15), respectively, are almost equal; that is, the x and z components of the 3$-$dimensional model behaves like the x and y component of the 2$-$dimensional model.

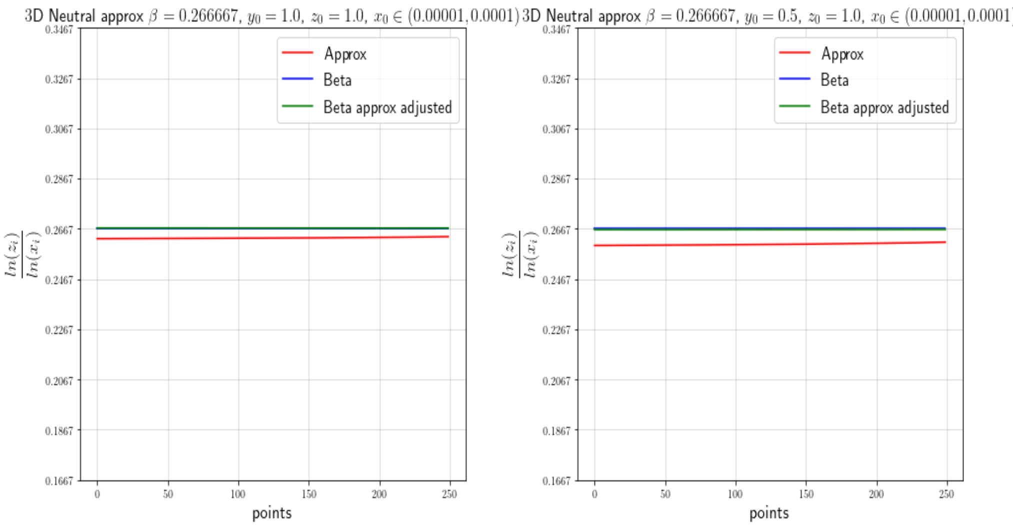

$a)$ $b)$

Figure 8.7: Numerical experimentation for the Neutral model with $\beta = 0.2666$

Figure 8.7 $a)$ and $b)$ show us the numerical results obtained for the case $\beta = 0.2666$ with $y_0 = 1.0$ and $y_0 = 0.5$, respectively. The results for this case are similar to the ones of the previous case. The constants for the adjusted beta approximation are $c(z_0) = \ln(1.06)$ and $c(z_0) = \ln(1.08)$ for Figure 8.7 a and b, respectively. Once again, the constants $c(z_0)$ of the 3−dimensional model and $c(y_0)$ of the 2−dimensional model are almost equal and $c(z_0)$ is not drastically affected when y changes.

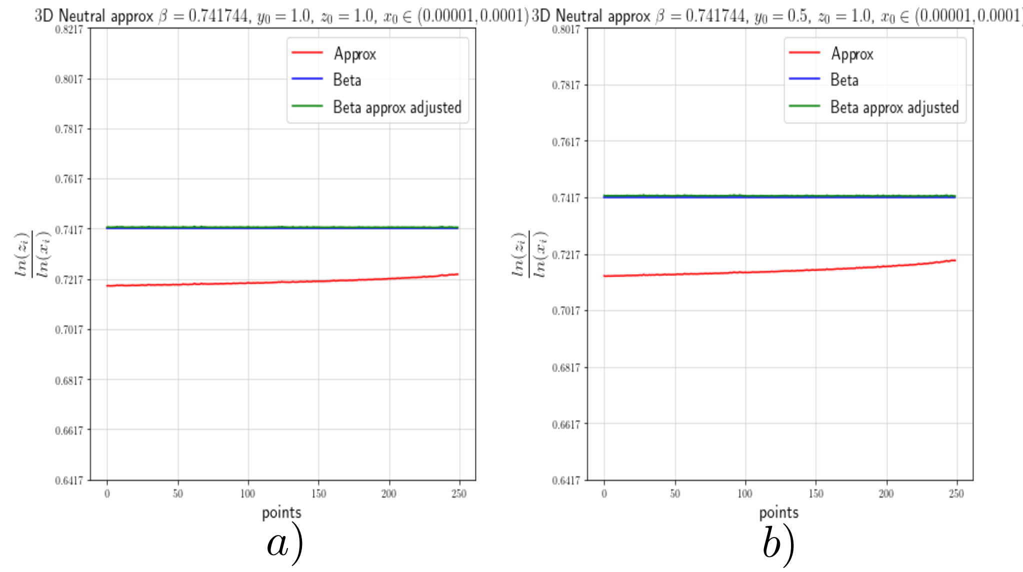

Figure 8.8: Numerical experimentation for the Neutral model with $\beta = 0.741743$

Figure 8.8 a) and b) show us the numerical results obtained for the case $\beta = 0.741743$ with $y_0 = 1.0$ and $y_0 = 0.5$, respectively. The results for this case and the ones of the previous cases are alike. The constants for the adjusted beta approximation are $c(z_0) = \ln(1.26)$ and $c(z_0) = \ln(1.3)$ for Figure 8.7 a and b, respectively. As before, the constants $c(z_0)$ and $c(y_0)$ of the 3$-$dimensional and the 2$-$dimensional model, respectively, are almost equal. Moreover, $c(z_0)$ is not drastically affected by the changes of y value.

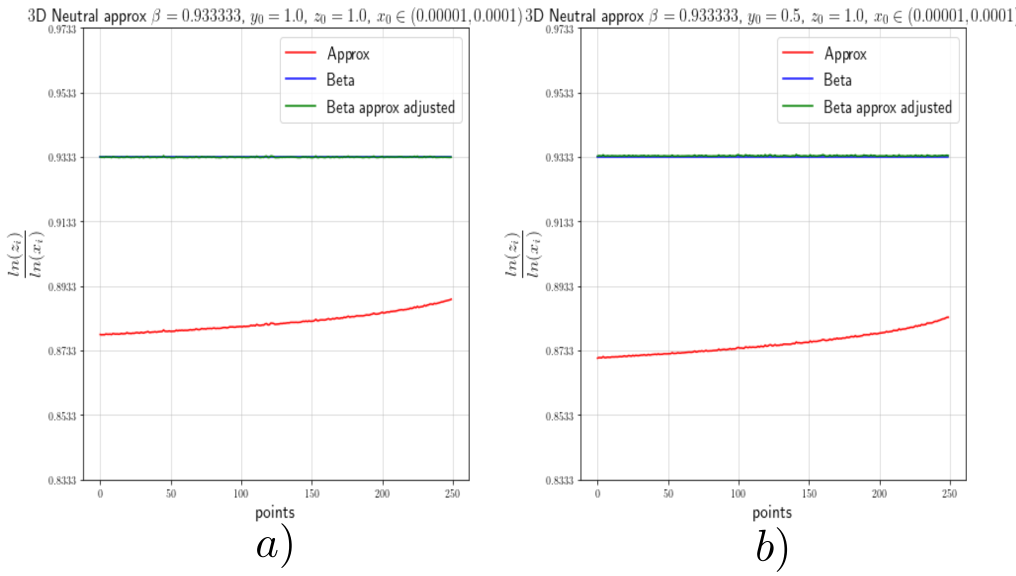

Figure 8.9: Numerical experimentation for the Neutral model with $\beta = 0.741743$

Figure 8.9 a) and b) display the numerical results obtained for the case $\beta = 0.933$ with $y_0 = 1.0$ and $y_0 = 0.5$, respectively. Once more, the results for this case and the ones of the previous cases are similar. The constants for the adjusted beta approximation are $c(z_0) = \ln(1.7)$ and $c(z_0) = \ln(1.78)$ for Figure 8.7 a and b, respectively. The constants $c(z_0)$ and $c(y_0)$ of the $3-$dimensional and the $2-$dimensional model, respectively, are again almost equal. Furthermore, $c(z_0)$ is not drastically affected by the changes of y value.

We will consider now the Neutral model 2 given by Equation (8.1) and present the numerical results obtained by performing the same experiments we did for the Neutral model 1. We start considering the case for $\beta = 0.40$. Figure 8.10 a) and b) show us the the numerical approximations of the Neutral model 2 for $y_0 = 1.0$ and $y_0 = 0.5$, respectively. We notice that the adjusted approximation of beta with constant $c(z_0) = \ln(1.12)$ for both Figure 8.10 a) and b) agrees with Equation (8.18). Moreover, observe that the constant $c(z_0)$ is the same for both cases $y_0 = 1.0$ and $y_0 = 0.5$, this was expected since the x and z component are independent of the y component. Once more, we observe that the constants $c(z_0)$ and $c(y_0)$ from Equation (8.18) and Equation (8.15), respectively, are almost equal; that is, the x and z

components of the 3−dimensional model behaves like the x and y component of the 2−dimensional model.

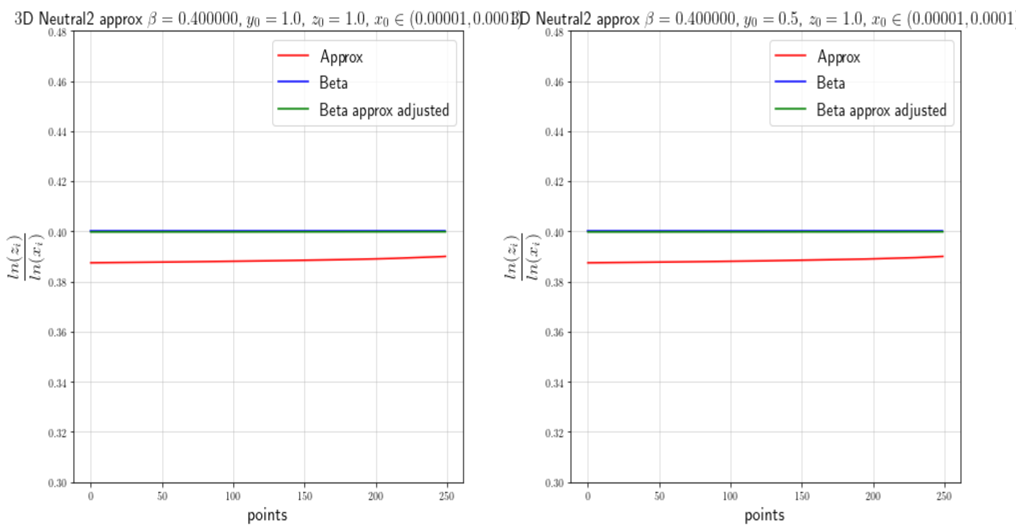

$a)$ $b)$

Figure 8.10: Numerical experimentation for the Neutral model 2 with $\beta = 0.40$

Figure 8.11 $a)$ and $b)$ show us the numerical results obtained for the case $\beta = 0.2666$ with $y_0 = 1.0$ and $y_0 = 0.5$, respectively. The results for this case are similar to the case $\beta = 0.40$. The constants for the adjusted beta approximation are $c(z_0) = \ln(1.08)$ for both Figure 8.11 a and b. Once again, the constants $c(z_0)$ of the 3−dimensional model and $c(y_0)$ of the 2−dimensional model are almost equal.

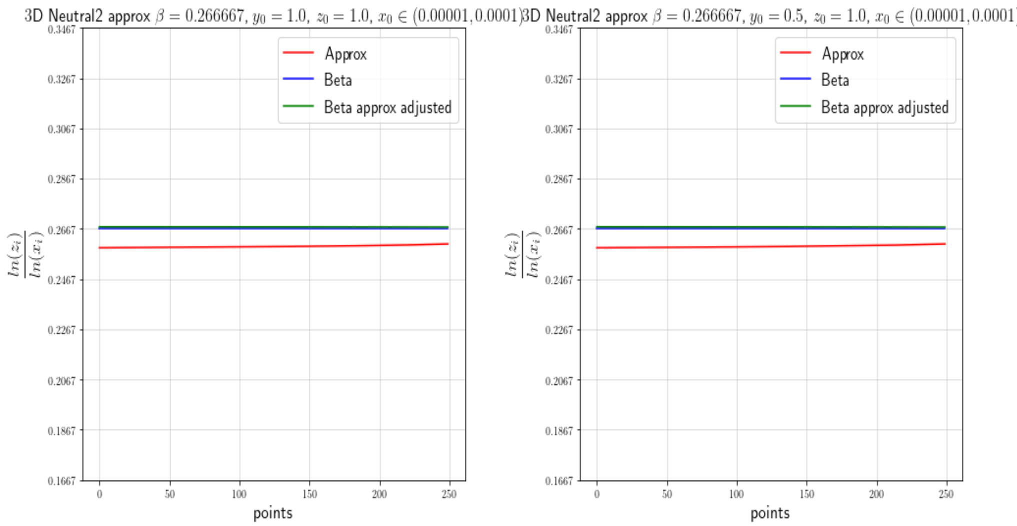

$a)$ $b)$

Figure 8.11: Numerical experimentation for the Neutral model 2 with $\beta = 0.2666$

Figure 8.12 $a)$ and $b)$ show us the numerical results obtained for the case $\beta = 0.741743$ with $y_0 = 1.0$ and $y_0 = 0.5$, respectively. The results for this case are similar to the ones of the previous cases. The constants for the adjusted beta approximation are $c(z_0) = \ln(1.31)$ for both Figure 8.12 a and b. Once again, the constants $c(z_0)$ of the 3−dimensional model and $c(y_0)$ of the 2−dimensional model are almost equal.

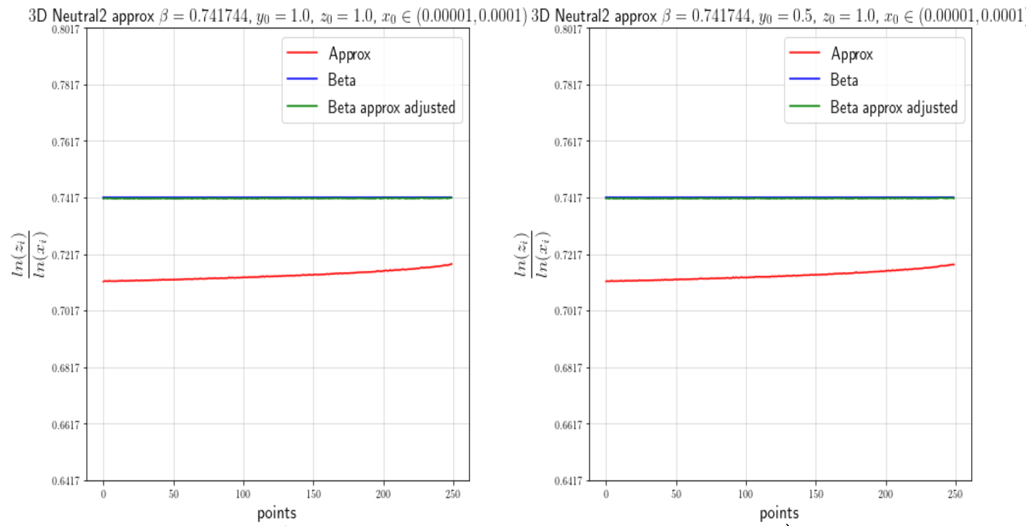

$a)$ $b)$

Figure 8.12: Numerical experimentation for the Neutral model 2 with $\beta = 0.741743$

Figure 8.13 $a)$ and $b)$ show us the numerical results obtained for the case $\beta = 0.933$ with $y_0 = 1.0$ and $y_0 = 0.5$, respectively. The results for this case and the ones of the previous cases are alike. As before, the constants for the adjusted beta approximation are $c(z_0) = \ln(1.8)$ for both Figure 8.13 a and b. The constants $c(z_0)$ and $c(y_0)$ of the 3−dimensional and the 2−dimensional model, respectively, are again almost equal.

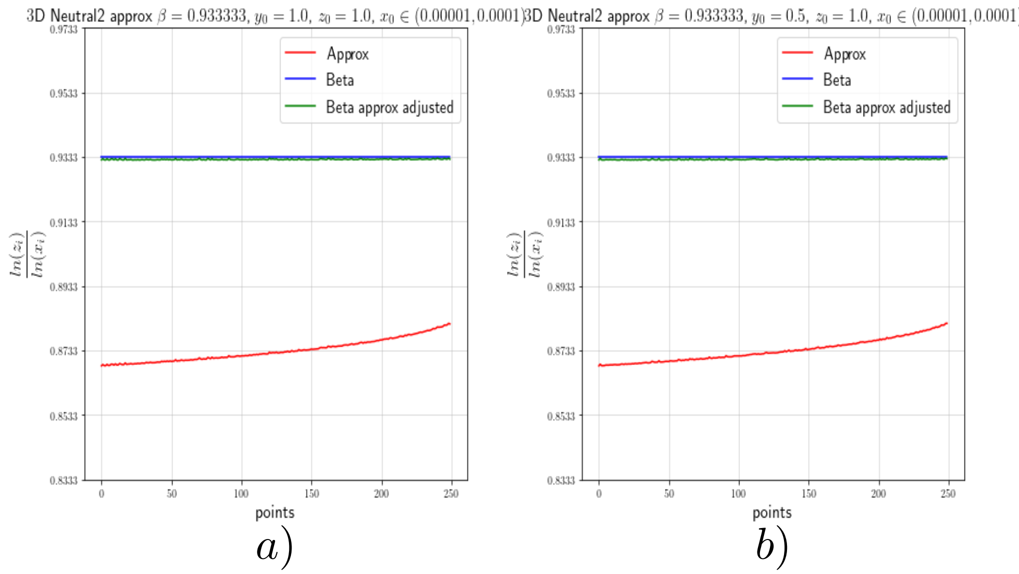

Figure 8.13: Numerical experimentation for the Neutral model 2 with $\beta = 0.933$

Until now we have performed the numerical experiments for the Neutral model 1 and 2 corresponding to the normal forms given by Equation (8.16) and (8.1), respectively. We saw there that for both models, the asymptotic behaviour of the x and z components are the same as the x and y component of the 2−dimensional model studied in the previous subsection. Recall that for this two models we had explicit formulas for the map $N : \Sigma \to S$ and hence for the modified Poincaré map $P_{\text{Neu}} : \Sigma \to \Sigma$. Our goal is to see that the asymptotic behaviour of the Neutral model 3 given by Equation (8.11) is similar to the other two models. Therefore, the numerical results obtained for the Neutral models 1 and 2 will be our reference and we will compare them to the numerical results obtained for the third model.

We start considering the case for $\beta = 0.40$. Figure 8.14 $a)$ and $b)$ display the the numerical approximations of the Neutral model 3 for $y_0 = 1.0$ and $y_0 = 0.5$, respectively. We notice that the adjusted approximation of beta with constant $c(z_0) = \ln(1.12)$ for both Figure 8.14 $a)$ and $b)$ agrees again with Equation (8.18). Moreover, observe that the constant $c(z_0)$ is the same for both cases $y_0 = 1.0$ and $y_0 = 0.5$, it is worth to recall that for this model the x and z component are not independent from the y component. Like in the previous models, we observe that the constants $c(z_0)$ and $c(y_0)$ from Equation (8.18) and Equation (8.15), respectively, are almost equal; that is, the x and z components of the 3−dimensional model behaves like the x and y component of the 2−dimensional model.

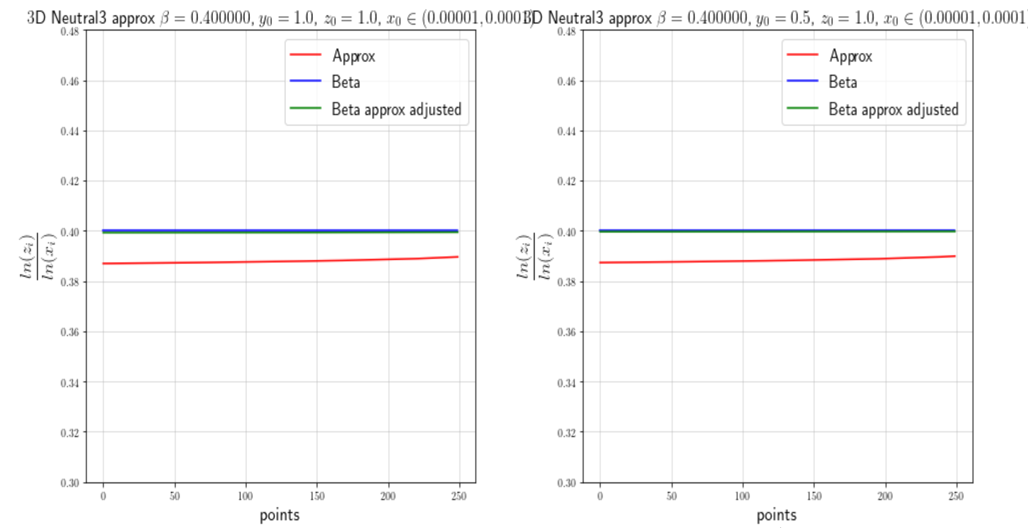

$a)$ $b)$

Figure 8.14: Numerical experimentation for the Neutral model 3 with $\beta =$ 0.40

Figure 8.15 $a)$ and $b)$ show us the numerical results obtained for the case $\beta = 0.2666$ with $y_0 = 1.0$ and $y_0 = 0.5$, respectively. The results for this case are similar to the case $\beta = 0.40$. The constants for the adjusted beta approximation are $c(z_0) = \ln(1.07)$ for both Figure 8.15 a and b. Once again, the constants $c(z_0)$ of the 3−dimensional model and $c(y_0)$ of the 2−dimensional model are almost equal.

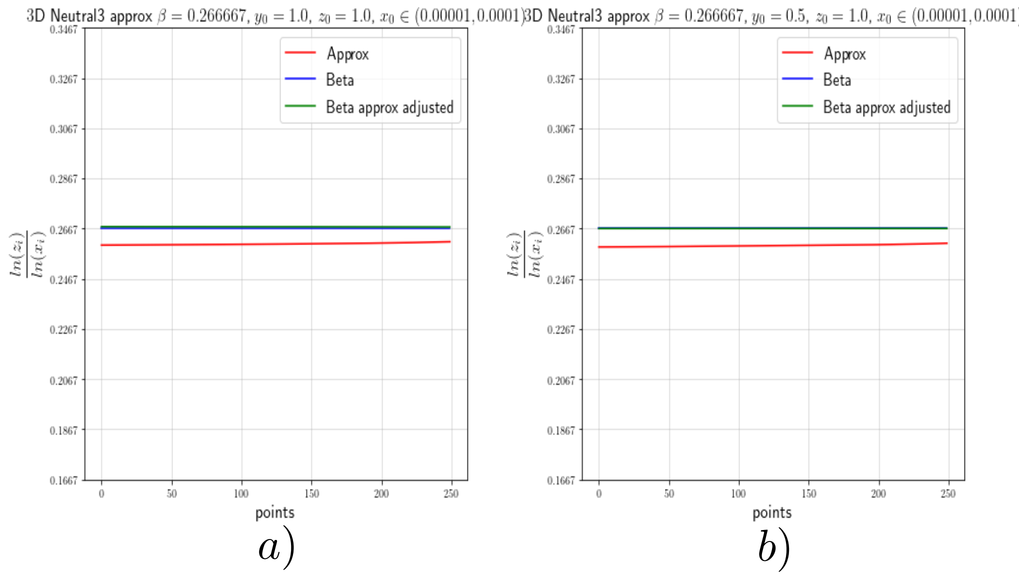

Figure 8.15: Numerical experimentation for the Neutral model 3 with $\beta = 0.2666$

Figure 8.16 $a)$ and $b)$ show us the numerical results obtained for the case $\beta = 0.741743$ with $y_0 = 1.0$ and $y_0 = 0.5$, respectively. The results for this case are similar to the ones of the previous cases. The constants for the adjusted beta approximation are $c(z_0) = \ln(1.3)$ for both Figure 8.16 a and b. Once again, the constants $c(z_0)$ of the $3-$dimensional model and $c(y_0)$ of the $2-$dimensional model are almost equal.

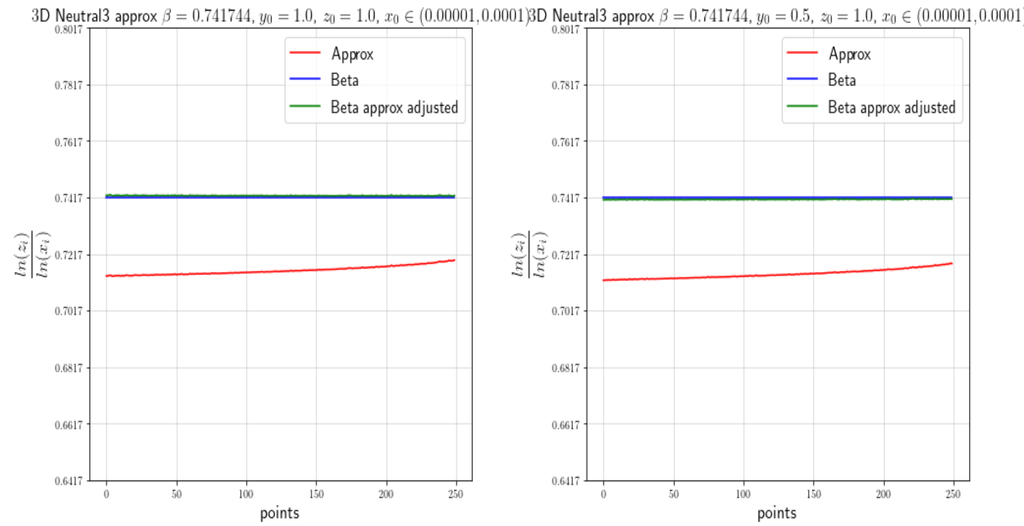

$a)$ $b)$

Figure 8.16: Numerical experimentation for the Neutral model 3 with $\beta = 0.741743$

Figure 8.17 $a)$ and $b)$ show us the numerical results obtained for the case $\beta = 0.933$ with $y_0 = 1.0$ and $y_0 = 0.5$, respectively. The results for this case and the ones of the previous cases are alike. As before, the constants for the adjusted beta approximation are $c(z_0) = \ln(1.8)$ for both Figure 8.17 a and b. The constants $c(z_0)$ and $c(y_0)$ of the 3−dimensional and the 2−dimensional model, respectively, are again almost equal.

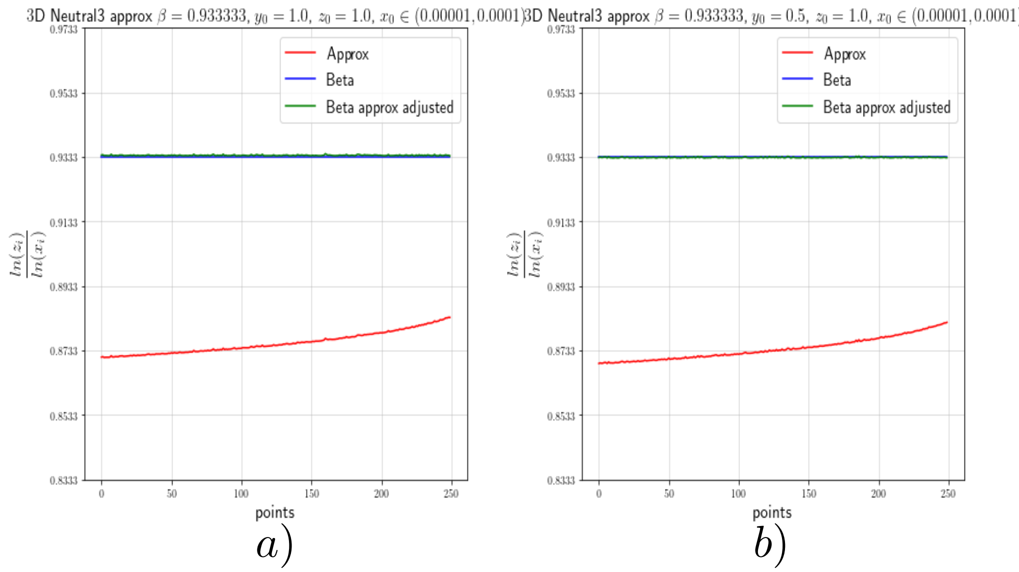

Figure 8.17: Numerical experimentation for the Neutral model 3 with $\beta = 0.933$

8.2.3 Numerics of the tails of the return map in the 3−dimensional case

In this subsection, we will perform the numeric experiments for the 3−dimensional models and see the approximations for the exponent of the decay of correlations; that is, for the exponent β_2. The general Neutral model or Neutral model 3 is given by

$$\begin{pmatrix} \dot{x} \\ \dot{y} \\ \dot{z} \end{pmatrix} = N \begin{pmatrix} x \\ y \\ z \end{pmatrix} = \begin{pmatrix} x(a_0x^2 + a_1y^2 + a_2z^2) \\ -\ell y(1 + c_0x^2 + c_2z^2) \\ -z(b_0x^2 + b_1y^2 + b_2z^2) \end{pmatrix} + \mathcal{O}(4), \tag{8.19}$$

where $a_0,\ a_1,\ a_2,\ b_0,\ b_1,\ b_2,\ c_0,\ c_2$ and $\ell > 0$ and $\Delta := a_2b_0 - a_0b_2 \neq 0$. Note that the Neutral model 1 and the Neutral model 2 are obtained from the general Neutral model if we let $c_0,\ c_2 = 0$ and if we let $a_1,\ b_1 = 0$, respectively.

In the previous subsection we saw the numerical analysis on $N : \Sigma \to S$ and showed, with the numeric experimentation, that the x and z components behaves like the 2−dimensional model regardless of the y value. For the numerical analysis we are about to perform, we will take an unstable leaf $W^u(x, y_0, z_0)$ and a stable leaf $W^s(1, 0, 0)$, where $y_0 = 1.0$ and $z_0 = 1.0$. From the estimates obtained in Theorem 4.2.2 we can see that

$$\beta_2 \approx -\frac{\ln(x)}{\ln(t)}, \tag{8.20}$$

where t is the flow time that it takes a point from the unstable leaf to hit the stable leaf and $x \in [1.0 \times 10^{-5}, 1.0 \times 10^{-4}]$. We will actually show that

$$\beta_2 = \frac{\ln(c(z_0))}{\ln(t)} - \frac{\ln(x)}{\ln(t)} + \mathcal{O}\Big(\frac{1}{\ln(t)}\Big). \tag{8.21}$$

As before, we will use the Radau quadrature method and take 50 points for the values of x starting from 1.0×10^{-4} and ending with 1.0×10^{-5}; that is, point 0 and point 50 correspond to $x = 1.0 \times 10^{-4}$ and $x = 1.0 \times 10^{-5}$, respectively. We will consider the same values of β we considered in the previous subsection except for the value $\beta = 9333$. The approximation of β_2, corresponding to the red line in all figures, is done by taking the x value, ranging in $[1.0 \times 10^{-5}, 1.0 \times 10^{-4}]$, of each integral curve with initial condition (x, y_0, z_0) and divide it by the flow time t, the adjusted approximation of β_2, shown in green in all figures, is calculated by using Equation (8.21), and the theoretical value of β_2, corresponding to the blue graph in all figures, is obtained from the parameters a_2 and b_2; that is $\beta_2 = \frac{a_2+b_2}{2b_2}$.

We start considering the Neutral model 1. Figure 8.18 a) shows the approximation for $\beta_2 = 1.333$ which corresponds to the case $\beta = 0.40$, for the adjusted approximation the constant is $\ln(c(z_0)) = 0.06$, b) displays the approximation for $\beta_2 = 2.0$ corresponding to the case $\beta = 0.266$ with adjustment constant $\ln(c(z_0)) = 0.05$ and in c) we can see the approximation for $\beta_2 = 1.84$ with corresponding $\beta = 0.741743$ and adjustment constant $\ln(c(z_0)) = 0.2$

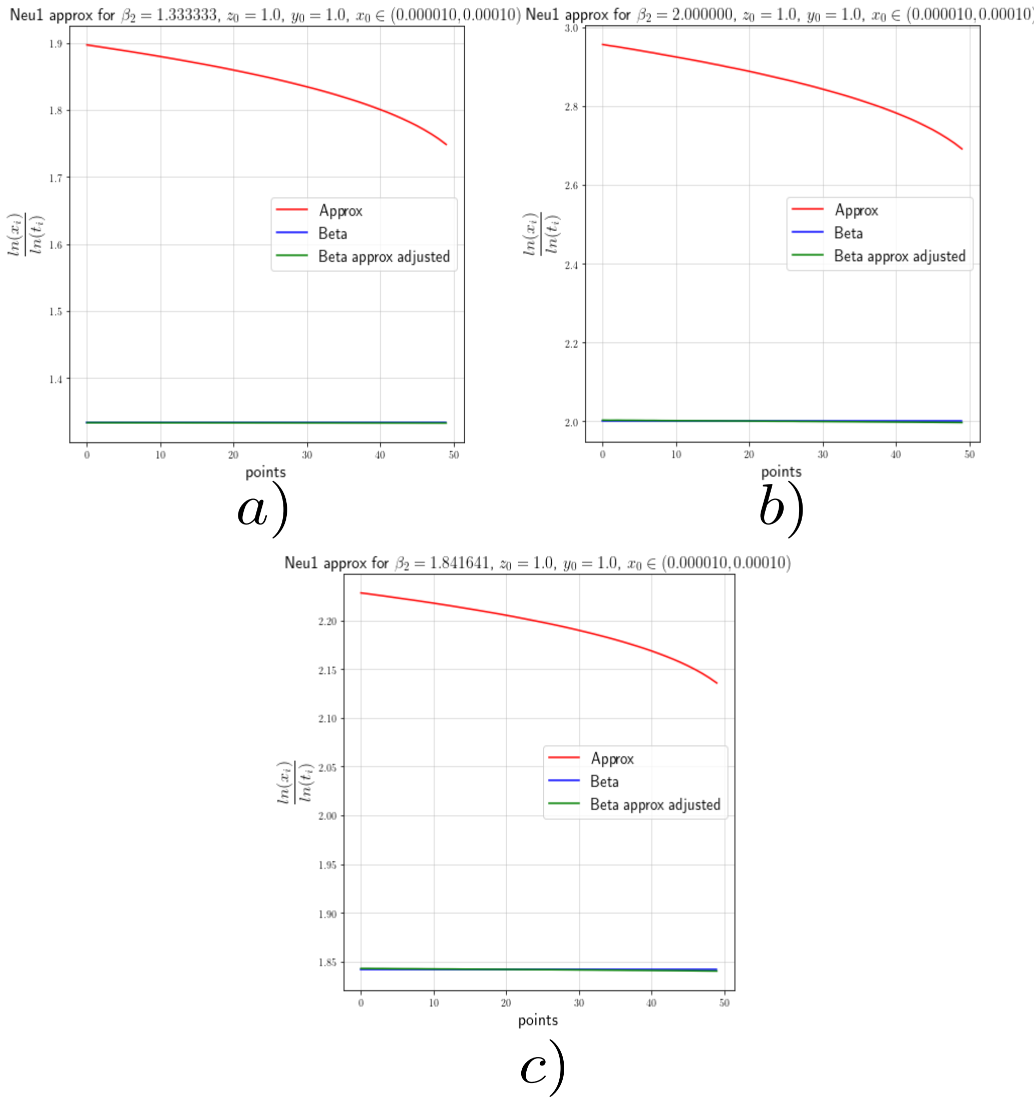

Figure 8.18: Numerical experimentation for β_2 approximation for the Neutral model 1

Next, we consider the Neutral model 2. Figure 8.19 $a)$ shows the approximation for $\beta_2 = 1.333$ which corresponds to the case $\beta = 0.40$, for the adjusted approximation the constant is $\ln(c(z_0)) = 0.06$, $b)$ displays the approximation for $\beta_2 = 2.0$ corresponding to the case $\beta = 0.266$ with adjustment constant $\ln(c(z_0)) = 0.04$ and in $c)$ we can see the approximation for $\beta_2 = 1.84$ with corresponding $\beta = 0.741743$ and adjustment constant $\ln(c(z_0)) = 0.18$

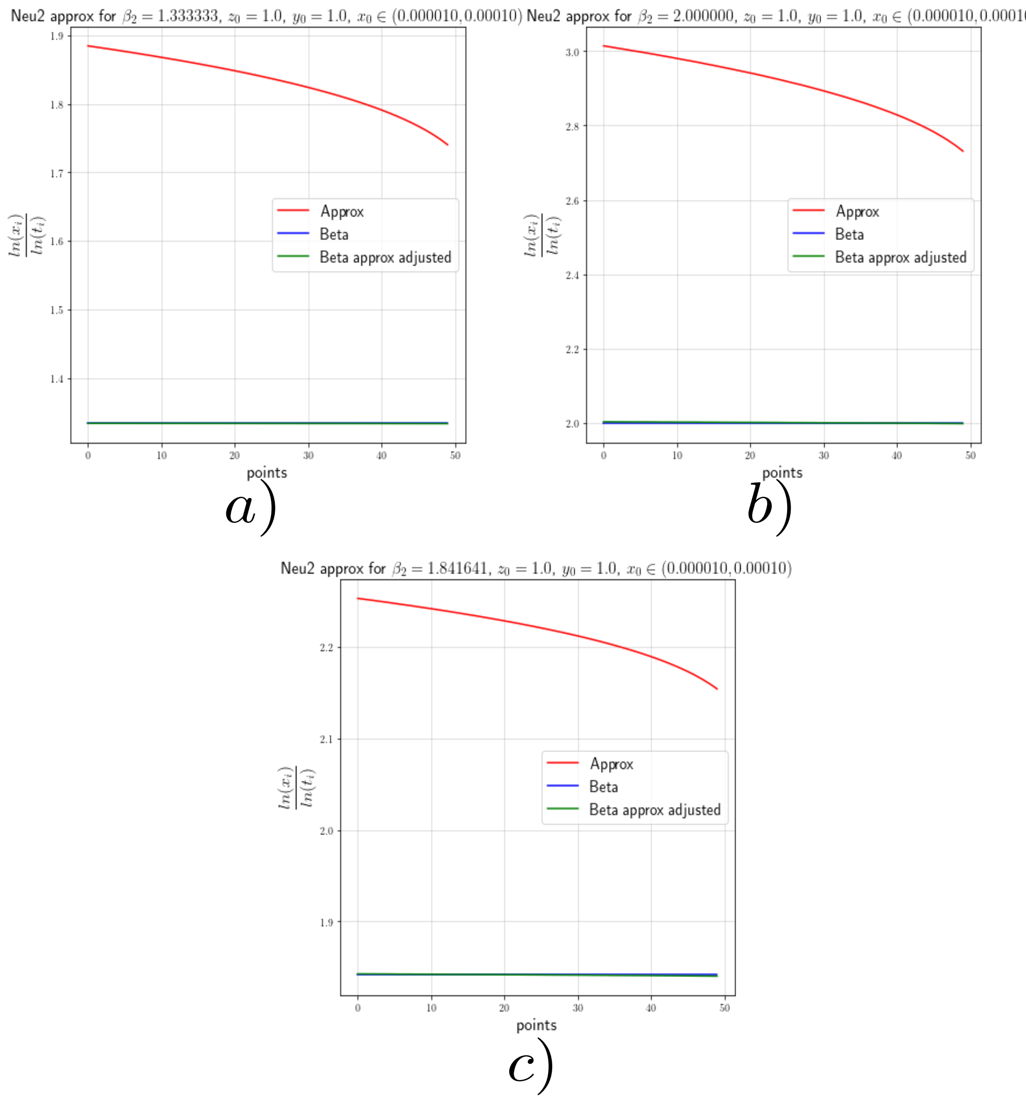

Figure 8.19: Numerical experimentation for β_2 approximation for the Neutral model 2

Last but not least, we consider the Neutral model 3. Figure 8.20 $a)$ shows the approximation for $\beta_2 = 1.333$ which corresponds to the case $\beta = 0.40$, for the adjusted approximation the constant is $\ln(c(z_0)) = 0.06$, $b)$ displays the approximation for $\beta_2 = 2.0$ corresponding to the case $\beta = 0.266$ with adjustment constant $\ln(c(z_0)) = 0.04$ and in c) we can see the approximation for $\beta_2 = 1.84$ with corresponding $\beta = 0.741743$ and adjustment constant $\ln(c(z_0)) = 0.19$

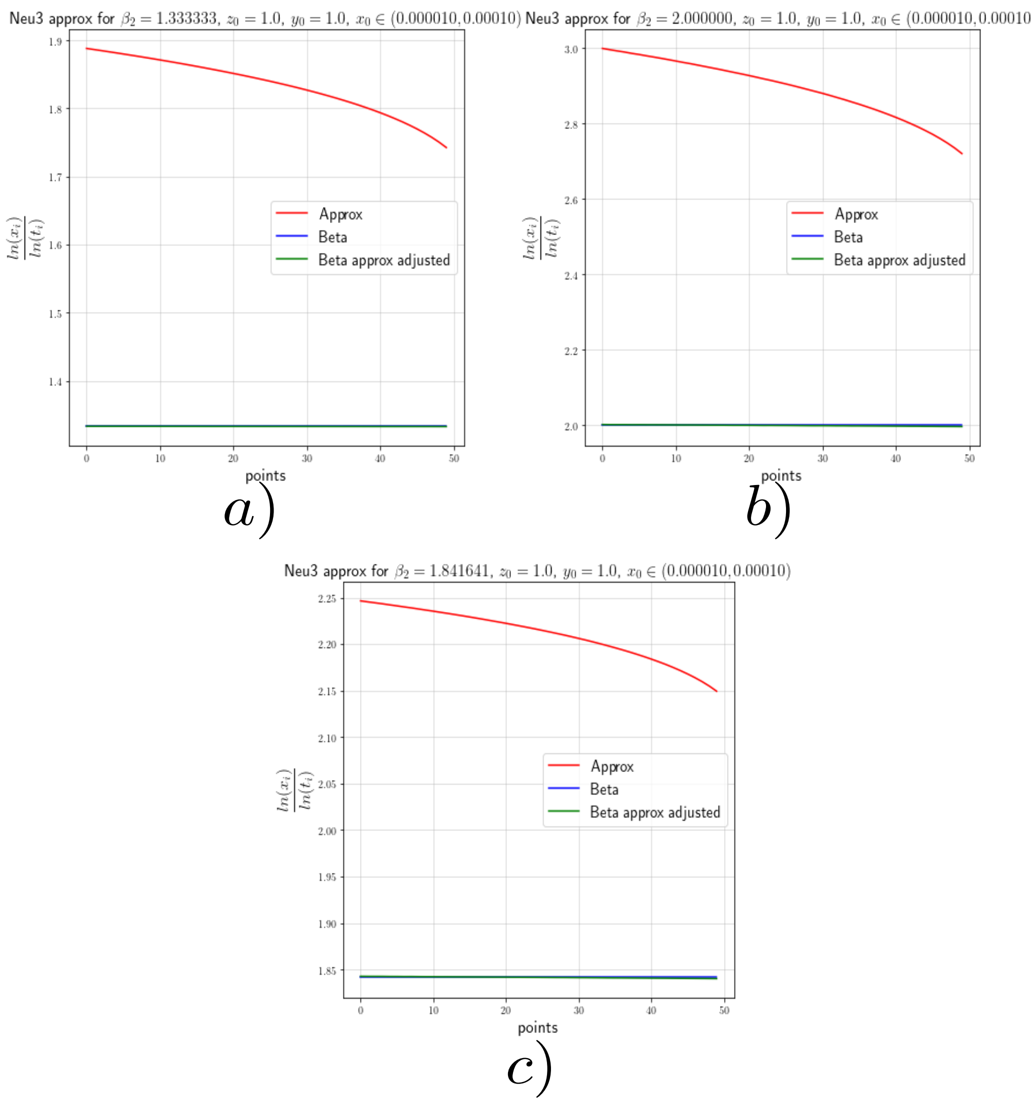

Figure 8.20: Numerical experimentation for β_2 approximation for the Neutral model 3

From these numerical results we can see that the asymptotic behaviour of all three Neutral models are similar. Thus, we can conclude that for the Neutral model 3 the image of the cross-section Σ under the map $N : \Sigma \to S$ will still have the cusp-shape as we saw in Chapter 4. Therefore, the Poincaré map of the modified Lorenz neutral model obtained by considering the Neutral model 3 will have the same properties we saw for the cases when we considered the Neutral model 1 and 2. Furthermore, the numerics showed us a good approximation of the exponent of the decay of correlations for the 3 Neutral models. From this we can deduce the same results concerning the decay of correlations. For completeness, we compress the results of this work in the following theorem.

8.2.1 Theorem. *Let Λ_{N}, $N_t : \Lambda_{\mathrm{N}} \to \Lambda_{\mathrm{N}}$ be the geometrical Lorenz neutral attractor, the geometrical Lorenz neutral flow obtained from the neutral form given by Equation* (8.16), (8.1) *and* (8.11)*, respectively, and μ its SRB measure. Then N_t has polynomial decay of correlations; that is, there exist $m \geq 1$ and a constant $C > 0$ such that for observables $v \in C^{\eta}(M) \cap C^{0,\eta}(M)$, $w \in C^{\eta,m}(M)$, and time $t > 1$ we have*

$$\rho_t(v, w) \leq C(\|v\|_{C^{\eta}} + \|v\|_{C^{0,\eta}}) \|w\|_{C^{\eta,m}} t^{-\beta_2}.$$

Bibliography

[1] Afraimovich, Valentin S., Bykov, VV and Shilnikov, Leonid P. *On the origin and structure of the Lorenz attractor*, DoSSR, Vol. 234, 11, 336–339 1977.

[2] Afraimovich, Valentin S., Bykov, VV and Shilnikov, Leonid P. *On attracting structurally unstable limit sets of Lorenz type attractors*, Trans. Moscow Math. Soc, Vol. 44, 11, 153–216 1983.

[3] Alligood, Kathleen, D. Sauer, Tim and Yorke, James A., *Chaos: An Introduction to Dynamical Systems*, Physics Today, 50, 1997.

[4] Anosov, Dmitri V., *Geodesic Flows on Closed Riemannian manifolds with negative curvature*, Steklov Inst. Math. Amer. Math. Soc., Vol. 90, 1967.

[5] Araújo, Vitor, and Varandas, Paulo, *Robust exponential decay of correlations for singular-flows*, Communications in Mathematical Physics, Springer, Vol. 311, 1, 215–246, 2012.

[6] Araújo, Vitor, Galatolo, Stefano and Pacifico, Maria José, *Open sets of Axiom A flows with exponentially mixing attractors*, Proceedings of the American Mathematical Society, Vol. 144, 7, 2971–2984, 2016.

[7] Araújo, Vitor, Galatolo, Stefano and Pacifico, Maria José, *Decay of correlations for maps with uniformly contracting fibers and logarithm law for singular hyperbolic attractors*, Mathematische Zeitschrift, Springer, Vol. 276, 3-4, 1001–1048, 2014.

[8] Araújo, Vitor and Melbourne, Ian, *Exponential Decay of Correlations for Nonuniformly Hyperbolic Flows with a $C^{1+\alpha}$ Stable Foliation, Including*

the Classical Lorenz Attractor, Annales Henri Poincaré, Springer, Vol. 17, 11, 2975–3004, 2016.

[9] Araújo, Vitor, Melbourne, Ian and Varandas, Paulo, *Rapid mixing for the Lorenz attractor and statistical limit laws for their time-1 maps*, Communications in Mathematical Physics, Springer, Vol. 340, 3, 901–938, 2015.

[10] Araújo, Vitor and Pacifico, Maria José, *Three-dimensional flows*, Springer Science & Business Media, Vol. 53, 2010.

[11] Avila, Artur, Gouëzel, Sébastien and Yoccoz, Jean-Christophe, *Exponential mixing for the Teichmüller flow*, Publications Mathématiques de l'IHÉS, 104, 143–211 2006.

[12] Bálint, Péter, Butterley, Oliver and Melbourne, Ian, *Polynomial decay of correlations for flows, including Lorentz gas examples*, Communications in Mathematical Physics, Springer, Vol. 368, 1, 55–111, 2019.

[13] Bálint, Péter and Melbourne, Ian *Decay of correlations for flows with unbounded roof function, including the infinite horizon planar periodic Lorentz gas*, preprint 2010.

[14] Bálint, Péter and Imre Péter, Tóth , *Correlation decay in certain soft billiards,* Commun. Math Phys. Springer, **243-1** (2003), 55–91.

[15] Boyarsky, Abraham and Gora, Pawel *Laws of chaos: invariant measures and dynamical systems in one dimension*, Springer Science & Business Media 2012.

[16] Brin, Michael I. and Pesin, Yakov B., *Partially hyperbolic dynamical systems*, Mathematics of the USSR-Izvestiya, IOP Publishing, Vol. 8, 1, 177 1974.

[17] Bruin, Henk, *On volume preserving almost Anosov flows*, arXiv preprint arXiv:1908.05675, 2019.

[18] Bruin, Henk and Melbourne, Ian and Terhesiu, Dalia, *Rates of mixing for non-Markov infinite measure semiflows*, Transactions of the American Mathematical Society, Vol. 371, 10, 7343–7386 2019.

[19] Bruin, Henk and Melbourne, Ian and Terhesiu, Dalia, *Sharp polynomial bounds on decay of correlations for multidimensional nonuniformly hyperbolic systems and billiards*, arXiv preprint arXiv:1811.07775, 2018.

[20] Bruin, Henk and Terhesiu, Dalia, *Regular variation and rates of mixing for infinite measure preserving almost Anosov diffeomorphisms*, Ergodic Theory and Dynamical Systems, Cambridge University Press, Vol. 48, 3, 663–698 2020.

[21] Bruin, Henk and Terhesiu, Dalia and Todd, Mike, *Pressure function and limit theorems for almost Anosov flows*, Communications in Mathematical Physics, Springer, Vol. 382, 1, 1–47 2021.

[22] Canales Farías, Hector Homero, *The dynamics of a taffy puller machine*, Masterarbeit, University of Vienna, urn:nbn:at:at-ubw:1-16285.78549.965471-0 2019.

[23] Chernov, N., *Decay of correlations and dispersing billiards,* Journal of Statistical Physics, Springer, **94** (1999), 513–556.

[24] Crovisier, Sylvain and Potrie, Rafael, *Introduction to partially hyperbolic dynamics*, School on Dynamical Systems, ICTP, Trieste, Vol. 3, 1 2015.

[25] Dolgopyat, D., *On decay of correlations in Anosov flows,* Ann. Math., JSTOR, **147-2** (1998), 357–390.

[26] Fathi, Albert and Laudenbach, François and Poénaru, Valentin, *Thurston's Work on Surfaces (MN-48)*, Princeton University Press, Vol. 48, 2012.

[27] Gouëzel, S., *Sharp polynomial estimates for the decay of correlations.* Israel J. Math. **139** (2004) 29–65.

[28] Guckenheimer, J., and Williams, R. F., *Structural stability of Lorenz attractors*, Inst. Hautes Etudes Sci. Publ. Math. **50** (1979), 59–72.

[29] Hennion, H. and Hervé, L., *Limit theorems for Markov chains and stochastic properties of dynamical systesm by quasi-compactness* , Lect. Nontes in Math. 1766, Springer 2000

[30] Hildebrand, Francis Begnaud *Introduction to numerical analysis*, Courier Corporation 1987.

[31] Hirsch, Morris. W., Smale, Stephen and Devaney, Robert. L., *Differential equations, dynamical systems, and an introduction to chaos*, Academic press, 2012

[32] Hu, Huyi, *Conditions for the existence of SBR measures for "almost Anosov" diffeomorphisms*, Transactions of the American Mathematical Society, Vol. 352, 5, 2331–2367 2000.

[33] Hu, Huyi and Young, Lai-Sang, *Nonexistence of SBR measures for some diffeomorphisms that are 'almost Anosov'*, Ergodic Theory and Dynamical Systems, Cambridge University Press Vol. 15, 1, 67–76 1995.

[34] Hu, Huyi and Zhang, Xu, *Polynomial decay of correlations for almost Anosov diffeomorphisms*, Ergodic Theory and Dynamical Systems, Cambridge University Press Vol. 39, 3, 832–864 2019.

[35] Lorenz, Edward N., *Deterministic nonperiodic flow*, Journal of the atmospheric sciences, Vol. 20 2, 130–141 1963.

[36] Natanson, I.P., *Theory of functions of a real variable*, Frederick Ungar Punl. Co., 1955.

[37] K. Petersen, *Ergodic Theory.* Cambridge University Press, Cambridge 1983.

[38] Pesin, Yakov B., *Lectures on partial hyperbolicity and stable ergodicity*, Vol. 34 European Mathematical Society 2004.

[39] Pugh, Charles and Shub, Michael, *Ergodicity of Anosov actions*, Inventiones mathematicae, Springer, Vol. 15 1, 1–23 1972.

[40] Robinson, Clark, *Dynamical systems: stability, symbolic dynamics, and chaos*, CRC press 1963.

[41] Sarig, O. M., *Subexponential decay of correlations.* Invent. Math. **150** (2002) 629–653.

[42] Schaefer, H.H., *Banach lattices and positive operators*, Die Grundlehren der mathematischen Wiessenschaften, Springer-Verlag, New York-Heidelberg 1974.

[43] Shub, Michael, *Global stability of dynamical systems*, Springer Science & Business Media 2013.

[44] Sinai, Y. G., *Dynamical systems with elastic reflections. Ergodic properties of dispersing billiards,* Uspekhi Matematicheskikh Nauk, Russian Academy of Science, **25-2** (1970), 141–192.

[45] Tao, Terence, *An introduction to measure theory*, American Mathematical Society Providence, Vol. 126, 2011.

[46] Tao, Terence, *Nonlinear dispersive equations: local and global analysis*, American Mathematical Society, 106, 2006.

[47] Tucker, Warwick, *The Lorenz attractor exists*, Comptes Rendus de l'Académie des Sciences-Series I-Mathematics, Elsevier, Vol. 328 12, 1197–1202 1999.

[48] Viana, Marcelo, *Stochastic dynamics of deterministic systems*, IMPA Rio de Janeiro, Vol. 21, 1997.

[49] Walters, Peter, *An introduction to ergodic theory*, Springer Science & Business Media, Vol. 79 2000.

[50] Young, Lai-Sang, *Statistical properties of systems with some hyperbolicity including certain billiards,* Ann. Math., **147** (1998), 585–650.

Index